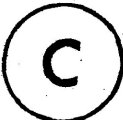


THERMODYNAMIC STUDIES OF THE SORPTION OF AMMONIA
ON NATURAL AND MODIFIED CHRYSOTILE ASBESTOS

BY
 JANE E. TODD

A THESIS SUBMITTED TO THE DEPARTMENT OF CHEMISTRY
IN PARTIAL FULFILLMENT OF THE REQUIREMENTS FOR
THE DEGREE OF MASTER OF SCIENCE
LAKEHEAD UNIVERSITY
THUNDER BAY, ONTARIO, CANADA
OCTOBER, 1981

ProQuest Number: 10611685

All rights reserved

INFORMATION TO ALL USERS

The quality of this reproduction is dependent upon the quality of the copy submitted.

In the unlikely event that the author did not send a complete manuscript and there are missing pages, these will be noted. Also, if material had to be removed, a note will indicate the deletion.



ProQuest 10611685

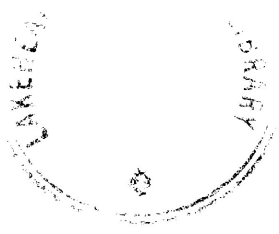
Published by ProQuest LLC (2017). Copyright of the Dissertation is held by the Author.

All rights reserved.

This work is protected against unauthorized copying under Title 17, United States Code
Microform Edition © ProQuest LLC.

ProQuest LLC.
789 East Eisenhower Parkway
P.O. Box 1346
Ann Arbor, MI 48106 - 1346

THESES
M.Sc.
1982
T64
C.1



(c) Jane E. Todd 1981

295229

ACKNOWLEDGEMENTS

The work in preparation for this thesis was carried out in the Department of Chemistry at Lakehead University, Thunder Bay, Ontario, Canada. The author wishes to thank her supervisor Dr. R. A. Ross, DSc(Strath.), PhD, BSc(Glas.), ARCST, CEng, F Inst E, FCIC, C Chem, FRSC(U. K.), Professor of Chemistry, for his advice and encouragement throughout this work. Thanks are also due to the technical staff of the Faculty of Science, Lakehead University for technical assistance.

The financial assistance of Imperial Oil Co. Ltd. is also gratefully acknowledged.

TABLE OF CONTENTS

CHAPTER	PAGE
ACKNOWLEDGEMENTS	ii
TABLE OF CONTENTS	iii
SUMMARY	viii
I. INTRODUCTION	1
1.1. Scope of Investigation	4
1.2. Adsorbent	5
1.2.1. Chrysotile	5
1.3. Adsorbate	8
1.3.1. Ammonia	8
1.4. Outline of Experimental Approach ..	10
II EXPERIMENTAL	12
2.1. Adsorbents	12
2.1.1. Chrysotile Asbestos	12
2.1.2. Material Supported on Asbestos ...	12
2.1.2.1. Sodium Nitrate/Californian	
Chrysotile	12
2.1.2.2. Water/Californian Chrysotile	13
2.2. Adsorbates	13
2.2.1. Ammonia	13
2.2.2. Nitrogen	14
2.2.3. Helium	14
2.3. Apparatus	15
2.3.1. Calorimetric Measurement of Heats	
of Adsorption	15

2.3.2.	Calculation of Entropies of Adsorption	27
2.3.3.	Surface Area and Pore Volume Measurement	32
2.3.4.	Mass Spectrometry	37
2.3.5.	Electron Microscopy	38
III.	RESULTS	40
3.1.	Introduction	40
3.2.	Adsorption/Desorption of Ammonia on Californian Chrysotile at 273 and 298 K	40
3.2.1.	Calorimeter Experiments	40
3.2.2.	Entropy Calculations	44
3.2.3.	Adsorption/Desorption Isotherms ..	47
3.3.	A Comparison of the Sorption Characteristics at 266, 273, 288, 298 and 308 K of Ammonia on Californian Chrysotile Heat-Treated at 500°C	50
3.3.1.	Calorimeter Experiments	50
3.3.2.	Entropy Calculations	53
3.3.3.	Adsorption/Desorption Isotherms ..	55
3.4.	Adsorption/Desorption of Ammonia on Quebec Chrysotile at 273 and 298 K ..	57
3.4.1.	Calorimeter Experiments	57
3.4.2.	Entropy Calculations	60
3.4.3.	Adsorption/Desorption Isotherms ..	60

3.5.	A Comparison of the Sorption Characteristics at 266, 273, 288, 298 and 308 K of Ammonia on Quebec Chrysotile Heat-Treated at 500°C	66
3.5.1.	Calorimeter Experiments	66
3.5.2.	Entropy Calculations	69
3.5.3.	Adsorption/Desorption Isotherms ..	69
3.6.	Adsorption/Desorption of Ammonia on Californian Chrysotile Pre-Treated with Boiling Water	72
3.6.1.	Calorimeter Experiment	72
3.6.2.	Entropy Calculations	72
3.6.3.	Adsorption/Desorption Isotherms ...	73
3.7.	Adsorption/Desorption of Ammonia on Californian Chrysotile Pre-Treated with Sodium Nitrate	75
3.7.1.	Calorimeter Experiment	75
3.7.2.	Entropy Calculations	75
3.7.3.	Adsorption/Desorption Isotherm ...	78
3.8.	Efficiency of Desorption of Ammonia from Heat-Treated Californian and Quebec Chrysotiles	78
3.8.1.	Introduction	78
3.8.2.	Californian Chrysotile	82
3.8.3.	Quebec Chrysotile	82
3.9.	Mass Spectrometer Analysis	85

3.10.	Studies of the Physical Structure of the Adsorbents	85
3.10.1.	Introduction	85
3.10.2.	Californian Chrysotile	85
3.10.2.1.	Low-Temperature Nitrogen Adsorption	85
3.10.2.2.	Electron Microscopy	92
3.10.3.	Quebec Chrysotile	92
3.10.3.1.	Low-Temperature Nitrogen Adsorption	92
3.10.3.1.	Electron Microscopy	98
3.10.4.	Californian Chrysotile Treated with Water and Sodium Nitrate	103
3.10.4.1.	Low-Temperature Nitrogen Adsorption	103
3.10.4.2.	Electron Microscopy	106
IV	DISCUSSION	108
4.1.	Introduction	108
4.2.	Adsorptions on Californian Chrysotile	108
4.3.	Adsorptions on Quebec Chrysotile ...	122
4.4.	Desorption Efficiency of Californian Chrysotile	125
4.5.	Desorption Efficiency of Quebec Chrysotile	126
4.6.	Adsorption of Ammonia on Californian Chrysotile Treated with Water and Sodium Nitrate	127

4.7	The Physical Structure of the Adsorbents	129
4.7.1.	Californian Chrysotile	129
4.7.2.	Quebec Chrysotile	130
4.7.3.	Water and Sodium Nitrate-Treated Californian Chrysotile	131
4.8.	Conclusion	131
REFERENCES	133
APPENDICES		
Appendix A.	Calculations	138
Appendix B.	DEC2020 Programmes	142
Appendix C.	Desorption Efficiency Data .	150

SUMMARY

The sorption of ammonia was studied at 273 and 298 K on Californian and Quebec chrysotile heat-treated at 150, 300, 500 and 700°C. Another ammonia sorption study involving the two chrysotiles treated at 500°C at isotherm temperatures of 266, 273, 288, 298 and 308 K was carried out. The variation of the calorimetric heats of adsorption with surface coverage and adsorption/desorption isotherms were determined. From these data experimental differential molar entropies of adsorption were calculated.

The results indicated that the high heats of adsorption observed initially may have been due to a weak chemisorption reaction perhaps involving ammonium complex formation with impurities on the chrysotile surface. Hydrogen bonding and van der Waals forces could possibly have accounted for the lower heats of adsorption observed at higher surface coverages.

The present studies appeared to belong to an unusual class of adsorption phenomena where the heat of adsorption was less than the heat of liquefaction of the ammonia. This was attributed to the two hypotheses of significant entropy involvement in the adsorption and capillary adsorption.

Minor studies of the adsorption/desorption of ammonia on Californian chrysotile treated with sodium nitrate and boiling water were also performed. Heats of adsorption at all degrees of surface coverage were approximately three

times those in the other experiments. This was attributed to the highly hydroxylated surface which may have facilitated chemisorption.

A group of experiments were carried out to determine the desorption efficiencies of the two chrysotiles. The Quebec samples generally proved to desorb the ammonia more efficiently.

All adsorbents were characterised by low-temperature (77 K) nitrogen adsorption/desorption isotherms from which surface area and pore size distribution data were obtained. Also, direct examination of the topographical and structural features of the adsorbents was made by transmission electron microscopy and selected area electron diffraction.

CHAPTER I

1. Introduction

The adsorption of gases on solid surfaces is a complex phenomenon. Most surfaces are not uniform, having sites with a broad distribution of adsorption energies. The sites and molecules present may be independent of one another or they may interact (1). The density of adsorptive sites may vary from extremely low to very high. The adsorption forces which hold molecules at a surface may be chemical in nature and involve molecular orbital overlap or they may be physical - including Van der Waals attraction and the forces developed by ions and dipoles as they approach the surface. Disturbances of surface atoms or ions may occur as a result of adsorption (2).

In spite of the many theoretical studies of the adsorption of gases on solid surfaces that have been made (1, 3 and 4), the mechanism and precise description of the changes produced in both the adsorbate and adsorbent have remained elusive except in the simplest of cases (5). Theoretical treatments of adsorption must note the changes in the thermodynamic properties of the system and this can be accomplished by using classical thermodynamic equations that have been derived for the adsorption process (6, 7) although these equations are too general to provide a detailed description of the process. In cases where more detailed descriptions are

required, assumptions are usually made regarding the specific adsorption model which can only give an approximation to the real system (7). It is the uncertainty involved in this method that has prevented precise analyses of adsorption systems in the past, and progress in the future will probably involve more sophisticated models which will reduce the uncertainty between the model and that which occurs in practice.

However, a large amount of useful information can still be obtained from a classical thermodynamic description of the adsorption process. In many cases experimentally determined values of the changes in enthalpy and entropy enable estimates to be made of the type of bonding and the mobility of the adsorbed gas on the surface (8).

The enthalpy and entropy of a system are related by the Gibbs free energy (G) equation:

$$G = H - TS \text{ ----- (1)}$$

where H, T and S are the enthalpy, temperature and entropy respectively.

Thus, when a gas is adsorbed on a solid surface, the changes that result in these thermodynamic properties can be described by:

$$\Delta G = \Delta H - T\Delta S \text{ ----- (2)}$$

where ΔG , ΔH and ΔS are the changes in Gibbs free energy, enthalpy (heat of adsorption) and entropy respectively.

Since the Gibbs free energy must decrease for any spontaneous process, and since adsorption is one such process

which is accompanied by a decrease in entropy, then from equation (2), ΔH , the heat of adsorption, is negative. Hence, adsorption is expected to be an exothermic process and for most adsorption systems this is a valid conclusion (8).

The heat of adsorption is the simplest thermodynamic quantity that can be measured and it is probably the most useful. It is the best single criterion to decide whether the "bonding" involved is of van der Waals type as in physical adsorption or if it is chemical in nature since the heat of physical adsorption rarely exceeds two or three times the heat of liquefaction of the gas (usually $<63 \text{ kJ mol}^{-1}$) whereas the heat of chemical adsorption can be much higher (usually $>85 \text{ kJ mol}^{-1}$) (9). In addition, molar entropies of adsorption can be calculated from the heats of adsorption and provide further information regarding the mobility of the adsorbed gas.

A knowledge of the magnitude of the heat of adsorption is also very important in understanding the nature of catalytic reactions. For example, if the heat of adsorption is very large for any reaction species, that species may be held too strongly at the surface and will therefore hinder catalysis. If the heat is too low, the species may not be held long enough to facilitate the reaction. Thus the mechanisms of heterogeneously catalyzed reactions may often be elucidated considerably from a knowledge of the heats of adsorption for the reactants, products and intermediates.

It can be noted from equation (2) that the magnitude

of the heat of adsorption will depend on temperature and on the physical and chemical nature of the adsorbate and adsorbent. It is therefore necessary to identify these variables as much as possible before reliable interpretation of the results can be made (6).

The study of the adsorption of gases on solid surfaces is of major theoretical interest but it is equally important in practice since any process involving solid/gas interactions must include adsorption as one of the operating stages (2).

1.1. Scope of the Investigation

A number of studies (10-13) have been reported of the interactions of gaseous ammonia on solid adsorbents but few have been detailed and fewer still have included thermodynamic measurements. In step with this, little work (14-17) has been reported regarding the sorption of gases on chrysotile and only recently has a study been reported (14) on the sorption of sulfur dioxide on Californian and Quebec chrysotiles which emphasized thermodynamic measurements.

In the present study ammonia was adsorbed at temperatures ranging from 266 K to 308 K on heat-treated Californian and Quebec chrysotiles. In addition, the adsorption of ammonia on Californian chrysotile treated with sodium nitrate and water was also briefly studied at 298 K.

The specific aims of the project were then:

- (i) to measure the heats of adsorption, and from these data, to calculate the entropy of the

adsorbed species to find its mobility;

- (ii) to contrast the two types of chrysotiles with particular reference to the effect of brucite impurity in the Quebec sample;
 - (iii) to study the effect of chemical treatment on the surface of chrysotile;
 - (iv) to characterise the physical structure of the adsorbents with respect to surface area, pore size distribution and predominant topographical features;
- and (v) to study the "bonding" mechanism and possibly to elucidate the nature of the adsorbed complex formed by ammonia with the adsorbents.

1.2. Adsorbents

1.2.1. Chrysotile

All asbestos is derived from two large groups of rock-forming minerals, the serpentines and the amphiboles (18). In this work chrysotile asbestos was used exclusively. It is the only species in the serpentine group and the most abundant type.

Chrysotile has many applications including fibrous reinforcement in cement, asphalt and tile as well as use in textiles and automotive products (18-20). A satisfactory replacement for asbestos has not been found and most of the above products utilize the substance because of its unique physical and chemical properties.

The relationship between the inhalation of asbestos fibres

and the initiation of respiratory disease has been the subject of extensive research (21-24). It has been suggested, however, that common asbestos-related respiratory diseases cannot be caused solely by asbestos inhalation (25). In view of the reported synergetic relationship (26) which exists between cigarette smoking and asbestos-related disease, studies of the sorption of gases on asbestos with emphasis on possible synergetic relationships may have some added interest to the health sciences. The key to understanding certain asbestos-related diseases may then lie in evaluating the effects of co-inhalation of the fibres with various pollutant gases.

With respect to the structure of chrysotile, each fibre is formed of several scrolls of individual crystallites (18). Each scroll is composed of a closely connected double layer with magnesium hydroxide units on its external face and silica units on its inner face. The unit cell is based on the formula $Mg_3(Si_2O_5)(OH)_4$. A diagrammatic representation of chrysotile is shown in Figure 1.

The magnesium hydroxide (brucite) layer has larger dimensions than the silicate layer thus causing the layers to mismatch which results in the formation of the curvilinear structure or scroll form (18).

Because of the presence of brucite on the external surface, the chrysotile fibre has strongly basic properties, a high surface potential for water and marked hydrophyllic tendencies. The surface can therefore be leached by water or the brucite removed by acid.

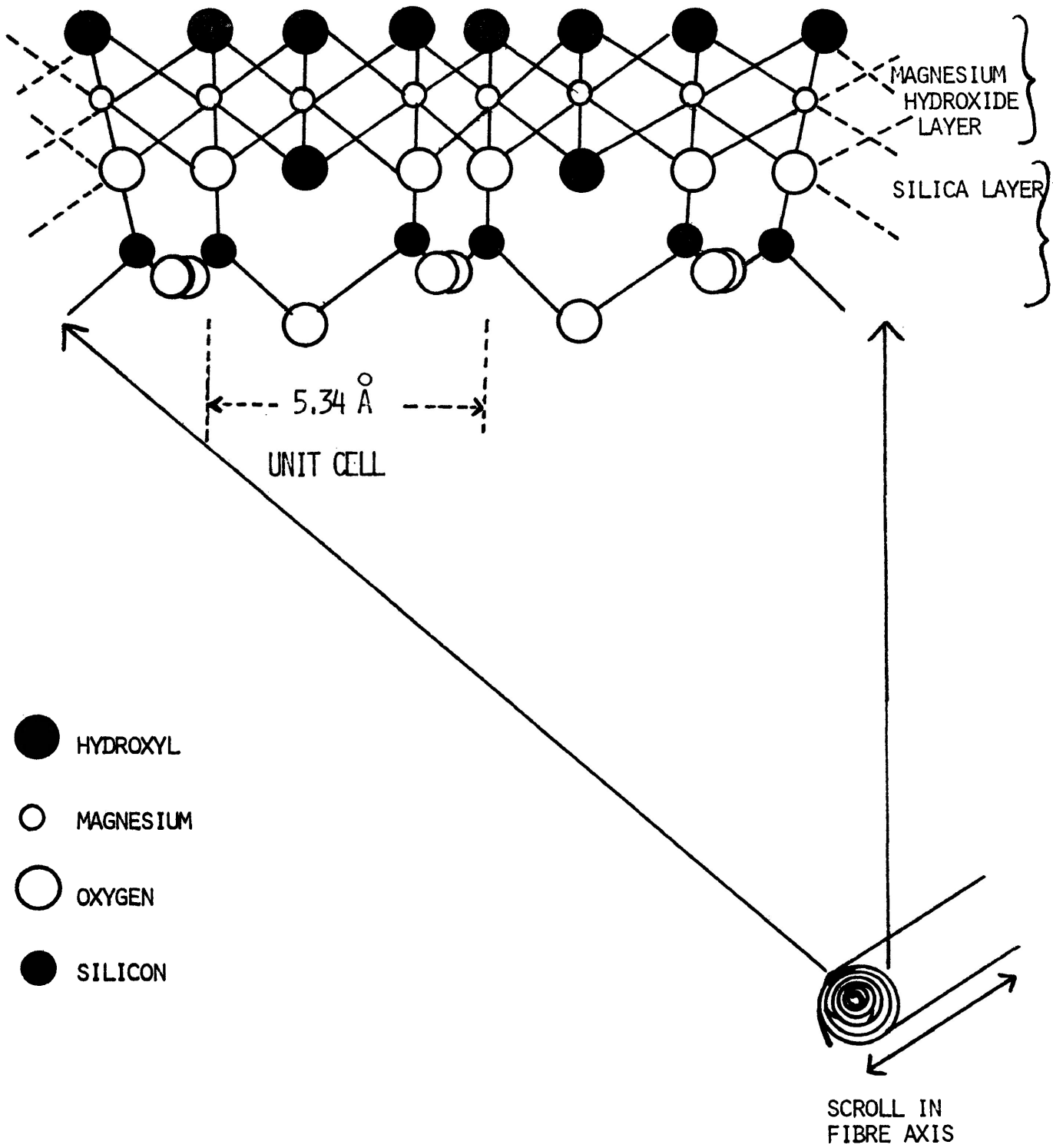
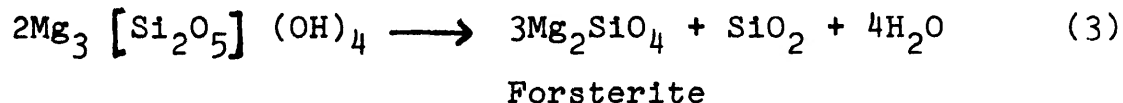


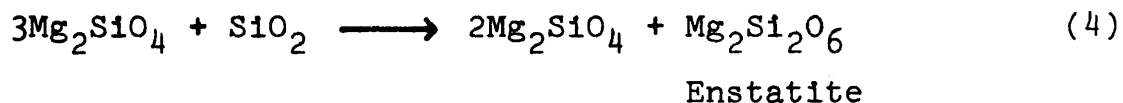
FIGURE 1 CHRYSOTILE STRUCTURE

Holt, Clark and Reimschuessel (22) extracted chrysotile with boiling water and found that the solution contained both magnesium and soluble silicic acid. They postulated that the chrysotile decomposed by dissolution of magnesium, leaving a residue of colloidal silica that hydrolyzed to orthosilicic acid. Soxhlet extraction studies showed that for the first three to four hours the magnesium concentration was high in the solution but it decreased later, accompanied by the formation of a precipitate of amorphous magnesium silicate.

All forms of asbestos break down to simpler components when heated to around 600 to 1000°C (27-39). Dehydroxylation generally occurs from 500 to 780°C and from 800 to 850°C the anhydride breaks down to form forsterite and silica as shown:



Equation 4 shows the formation of some enstatite at temperatures well above 1000°C:



1.3. Adsorbate

1.3.1. Ammonia

No previous studies of ammonia adsorbed on chrysotile surfaces were found in the literature. The only fairly comparable studies were concerned with ammonia adsorption on

silica, silica-alumina and carbon black surfaces (10-13, 40-42).

Clark, Holm and Blackburn (12) made adsorption measurements on a vacuum microbalance using eleven silica-alumina gels ranging in composition from pure alumina to pure silica. Results showed limiting heats of adsorption in the order of 50 kJ mol^{-1} for pure alumina down to less than 15 kJ for pure silica. Heats of adsorption were not determined directly in a calorimeter but rather, indirectly by application of the integrated form of the Clausius-Clapeyron equation. The value of experimental differential molar entropy corresponded to that calculated for a two-dimensional mobile model for most samples. The best correlations were obtained for the 55 to 90 percent silica samples.

A study of the heat of adsorption of ammonia on silica-alumina catalysts by Hsieh (11) indicated limiting heats of adsorption of 25 kJ mol^{-1} . Hsieh also found evidence of strong adsorbate-adsorbate interactions.

Studies of ammonia sorption on silica xerogel and modified silica xerogel (13) indicated that the adsorption pattern was complex and exhibited both physical and chemical adsorption characteristics in terms of the classical description of the phenomena.

Various other sources (40-42) have discussed the possibility of hydrogen bonding of ammonia to silica (40,41) and carbon black (42) and also the non-quantitative formation of NH_4^+ when ammonia is chemisorbed on cracking catalysts.

The past studies provided a useful base for the present investigation, particularly the work involving the surface reactions of ammonia on silica gel since some correlation may be drawn between the silica gel surface and the outer silica layer of the chrysotile. However, other aspects of the chrysotile structure make it somewhat unique and therefore the present work cannot be extensively compared with that reported previously.

1.4. Outline of Experimental Approach

A major section of this work was devoted to the measurements of the heats of adsorption of ammonia at various temperatures on two types of heat and chemically-treated chrysotiles. It was hoped that these measurements would provide useful information on the nature of the adsorbate/adsorbent interactions and also on the key chemical and physical characteristics of the surfaces involved. This information was supported by the calculation of the differential molar entropies of the adsorbed gases and comparing these with theoretical values calculated for models of mobile and immobile adsorption. In spite of recognised limitations, such classical entropy calculations have provided very useful insights concerning the mobility of the adsorbed phases (8, 43, 44).

Adsorption isotherms were determined on both adsorbents using an established volumetric method which provided information regarding the nature of the process.

The physical structures of the adsorbents were characterized by two independent techniques. The first involved measurement of low-temperature (77 K) nitrogen adsorption/desorption isotherms which has been used regularly to evaluate the effects of heat treatment on porous oxide structures (45-47). The classical B. E. T. method (48) was applied to obtain the surface area of the adsorbents, and analysis of the isotherms using the techniques of Cranston and Inkley (49) and Dollimore and Heal (50) yielded pore size distribution data. These results were compared with independent measurements on the electron microscope. This technique provided information regarding the shapes and sizes of the pores, and also the topographical features of the surface.

Other useful data were obtained from analysis of desorbed products by mass spectrometry.

CHAPTER II

2. Experimental

2.1. Adsorbents

All heat treatments and other modification procedures were carried out in air.

2.1.1. Chrysotile Asbestos

Two types of chrysotile asbestos were used in this work. One was supplied by Lake Asbestos, Black Lake, Quebec (sample 7T-5, Quebec chrysotile) and the other by Union Carbide Corporation (Calidria asbestos sample HPO, Californian chrysotile). The major impurities were brucite ($\text{Mg}(\text{OH})_2$), 10% w/w in the Quebec sample and magnetite (Fe_3O_4), 3.75% in the Quebec and 0.75% in the Californian sample. Surface areas were determined from nitrogen adsorption/desorption isotherms at 77 K, giving 60 and 40 $\text{m}^2 \text{g}^{-1}$ for Californian and Quebec chrysotiles, respectively.

2.1.2. Material Supported on Asbestos

An impregnation technique was used to prepare the modified adsorbent (13). In general, no attempt was made to control strictly the conditions of impregnation since subsequent analysis of the adsorbent by physical and chemical methods characterized the material.

2.1.2.1. Sodium Nitrate/Californian Chrysotile

Untreated Californian chrysotile was impregnated with

10g. NaNO_3 in 100 dm^3 of boiling water for 5 h., as described by Boyle et al (13). After filtering and repeated washings with distilled water to remove traces of nitrate, the sample was dried in a furnace for 48 h. at 150°C . Flame photometric analysis showed 3.7% sodium present.

2.1.2.2. Water/Californian Chrysotile

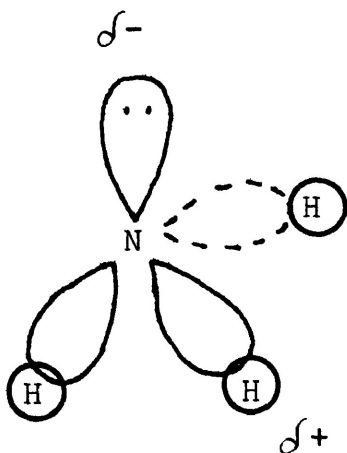
As a "control" for the sodium nitrate impregnation experiment, untreated Californian chrysotile was boiled in distilled water for 5 h. in order to determine any effect of water on the chrysotile surface.

2.2. Adsorbates

2.2.1. Ammonia

Physical Properties

- sp_3 hybridization of orbitals
- pyramidal shape



The ammonia molecule is pyramidal with nitrogen placed at the apex about 0.4 \AA above a triangular base defined by three hydrogen atoms (51).

Ammonia boils at -33.35°C (101.1 kPa), with a latent heat of vaporization of 1.369 kJ g^{-1} (52); it has a critical temperature of 133.0°C (53) and a dipole moment of 1.3×10^{-18} e.s.u.

In these experiments the ammonia (Matheson, Co.) was anhydrous quality (99.99%) and was drawn, after line flushing, from the cylinder to a trap attached to the adsorption apparatus. A 40 cm. potassium hydroxide (Analar) column was inserted in the line before the trap in the apparatus in order to further dry the gas. It was then outgassed three times at 1.33×10^{-4} kPa and vacuum distilled over trays of "Analar" potassium hydroxide, the first and last fractions being discarded. The distilled gas was stored at liquid nitrogen temperature. Mass spectrometric analysis showed the gas to be 99.99% pure.

2.2.2. Nitrogen

The nitrogen used in the low-temperature adsorption experiments was supplied by Canadian Liquid Air with a stated minimum purity of 99.99%. The main impurities were argon (80 ppm), oxygen (20 ppm), and water (10 ppm). The purity, including argon, was 99.998%.

2.2.3. Helium

Helium was used for calibrating dead spaces. It was

supplied by Canadian Liquid Air Ltd., minimum purity, 99.995%, and was used as supplied after repeated line flushing.

2.3. Apparatus

2.3.1. Calorimetric Measurement of Heats of Adsorption

Introduction

The heat of adsorption can be measured directly, using a calorimeter, or indirectly, by applying the Clausius-Clapeyron equation to a series of adsorption isosteres derived from adsorption isotherms (8). The calorimetric approach involves fewer assumptions (54) than the Clausius-Clapeyron method, and has been used widely for the determination of heat capacities (55), and entropies (56), as well as heats of adsorption for various gas/solid systems.

The calorimetric technique involves the admission of successive increments of gas to the surface of an outgassed adsorbent and measurement of the heat liberated by each dose. The heats are approximately equivalent to differential heats of adsorption (57) and are normally plotted as a function of the amount of gas adsorbed.

The design of a calorimeter is dictated largely by the nature of the adsorbent. For powdered samples, it has not changed basically from that of early versions (58, 59), the major improvement arising from small refinements in construction and the use of more sensitive instrumentation.

Apparatus

The calorimeter is shown in Figure 2. The apparatus consisted of an adsorption chamber of glass tube 30.0 x 1.5 cm. diameter with a constriction 2.0 cm. from the base. About 5mm. above the base, the calibration heater was fixed horizontally in a thin-walled glass tube 3 mm. i.d. The heater was made from 30 cm. of 32 tr Kanthal wire and had a resistance of 35 ohms. It was sealed through tungsten/glass seals to thick copper leads 3 mm. in diameter which were themselves sealed again to thick tungsten leads before final sealing through the outer glass jacket. The temperature sensor used was a thermistor (Yellow Springs Instrument, Co. Ltd.) with a resistance at 0°C of 9795 ohms. The thermistor had a very rapid response and was well suited for measurement of small temperature changes from -10 to 150°C. A typical temperature change in a given experiment was about 0.5 to 1.0°C. It was established that the thermistor had a linear temperature-resistance relationship from -10 to 150°C. It was positioned at the bottom of a narrow, thin-walled glass probe. The probe widened above the constriction in the adsorption chamber and was a close fit to the wall of the chamber (thus reducing the dead space in the calorimeter). The lower portion of the adsorption chamber was surrounded by an outer jacket, 18 x 6 cm., which could be evacuated or filled with helium depending on whether the calorimeter was operated in an isothermal or adiabatic mode.

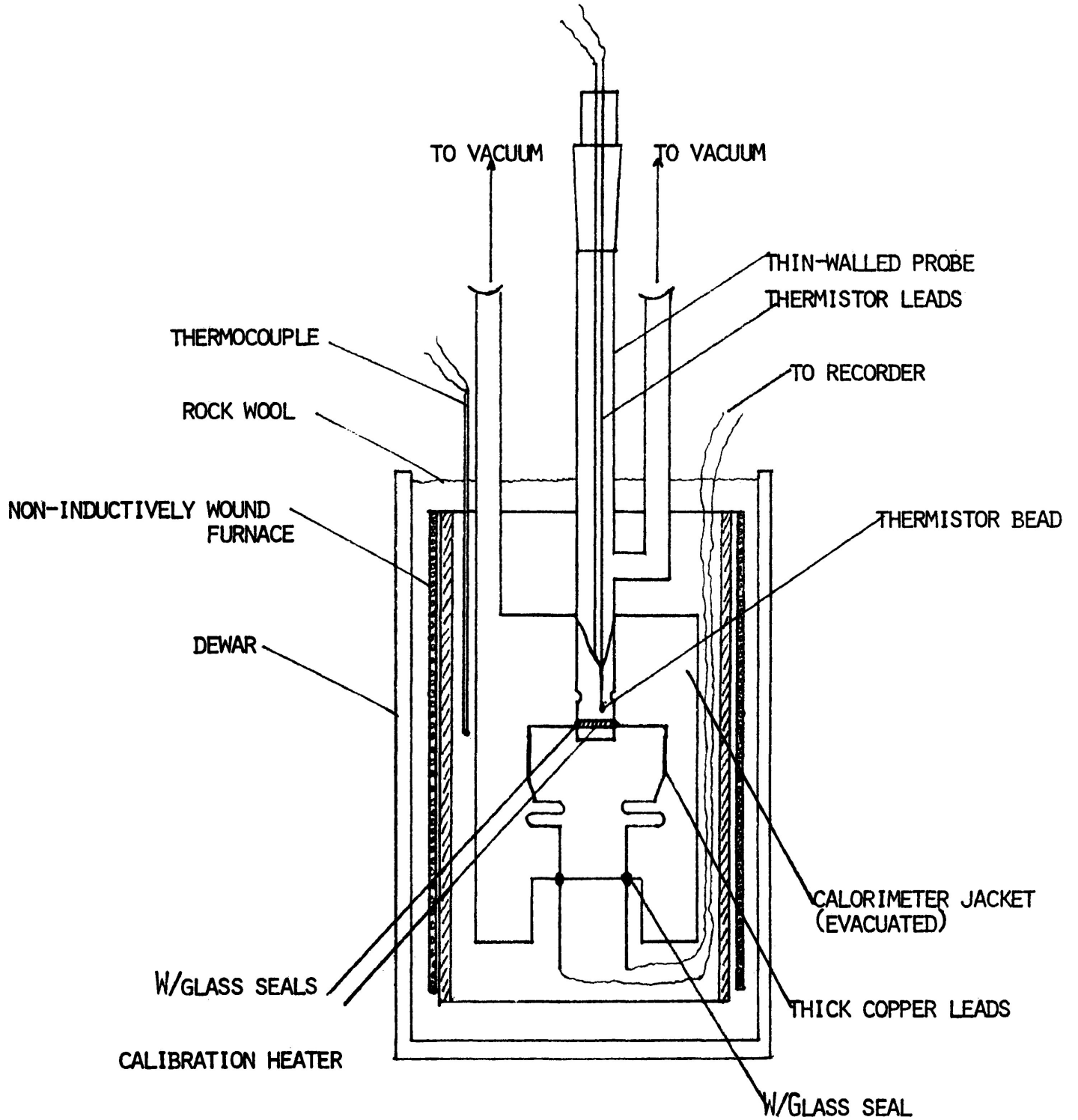


FIGURE 2 CALORIMETER AND FURNACE ASSEMBLY

The calorimeter was placed in an ethylene glycol bath maintained at constant temperature with a Masterline constant temperature bath and circulator (Forma Scientific; Model 70). This apparatus was operated in the circulating mode with a copper cooling coil immersed in the bath and connected to the circulator by rubber tubing. There was a slight temperature change over the length of rubber tubing but the circulator was adjusted to accommodate this difference. All final temperatures were accurately measured using the thermistor. The constant temperature glass bath enclosing the calorimeter was surrounded with 3.5 cm. styrofoam insulating material. With vigorous mechanical stirring, the apparatus maintained temperatures from -7 to 35°C to $\pm 0.1^{\circ}\text{C}$.

All adsorbent samples were outgassed for 24 h. at 1.33×10^{-4} kPa and 423 K. To achieve this temperature a non-inductively wound furnace was used. The windings were insulated from the metal core with asbestos tape, and from each other by asbestos rope. The furnace was then placed in a large Dewar flask (37 x 14 cm.). The bottom of the flask, and the gap between the furnace and the flask were filled with rock wool. The calorimeter was positioned centrally in the furnace, with rock wool packed around it and on top of it. A chromel-alumel thermocouple was used as a temperature sensor for a stepless, proportional controller (Thermo Electric Ltd.; Model 400) and was positioned level with the sample in the adsorption chamber. A constant voltage regulator (Solar

Electric; Type CVS 500 VA) controlled the supply voltage to 118 ± 1 V AC. Temperatures could be controlled to $\pm 0.10^\circ\text{C}$ indefinitely with this system. If the outer jacket of the calorimeter was evacuated to less than 1.33×10^{-4} kPa, temperatures could be controlled to $\pm 0.003^\circ$ indefinitely.

The gas-handling section of the apparatus is shown in Figure 3. A vacuum of 1.33×10^{-5} kPa was obtained using a mercury diffusion pump (Edwards High Vacuum Ltd. ; Type EMZ) backed by a two-stage rotary oil pump (Edwards High Vacuum Ltd.; Type ED100). A de-mountable liquid nitrogen trap was used to prevent mercury vapour from entering the low vacuum side of the apparatus and also to prevent damage to the pump from corrosive vapours. The vacuum was measured using a Pirani gauge (Edwards High Vacuum Ltd.; Type G5C-2, range 1.33×10^{-4} to .133 kPa) connected to a control unit (Edwards High Vacuum Ltd., Model 8/2).

Adsorbate doses and equilibrium pressures were measured using a combined differential mercury manometer and gas burette. The mercury levels in the limbs of the manometer were measured using a cathetometer (± 0.001 cm.) (Gaertner Scientific Corporation; Model 3380A).

The thermistor formed one arm of an initially balanced Wheatstone bridge circuit (Sigma Instruments; Ruhstat, Type SFM). The output from the galvanometer was connected to a potentiometric recorder (Beckman Instruments; Model 1005). Thus any change in the resistance of the thermistor caused by a

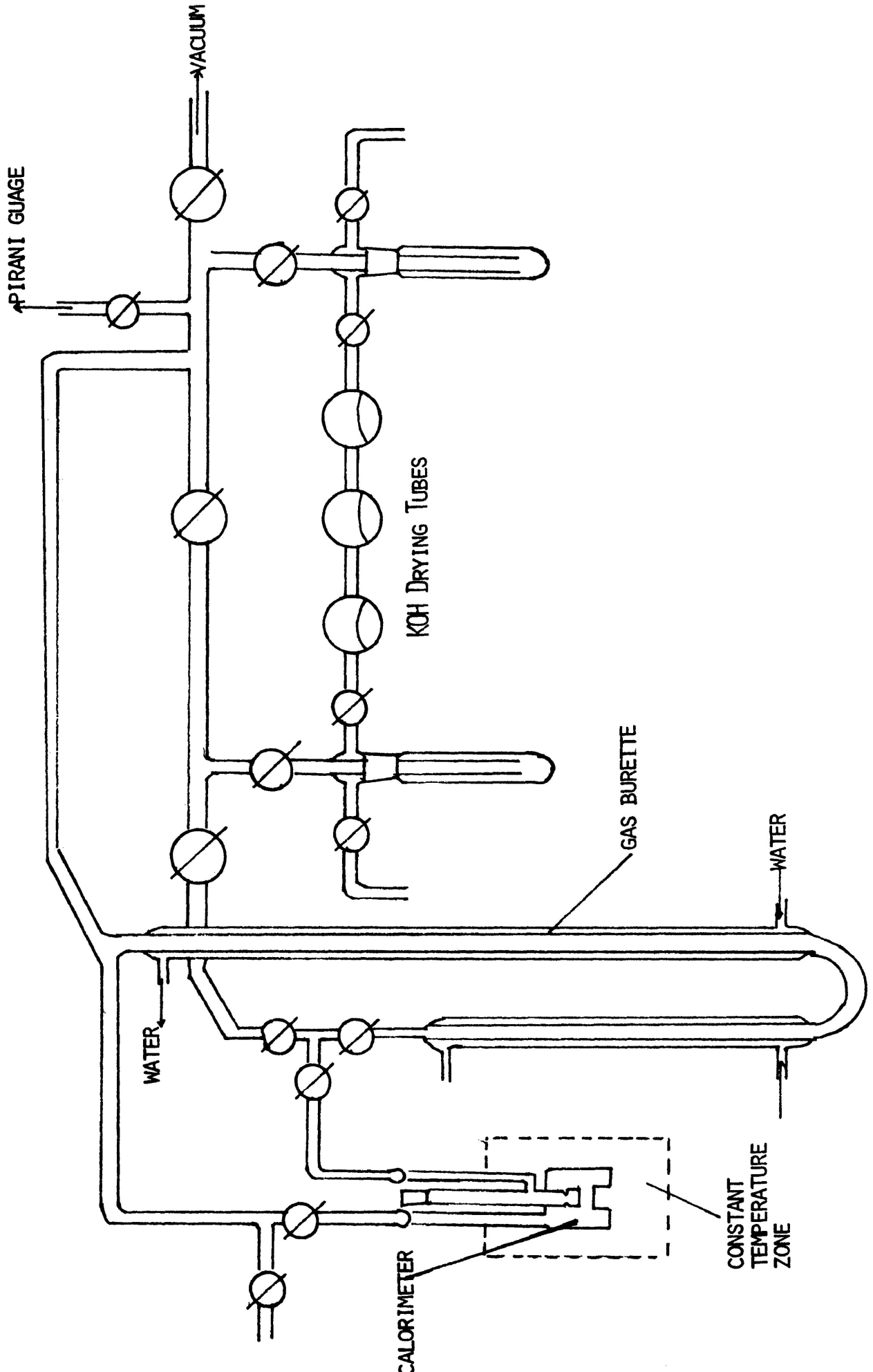


FIGURE 3 CALORIMETER APPARATUS

temperature change was recorded. Normally the 1 mV span and a chart speed of 300 mm/h. was used.

The electrical calibration circuit, Figure 4, consisted of a 6V wet cell battery reduced to 2V using suitable resistors, connected in series to an ammeter (General Electric Co. Ltd.) and the calibration heater. The voltage across the internal calibration heater was measured with a standard voltmeter (0-5V; General Electric Co. Ltd.). The time of calibration was determined by a timer (Leybold) which started immediately on closing the calibration switch. The timer could measure to 0.01 s. and was driven by a synchronous motor operated from a constant voltage supply. At all temperatures the calorimeter was operated adiabatically with its outer jacket evacuated and thus temperature control of the required accuracy was maintained.

In operation, successive doses of adsorbate were admitted to the calorimeter and the process repeated until the desired amount of gas had been adsorbed at equilibrium. The recorder traced the temperature/time plot for each addition. The plot showed a rapid initial rise followed by a slow fall, returning to the base line in about 30 min. The area under this curve was proportional to the quantity of heat evolved in the calorimeter and was determined by reference to the calibration curve. These areas were measured by counting the squares of the chart paper grid under the curves. Calibrations were carried out after each successive dose of gas was adsorbed (60)

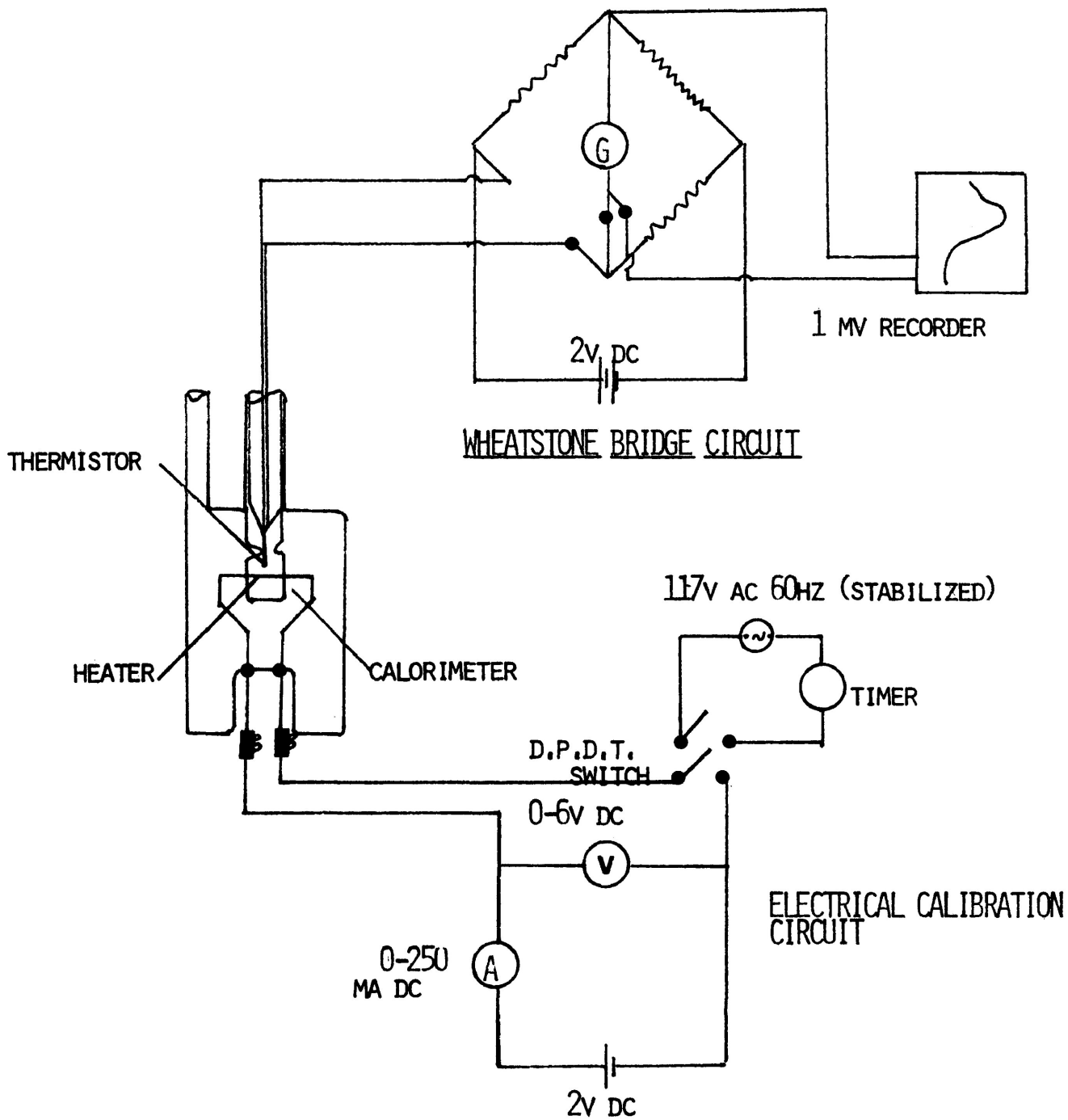


FIGURE 4 CALORIMETER -ELECTRICAL CIRCUITS

and were reproducible to within $\pm 5\%$ with no significant trends. The shapes of the temperature/time calibration traces were almost identical to those given by the gas additions.

A typical temperature/time curve is shown in Figure 5. A cooling correction was applied to the observed temperature rise by extrapolating the linear portion of the cooling curve immediately after the maximum, to a point midway between " t_{\max} " and " t_0 ". This measurement technique was adapted from that used by Smith and Ford (61). The quantity of heat evolved was proportional to the extrapolated peak height and was determined by comparison with the calibration curve.

Calculation of Heats of Adsorption

The method of calculation is described in Table 2.1.

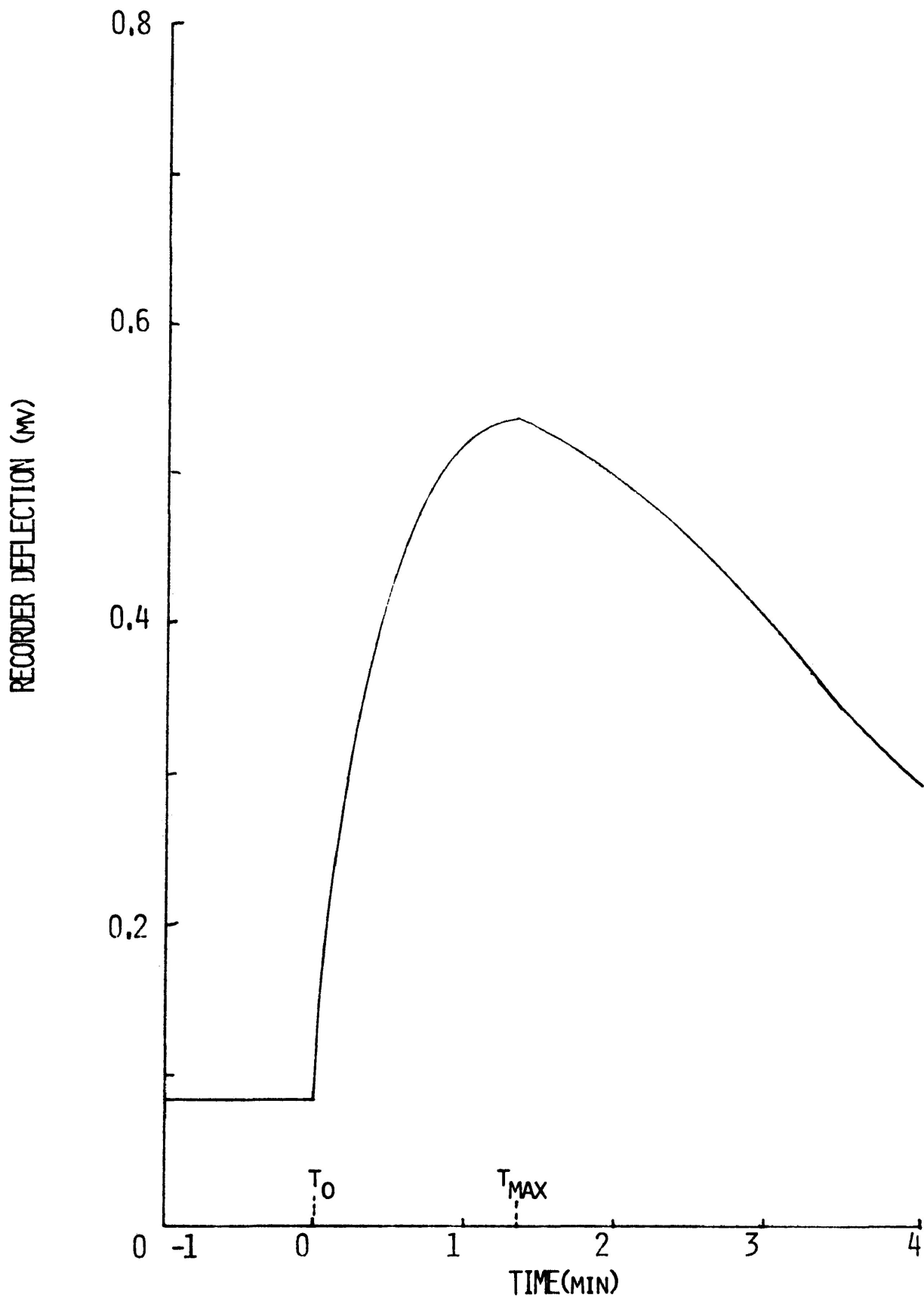


FIGURE 5 A TYPICAL RECORDER TRACE.

Table 2.1.

Calculation of Adiabatic Calorimetric Heats of Adsorption

Data

- 1) Pressure
 - (a) The pressure of gas in burette before admission to calorimeter.
 - (b) The pressure of gas in burette after admission to calorimeter at time " t_{\max} ".
 - (c) The equilibrium pressure.
- 2) Volume (calculated)
 - (a) The volume of gas in burette before admission to calorimeter.
 - (b) The volume of gas in burette after admission to calorimeter at time " t_{\max} ".
 - (c) Volume of gas in burette at equilibrium.
- 3) The volume of gas in calorimeter dead space at experimental temperature T, corrected to S. T. P.
- 4) Weight of sample.
- 5) The surface area of the sample measured using low temperature nitrogen adsorption apparatus.

Calculation

- 1) Calculate the initial volume of gas in the burette before admission to the calorimeter and correct to S. T. P.
- 2) Calculate the volume of gas in the burette at equilibrium and correct to S. T. P.
- 3) Calculate the amount of gas, at S. T. P. that is adsorbed at equilibrium by subtracting the equilibrium volume + the

calorimeter dead space volume from the initial volume.

- 4) To convert the amount adsorbed from dm^3 to $\mu\text{mol m}^{-2}$
divide by the sample weight x the sample area x the molar
volume.
- 5) To find the number of Joules produced for each adsorption,
compare the extrapolated peak areas to the calibration curve.
- 6) To calculate the heat of adsorption multiply Joules
produced x molar volume and divide by the amount adsorbed.

A typical calculation is given in Appendix A.

2.3.2 Calculation of Entropies of Adsorption

Prior to the more recent direct techniques used in studies of surfaces such as field emission microscopy, field-ion microscopy and infrared spectrophotometry, the mobility of an adsorbed species was almost solely determined by using classical and statistical thermodynamic methods (8, 43, 44).

Although there have been several valid criticisms (62, 63) of this approach to the study of mobility, the method can still provide useful information which, in conjunction with data from heats of adsorption etc., can help to elucidate the nature of the adsorbed species.

If the standard state (63) of the gas is one atmosphere, the experimental differential molar entropy of adsorption may be calculated (2) from the equation:

$$\bar{S}_s = S_g - R \ln p - (q_{st}/T) \text{-----(5)}$$

where \bar{S}_s is the differential molar entropy of the adsorbed species at temperature T, and the equilibrium pressure p, S_g is the entropy of the gas, and q_{st} is the isosteric heat of adsorption.

Since the differential heats of adsorption were measured experimentally, equation (5) may be re-written:

$$\bar{S}_s = S_g - R \ln p - (q_d + RT)/T \text{-----(6)}$$

$$\text{since } q_d \approx q_{st} - RT \text{-----(7)}$$

where q_d is the differential heat of adsorption.

Thus, if values of s_g are obtained from the literature (64-66) and the differential heat of adsorption and equilibrium

pressure are known at a variety of surface coverages, the differential molar entropy of adsorption at these coverages can be calculated.

The experimental entropy values thus obtained may be compared with theoretical values calculated for mobile and immobile layers by means of statistical thermodynamics. In the model of immobile adsorption the atoms are firmly bound to the adsorption sites and there are no translational or vibrational motions perpendicular or parallel to the surface. The only entropy of the adsorbed layer present is that of the differential molar configurational entropy (2) which is given by:

$$\bar{S}_{s_c} = -R \ln [\Theta / (1 - \Theta)] \text{ -----(8)}$$

where Θ is the degree of surface coverage.

The other extreme model of adsorption is that of a two-dimensional surface gas in which the degrees of rotation are retained and there is also the possibility of the adsorbed species moving perpendicularly to the surface (7).

In this case, the differential molar entropy of the species is given by:

$$\bar{S}_s = \bar{S}_{2t} + \bar{S}_{rot} + \bar{S}_{vib} \text{ -----(9)}$$

where \bar{S}_{2t} is the two-dimensional translational entropy of the adsorbed species and \bar{S}_{rot} and \bar{S}_{vib} are the corresponding rotational and vibrational entropies.

\bar{S}_{2t} , for an ideal surface gas, may be evaluated (2) from:

$$\bar{S}_{2t} = R \ln MTA + 63.8 \text{ -----(10)}$$

where M is the molecular weight of the gas, and A is the area

occupied per molecule which is a function of the number of moles adsorbed. \bar{S}_{rot} and \bar{S}_{vib} may be obtained from the literature or they can be calculated from the usual statistical thermodynamic equations (67).

The rotational and vibrational contributions to the entropy of ammonia were not calculated from the basic properties of the gas since the calculations are extremely complex and outside the scope of the present study. Thus the gas was assumed to behave in an ideal way and the sum of $(\bar{S}_{rot} + \bar{S}_{vib})$ was obtained by subtracting the translational entropy contribution given by (67):

$$S_t = R \ln M^{3/2} T^{5/2} - 2.30 \text{ ----- (11)}$$

from the total entropy of the ideal three-dimensional gas. Data for the total entropy of ammonia are listed in the literature (64). Since the "mobile" entropy curves are plotted for an ideal two-dimensional gas i.e. a gas that has lost only one degree of translational freedom, the \bar{S}_{rot} and \bar{S}_{vib} contributions will have the same value as that for the three-dimensional gas.

Numerous intermediate models of mobility can be calculated similarly and the results compared with those obtained experimentally.

Examples of the method of calculation of experimental and theoretical entropies for the models of mobile and immobile adsorption, are shown below.

Example. Consider the adsorption of ammonia at 298 K on Californian chrysotile asbestos heat-treated at 150°C.

If the experimental heat of adsorption is 7.47 kJ mol^{-1} at a coverage of $4.60 \mu\text{mol m}^{-2}$ and the corresponding equilibrium pressure is 112.32 Torr (14.94 kPa), and if the entropy of the gas at 298 K is $192.55 \text{ J deg}^{-1} \text{ mol}^{-1}$, then from equation (6) the experimental differential molar entropy \bar{S}_s is:

$$\begin{aligned}\bar{S}_s &= 192.55 - 8.3144 \ln \left(\frac{112.32}{760} \right) - \left[\frac{7470 + 8.3144 \times 298}{298} \right] \\ &= 175.07 \text{ J deg}^{-1} \text{ mol}^{-1}\end{aligned}$$

For the mobile model, the entropy of the adsorbed ammonia is given by equations (9) and (10). The rotational and vibrational contribution is given by equation (11). Thus the sum of the rotational and vibrational components of the entropy at 298 K is given by:

$$\begin{aligned}\bar{S}_{\text{rot}} + \bar{S}_{\text{vib}} &= 192.55 - 8.3144 \ln(17)^{3/2} (298)^{5/2} - 2.3 \\ &= 41.40 \text{ J deg}^{-1} \text{ mol}^{-1}\end{aligned}$$

The value of the differential translational component of the entropy at 298 K and coverage of $4.60 \mu\text{mol m}^{-2}$ is:

$$\begin{aligned}\bar{S}_{2t} &= 8.3144 \left\{ \ln \left[\frac{17 \times 298 \times 10^{-4}}{4.60 \times 10^5 \times 6.023 \times 10^{23}} \right] + 63.8 \right\} \\ &= 114.30 \text{ J deg}^{-1} \text{ mol}^{-1}.\end{aligned}$$

Hence the total differential molar entropy of a perfectly mobile adsorbed layer of ammonia at a coverage of $4.60 \times 10^{-6} \mu\text{mol m}^{-2}$ at 298 K, is given by:

$$\begin{aligned}\bar{S}_{\text{sm}} &= 114.30 + 41.40 \\ &= 155.70 \text{ J deg}^{-1} \text{ mol}^{-1}\end{aligned}$$

The entropy of an immobile adsorbed layer of ammonia is determined from equation (8). The cross-sectional area of an adsorbed ammonia molecule may be calculated using the liquid density, ρ , assuming close-packing, from the equation (68):

$$A = 1.091 \times \frac{M}{\rho N}^{2/3} \times 10^{16}$$

where M is the molecular weight, N is Avogadro's number, and 1.091 is the packing factor. For ammonia at 298 K this equation yields a value of 13.96 \AA^2 (0.14 nm^2), and on the basis of this value a monolayer of ammonia will be formed at 298 K if:

$$\frac{10^{20}}{13.96 \times 6.023 \times 10^{23}} \mu\text{mol m}^{-2} \text{ are adsorbed,}$$

i.e. a surface coverage of $11.94 \mu\text{mol m}^{-2}$ is equivalent to a monolayer.

Thus the differential configurational entropy of adsorbed ammonia at 298 K at a coverage of $4.60 \mu\text{mol m}^{-2}$ can be obtained:

$$\begin{aligned} \bar{s}_{s_c} &= - 8.3144 \ln \left[\frac{4.60/11.94}{1-(4.60/11.94)} \right] \\ &= 4.07 \text{ J deg}^{-1} \text{ mol}^{-1} \end{aligned}$$

Clearly, from these calculations the experimental differential molar entropy of ammonia adsorbed at 298 K at a coverage of $4.60 \mu\text{mol m}^{-2}$ approaches much more closely to the theoretical value for a mobile layer ($155.70 \text{ J deg}^{-1} \text{ mol}^{-1}$) than to the value for an immobile layer ($4.07 \text{ J deg}^{-1} \text{ mol}^{-1}$).

The accuracy of the experimental molar entropy values clearly depends on the accuracy of the measurement of the heat

of adsorption, and also on the validity of the assumption of ideal gas behavior for ammonia at 298 K. In general, the accuracy could not be claimed to be better than $\pm 8 \text{ J deg}^{-1} \text{ mol}^{-1}$ or 5% in this case.

2.3.3. Surface Area and Pore Volume Measurements

Introduction

Low-temperature nitrogen adsorption at 77 K provides one of the best and most widely used methods for the determination of surface areas and pore size distributions of solid adsorbents (69, 70). Relative surface areas can be determined fairly accurately but the method is not absolute (1, 48, 68).

It involves the determination of the volume of gas required to form a monolayer on the surface of the adsorbent. The number of molecules in the layer can be calculated, and if the area of the surface occupied by each molecule is known, the surface area which is available to the nitrogen molecules may be found by a simple calculation.

Brunauer, Emmett and Teller (48) extended the Langmuir theory of unimolecular layer adsorption to account for the multimolecular layer adsorption of gas on a solid surface. The most commonly used form of their equation is:

$$\frac{p}{V(P_0 - p)} = \frac{1}{V_m C} + \frac{(C-1).p}{V_m C.p_0} \text{-----(13)}$$

where V = volume of gas adsorbed at equilibrium pressure p

p_0 = saturation vapour pressure of adsorbate (kPa)

V_m = monolayer volume of gas adsorbed ($\text{dm}^3 \text{ g}^{-1}$)

C = a constant which is related to the heats of adsorption and liquefaction of the gas.

The B. E. T. theory has been criticized on several grounds (71) and it is generally accepted (9) that the theory has little theoretical justification. In general, however, it still remains the most satisfactory mathematical relationship available to describe low-temperature physical adsorption.

A plot of $p/V(p_0-p)$ against p/p_0 gives a straight line of slope $(C-1)/V_m C$ and intercept $1/V_m C$ which enables a value of V_m to be calculated:

$$V_m = \frac{1}{(\text{slope} + \text{intercept})} \text{-----(14)}$$

The equation is normally valid over the range $0.05 < p/p_0 < 0.35$, which is the portion of the isotherm usually associated with completion of the monolayer (48).

The specific surface area may be evaluated from V_m using the equation:

$$S = V_m (N/V) A_0 \text{-----(15)}$$

where V = molar volume ($22,400 \text{ dm}^3$ at N. T. P.)
 N = Avogadro's number ($N = 6.023 \times 10^{23} \text{ molecules mol}^{-1}$)
 A_0 = area occupied per molecule in the adsorbed phase.

The most widely accepted value for the cross-sectional area of the nitrogen molecule is 16.2 \AA^2 ($.16 \text{ nm}^2$) (48), derived from the density of liquid nitrogen; although Livingstone (71) has proposed a value of 15.4 \AA^2 ($.157 \text{ nm}^2$) based on the

van der Waal's constant 'b'.

Therefore, for nitrogen adsorption at 77 K equation (15) becomes:

$$A = 4.36 V_m \text{ ----- (16)}$$

Low-temperature gas adsorption may also be used to obtain information on pore size distribution. Cranston and Inkley (49) established a computational method for pore sizes by a development of the method of Barrett, Joyner and Halenda (72). Either the adsorption or desorption branch of the isotherm may be used to derive the data. The principle criticism of this method is the assumption that the adsorbents contain cylindrical pores with a closed end.

In terms of pore diameters, the equation is:

$$V_{12} = R_{12} (V_{12} - k_{12} \sum_{d_2 + \frac{1}{2}d}^{d_{\max}} \frac{d - 2t_{12}}{d} V_d \Delta d) \text{----- (17)}$$

where V_{12} = volume of pores having radii between r_1 , and r_2 (dm^3)

R_{12} = constant for a given range of diameters

K_{12} = factor to account for the layer of liquid in pores of larger diameter

d_{\max} = diameter of the largest pore

Δd = an increment of pore diameter (nm^2)

$V_d \Delta d$ = volumes of pores having diameters between
($d - \frac{1}{2} \Delta d$) and ($d + \frac{1}{2} \Delta d$)

The other method frequently used for calculating pore size distribution from adsorption isotherms was devised by Dollimore and Heal (50). It has been claimed to be more exact and less tedious than that of Cranston and Inkley (49).

A comparison of the results obtained by the application of the two methods was attempted. Pore size distributions were calculated from data taken from the desorption branch of the isotherms. The calculations were made using a DEC2020 computer. Details of the programme are given in Appendix B and the conclusions regarding the comparison of methods will be noted in the discussion of the results.

Apparatus

A constant volume apparatus similar to that of Joyner (73) was used for the measurements of low-temperature nitrogen isotherms, Figure 6.

The pumping system consisted of a single-stage mercury diffusion pump (Edwards High Vacuum Ltd., type EM2) backed by a rotary oil pump (Edwards High Vacuum Ltd., type ED100). Mercury vapour was prevented from entering the low pressure side of the apparatus by a liquid nitrogen trap. The vacuum was measured with a McLeod gauge and once established, the apparatus held a vacuum of 1.33×10^{-3} kPa for one week. Three taps were arranged so that small quantities of nitrogen could be admitted as required.

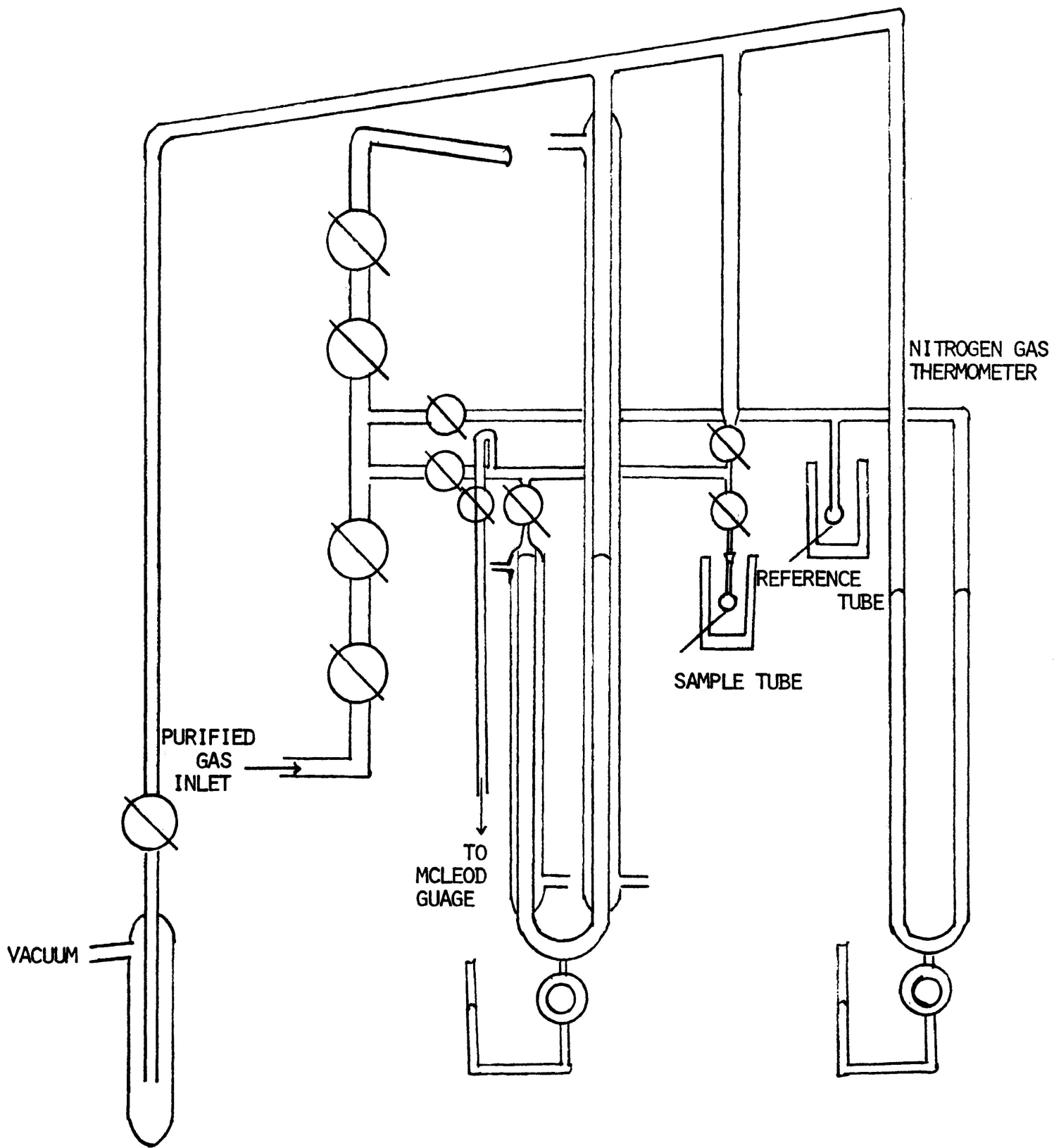


FIGURE 6 LOW-TEMPERATURE NITROGEN ADSORPTION APPARATUS

The measurement section of the apparatus contained a combined gas burette and manometer which was read using a cathetometer (± 0.001 cm.). The burette was thermostatted and precalibrated before use (one cm. movement on the cathetometer corresponded to 0.86 dm^3 of gas). The zero level on the burette was maintained by a mercury reservoir.

The apparatus "dead space" between the gas burette and sample bulb was minimized by using small taps and connecting tubing, and by containing the sample in a small round-bottomed flask with a long neck. The "dead space" (23.22 dm^3) and sample tube volumes were determined, in separate calibration experiments, with helium. The volume of the sample tube up to the fixed mark was determined by filling with mercury at room temperature and then weighing the mercury added, to determine the volume of the tube below liquid nitrogen.

All materials used were accurately weighed into the sample tube and then connected to the apparatus. The samples were then outgassed at 1.33×10^{-4} kPa at 100°C for 1 h. Care was taken to avoid sample entrainment. The sample was then cooled to liquid nitrogen temperature (77 K) and the isotherm measured by admitting successive doses of nitrogen to the sample. The results were calculated as described in Table 2.2. Computation was made with a DEC2020 computer. Details of the programme are outlined in Appendix B.

2.3.4. Mass Spectrometry

Analysis of the ammonia after distillation, before and

after use in adsorption experiments was performed on a Hitachi-Perkin Elmer RMU-7 mass spectrometer.

2.3.5. Electron Microscopy

Although the analysis of pore sizes by low-temperature nitrogen adsorption is valuable, the accuracy of the technique is limited by the validity of the pore model chosen. Direct observation using the electron microscope does not involve these assumptions.

Electron micrographs were made using a transmission electron microscope, Philips Model EM300. Samples were dispersed in n-butanol onto carbon form/var grids. Micrographs were taken at low beam intensities to prevent beam damage.

Table 2.2

Calculation of Low-Temperature Adsorption/Desorption Isotherms

- 1) Pressure - The equilibrium pressure measured at different points during the isotherm.
- 2) Calculate the volume of gas in the burette before admission to the sample tube.
- 3) Calculate the volume of gas in the burette after admission to the sample tube but above liquid nitrogen.
- 4) Calculate the volume of gas below the level of liquid nitrogen and above the sample.
- 5) To find the amount adsorbed subtract (3) + (4) from (2).
- 6) For all samples after the first, the amount of gas in the sample tube above and below liquid nitrogen must be added to (2) before subtracting (3) and (4).
- 7) To find the volume adsorbed in $\text{dm}^3 \text{g}^{-1}$, the answer in (5) is divided by the weight of the sample.
- 8) To find p/p_0 the pressure from (1) is divided by the saturation pressure.

Part of a typical calculation is given in Appendix A

CHAPTER III

3. Results

3.1. Introduction

The adsorption of ammonia was studied on Californian and Quebec chrysotiles using the technique described in Section 2.3. Changes in the adsorption behaviour caused by heat treatment of the materials were also examined. The physical effects of these treatments were analyzed by low-temperature nitrogen adsorption and by electron microscopy. The adsorption of ammonia on Californian chrysotile treated with water and sodium nitrate was also briefly studied.

3.2. Adsorption/Desorption of Ammonia on Californian Chrysotile at 273 and 298 K

3.2.1. Calorimeter Experiments

The calorimeter was operated adiabatically to determine the heat of adsorption at 273 and 298 K for ammonia on Californian chrysotile heat-treated at 150, 300, 500 and 700°C, Figures 7 and 8. These experiments were performed to obtain comparative data on the "limiting" heats given by the range of test samples at various operating temperatures. In the present context "limiting" is used as a convenient description for the final heat value determined for the adsorption process. In most runs the actual "limiting" heat was closely approached rather than clearly attained in a strict thermodynamic sense.

An approximate figure for the degree of surface coverage

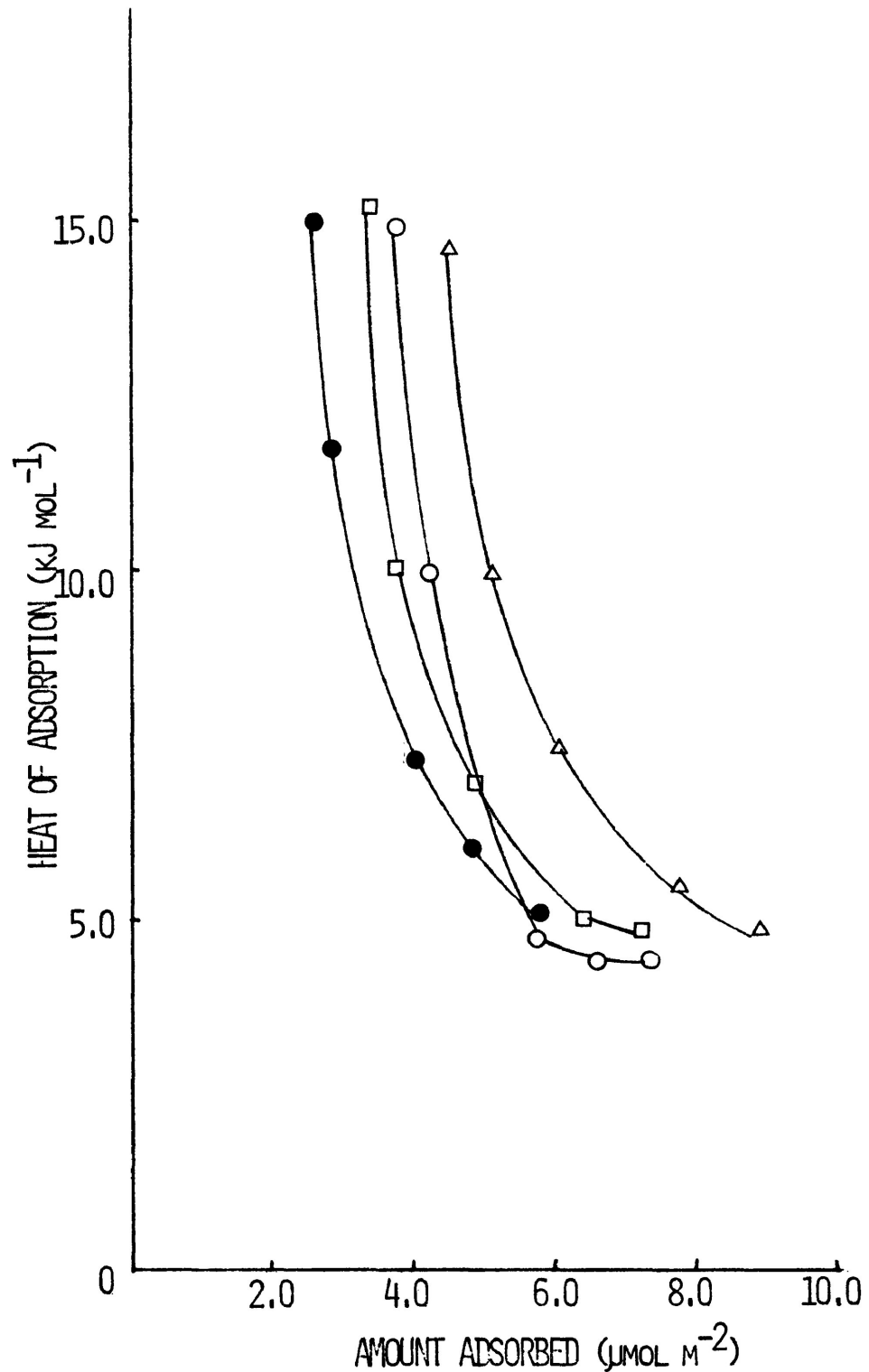


FIGURE 7 VARIATION OF HEAT OF ADSORPTION WITH AMOUNT OF AMMONIA ADSORBED ON HEAT-TREATED CALIFORNIAN CHRYSOTILE. HEAT TREATMENT AT 150 (○), 300 (△), 500 (□), AND 700 (●)°C. EXPERIMENTS AT 273K.

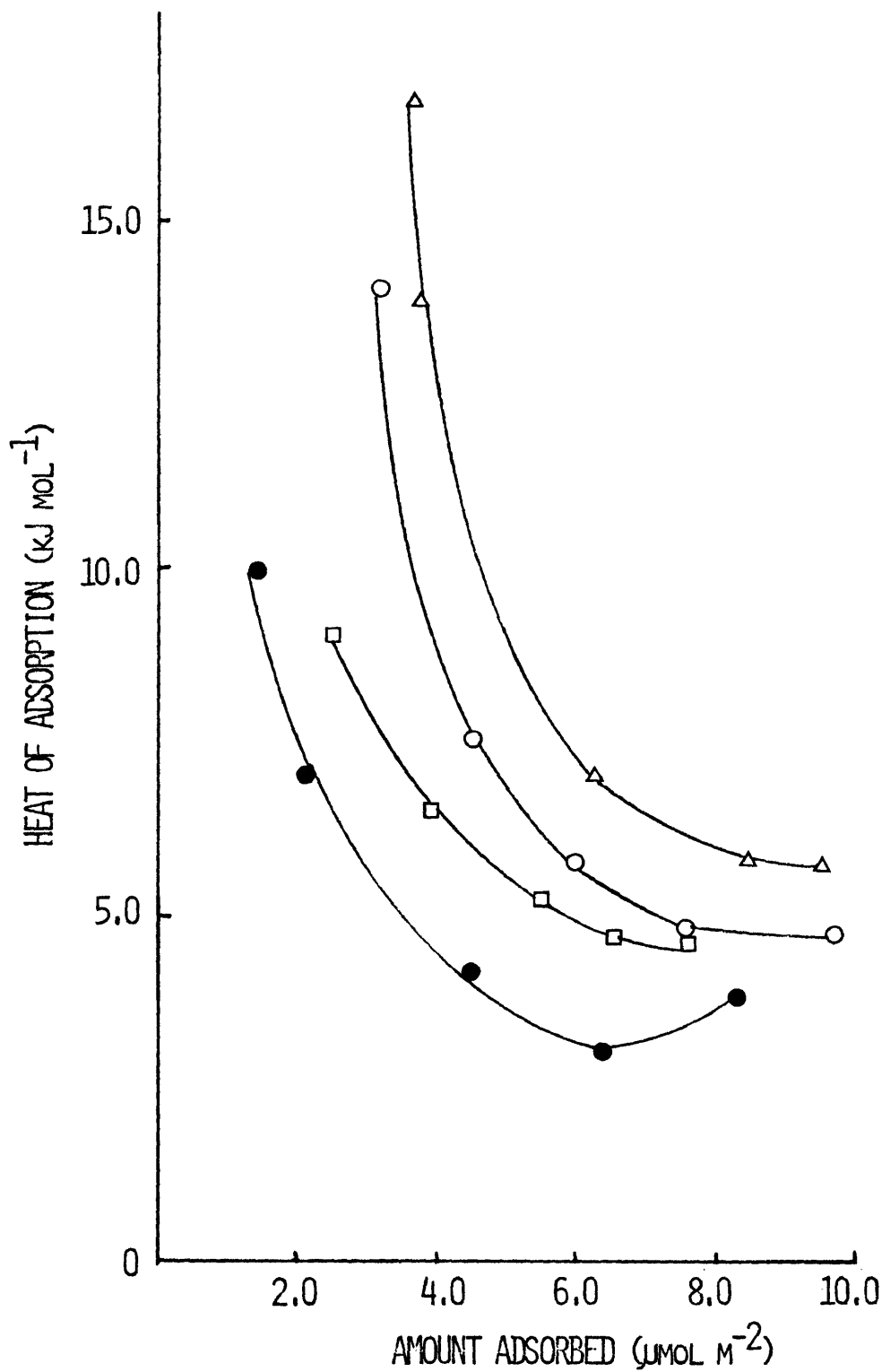


FIGURE 8 VARIATION OF HEAT OF ADSORPTION OF AMMONIA WITH AMOUNT ADSORBED ON HEAT-TREATED CALIFORNIAN CHRYSOTILE. HEAT TREATMENT AT 150(○), 300 (△), 500 (□), AND 700 (●)°C. EXPERIMENTS AT 298K.

was calculated assuming close-packing in the monolayer and a cross-sectional area of 13.86 \AA^2 ($.14 \text{ nm}^2$) for an adsorbed ammonia molecule at 298 K. With these assumptions, $8.0 \text{ } \mu\text{mol m}^2$ was shown to be approximately equivalent to seventy percent of a monolayer at that temperature (Section 2.3.2.).

In all cases the first addition of gas produced the highest heat of adsorption for a given heat treatment. Subsequently, there was a tendency for the heats to follow somewhat similar patterns on all of the adsorbents. However, the "limiting" values differed considerably depending on the activation temperature.

The heat curves determined at 273 K showed that the samples treated at 150 and 300°C exhibited the lowest limiting values in the region of 4.5 kJ mol^{-1} at surface coverages of 6.5 and $8.5 \text{ } \mu\text{mol m}^{-2}$, respectively. The samples treated at 500 and 700°C gave higher "limiting" values of approximately 5.0 kJ mol^{-1} at $6.0 \text{ } \mu\text{mol m}^{-2}$ for both samples.

The heat curves determined at 298 K showed some interesting differences. The limiting value for the sample treated at 300°C was 5.7 kJ mol^{-1} at $8.0 \text{ } \mu\text{mol m}^{-2}$. The curves for the samples treated at 150 and 500°C were "limited" at 4.5 kJ mol^{-1} for $7.5 \text{ } \mu\text{mol m}^{-2}$ surface coverage. The sample treated at 700°C indicated that a different adsorbate/adsorbent phenomenon was taking place with "limiting" heats of 3.2 kJ mol^{-1} at a surface coverage of $6.0 \text{ } \mu\text{mol m}^{-2}$. For all the heat-treated adsorbents the heat curves determined at 298 K showed a tendency to rise

after the onset of what is usually regarded as the "limiting" value. The phenomenon will be discussed later.

It should also be noted that at both operating temperatures the curves for the 150 and 300°C samples seem "out of order" in that results obtained from the sample heat-treated at the lower temperature would be expected to lie above that of the sample heat-treated at a higher temperature. The 300°C sample had generally identical or higher "limiting" heat values at higher surface coverages than those for the 150°C sample. It may be noted also that, in general, the "limiting" heats of all samples at 298 K were similar to those at 273 K except for the 700°C sample where the "limiting" heat was considerably less (i.e. 3.2 kJ mol⁻¹) at 298 K than at 273 K (i.e. 5.0 kJ mol⁻¹).

3.2.2 Entropy Calculations

The variation of the experimental differential molar entropy with surface coverage for the adsorption of ammonia at 273 and 298 K on the 150, 300, 500 and 700°C Californian samples is shown in Figures 9 and 10. At low surface coverages the entropies were small but increased rapidly with the adsorbed amount before levelling out. The values followed a path converse to that of the heats of adsorption. The variation of the operating temperature from 273 to 298 K altered the position of the entropy curves. When the experiments were carried out at 273 K the 150 and 300°C samples levelled out 5 J deg⁻¹ mol⁻¹

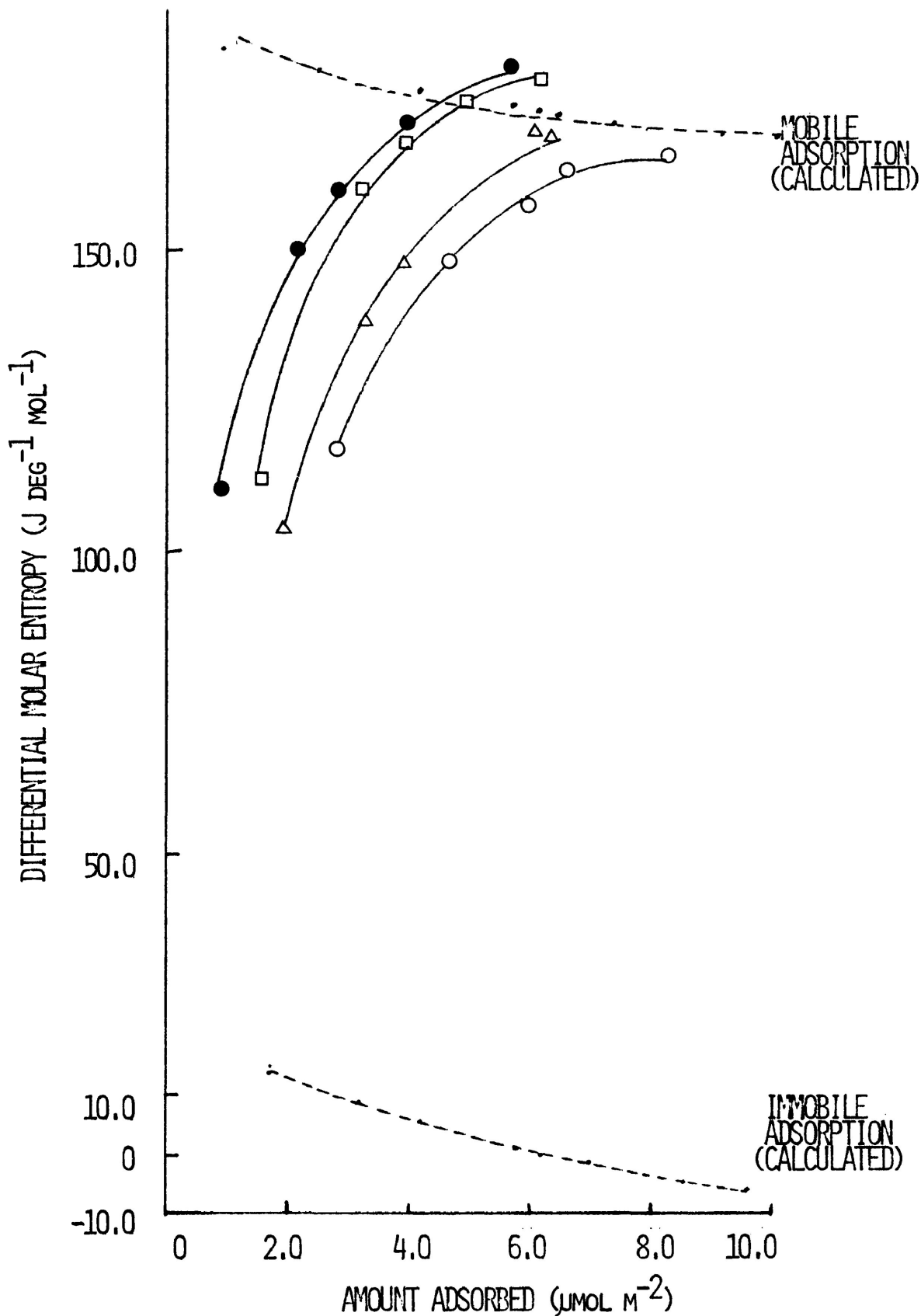


FIGURE 9 EXPERIMENTAL DIFFERENTIAL MOLAR ENTROPIES OF AMMONIA ADSORBED AT 273K ON CALIFORNIAN CHRYSOTILE HEAT-TREATED AT 150 (O), 300 (Δ), 500 (□), AND 700 (●)°C.

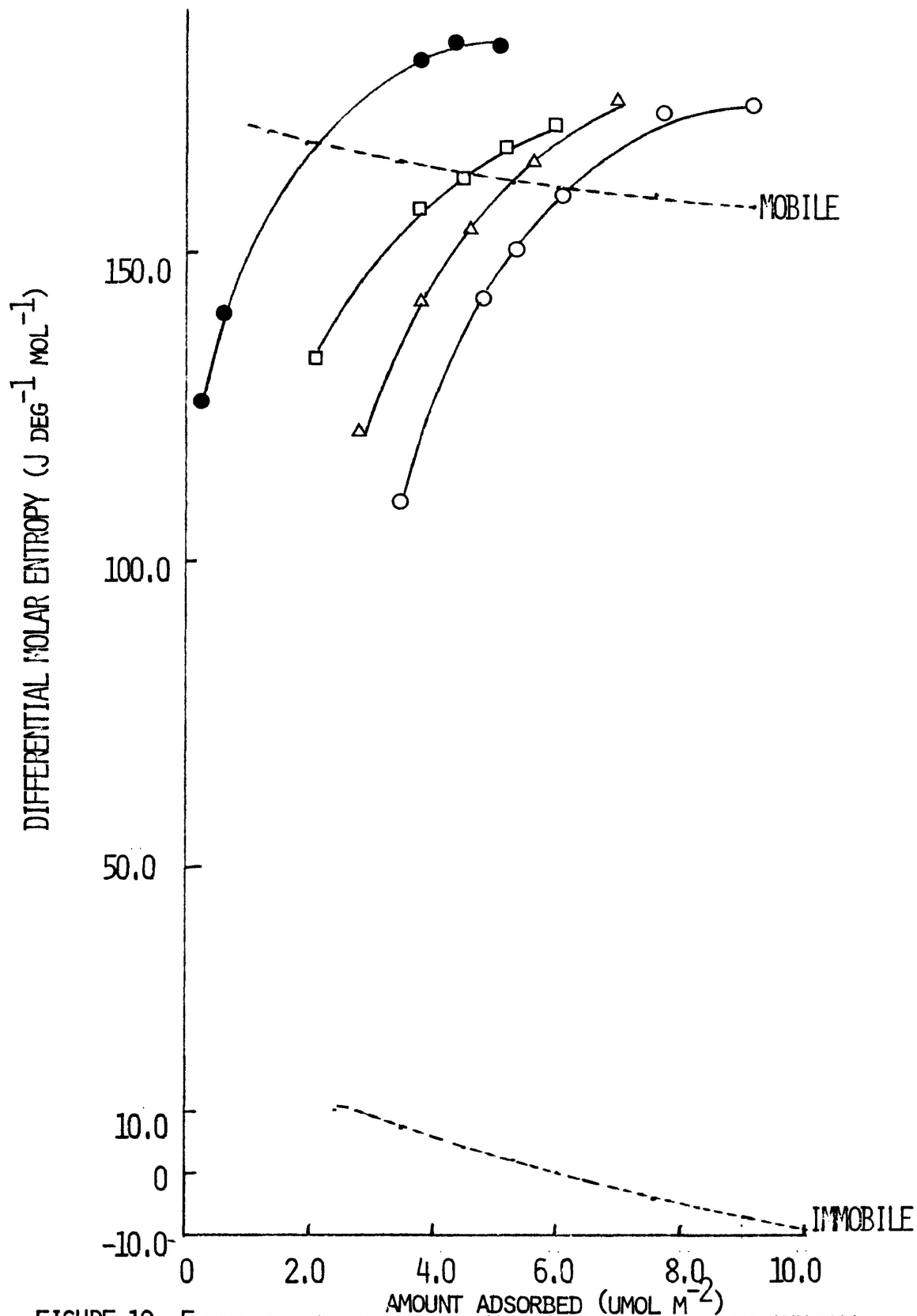


FIGURE 10 EXPERIMENTAL DIFFERENTIAL MOLAR ENTROPIES OF AMMONIA ADSORBED AT 298K ON CALIFORNIAN CHRYOTILE HEAT-TREATED AT 150 (○), 300 (△), 500 (□), AND 700 (●)°C.

below, and coincident with, the model calculated for mobile adsorption, respectively. The 500 and 700°C chrysotiles both levelled out at approximately $10 \text{ J deg}^{-1} \text{ mol}^{-1}$ above the values for the mobile adsorption model. Conversely, at 298 K, the experimental differential molar entropy for all the heat-treated samples levelled out above the curve for the mobile adsorption model - the 150, 300 and 500°C chrysotiles 15 to 19 $\text{J deg}^{-1} \text{ mol}^{-1}$ above; the 700°C sample 23 $\text{J deg}^{-1} \text{ mol}^{-1}$ above and at a surface coverage $2 \mu\text{mol m}^{-2}$ lower than that for the sample studied at 273 K.

3.2.3. Adsorption/Desorption Isotherms

The adsorption/desorption isotherms of ammonia at 273 and 298 K on Californian chrysotile heat-treated at 150, 300, 500 and 700°C are shown in Figures 11 and 12. At both operating temperatures, it can be noted from the desorption isotherms that adsorption was irreversible to some extent. The adsorption behaviour of certain samples was changed by varying the operating temperature. Figure 11 indicates that the adsorption capacity was identical at lower pressures of ammonia ($< 10 \text{ kPa}$) for the 150 and 300°C samples but decreased in amount for the 300°C sample at higher pressures. Further heating to 500°C lowered the adsorption capacity overall while treatment at 700°C drastically affected the pattern and extent of adsorption. Figure 12 which shows results for experiments at 298 K, indicates that the initial adsorption at low pressures of ammonia ($< 20 \text{ kPa}$) was not greatly affected by heat treatment; the

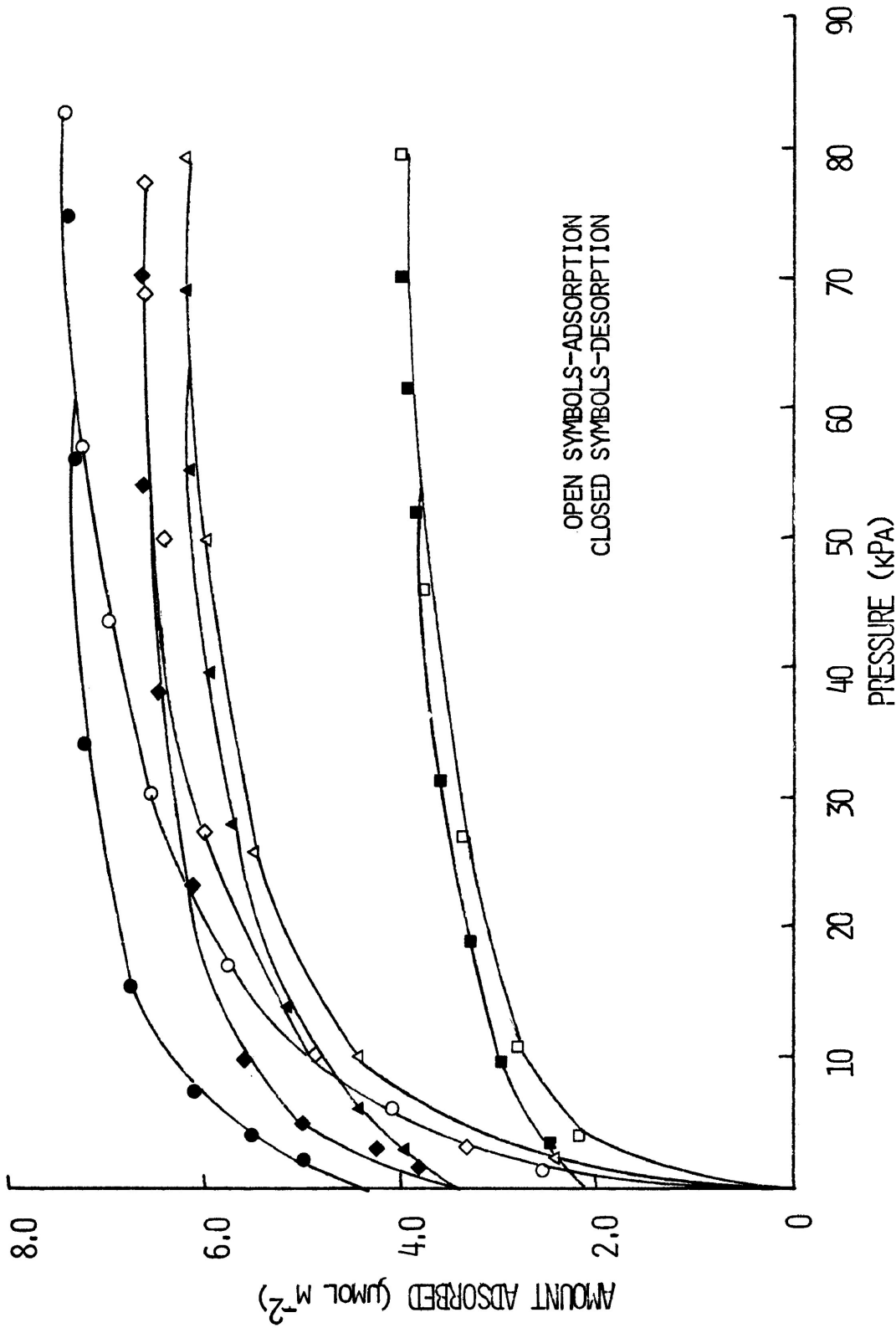


FIGURE 11 ADSORPTION/DESORPTION ISOTHERMS FOR AMMONIA AT 273K ON HEAT-TREATED CALIFORNIAN CHRYSOTILE. HEAT TREATMENT AT 150 (○), 300 (◇), 500 (△), AND 700 (□)°C.

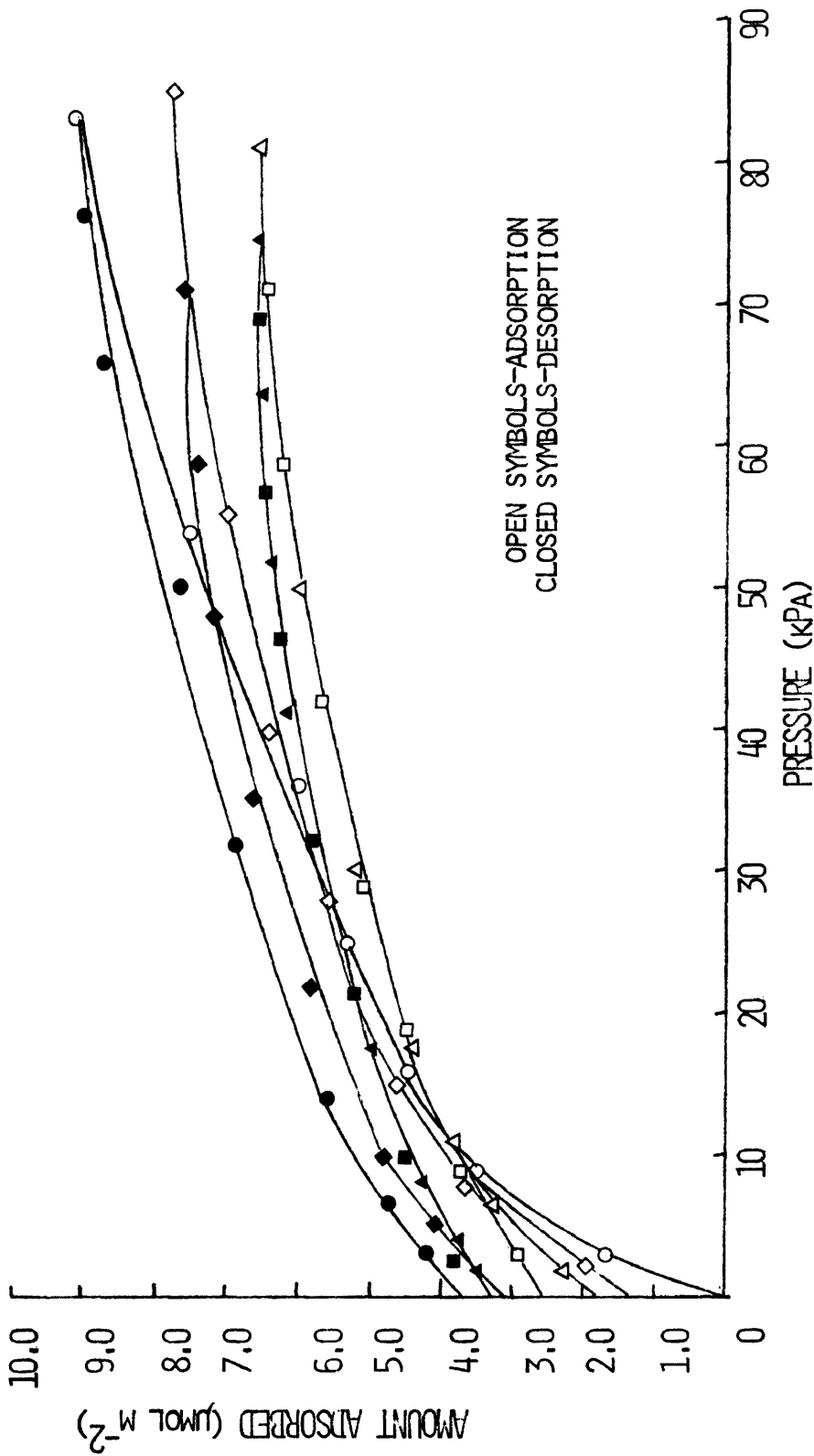


FIGURE 12 ADSORPTION/DESORPTION ISOTHERMS FOR AMMONIA AT 298K ON HEAT-TREATED CALIFORNIAN CHRYSOTILE. HEAT TREATMENT AT 150 (○), 300 (◇), 500 (△), AND 700 (□)°C.

adsorption isotherms diverging significantly only when pressures exceeded 50 kPa. In this case, the adsorption capacity at higher pressures was greatest for the 150°C sample followed by the 300°C sample. The isotherms for the 500 and 700°C samples were coincident over their entire range.

As indicated in Section 3.2.1, a monolayer appeared to be formed when $11.94 \mu\text{mol m}^{-2}$ had been adsorbed. If the assumptions involved in the calculation were correct then from the amount of gas adsorbed at the maximum pressures it may be deduced that fifty to seventy-five percent of a monolayer had formed.

Table 3.1 summarizes the principal characteristics for ammonia adsorbed on each of the heat-treated samples at the two temperatures used for isotherm evaluation.

3.3 A Comparison of the Sorption Characteristics at 266, 273, 288, 298 and 308 K of Ammonia on Californian Chrysotile Heat-Treated at 500°C

3.3.1. Calorimeter Experiments

The calorimeter was operated adiabatically to determine the heat of adsorption at 266, 273, 288, 298 and 308 K for ammonia on Californian chrysotile heat-treated at 500°C, Figure 13.

The shape of the heat curves determined at the various operating temperatures was very similar, falling rapidly from a high initial point to a "limiting" value. The heat curves

Table 3.1.

Surface Areas, Adsorption Capacities, "Limiting" Heats and Entropies of Adsorption of Ammonia on Heat-Treated Californian Chrysotile

Isotherm	Temperature	Surface Area	Adsorption	"Limiting"	"Limiting"
(K)	of Heat	(m ² g ⁻¹)	Capacity at	Heat of	Entropy at
	Treatment (°C)		30 kPa	Adsorption	7.0 $\mu\text{mol m}^{-2}$
			($\mu\text{mol m}^{-2}$)	(kJ mol ⁻¹)	(J deg ⁻¹
					mol ⁻¹)
273	150	60	6.5	4.5	165
"	300	60	6.0	4.5	172
"	500	60	5.5	4.8	178
"	700	62	3.5	5.0	183
298	150	60	5.8	4.5	166
"	300	60	5.8	5.7	175
"	500	60	5.2	4.5	175
"	700	62	5.2	3.2	183

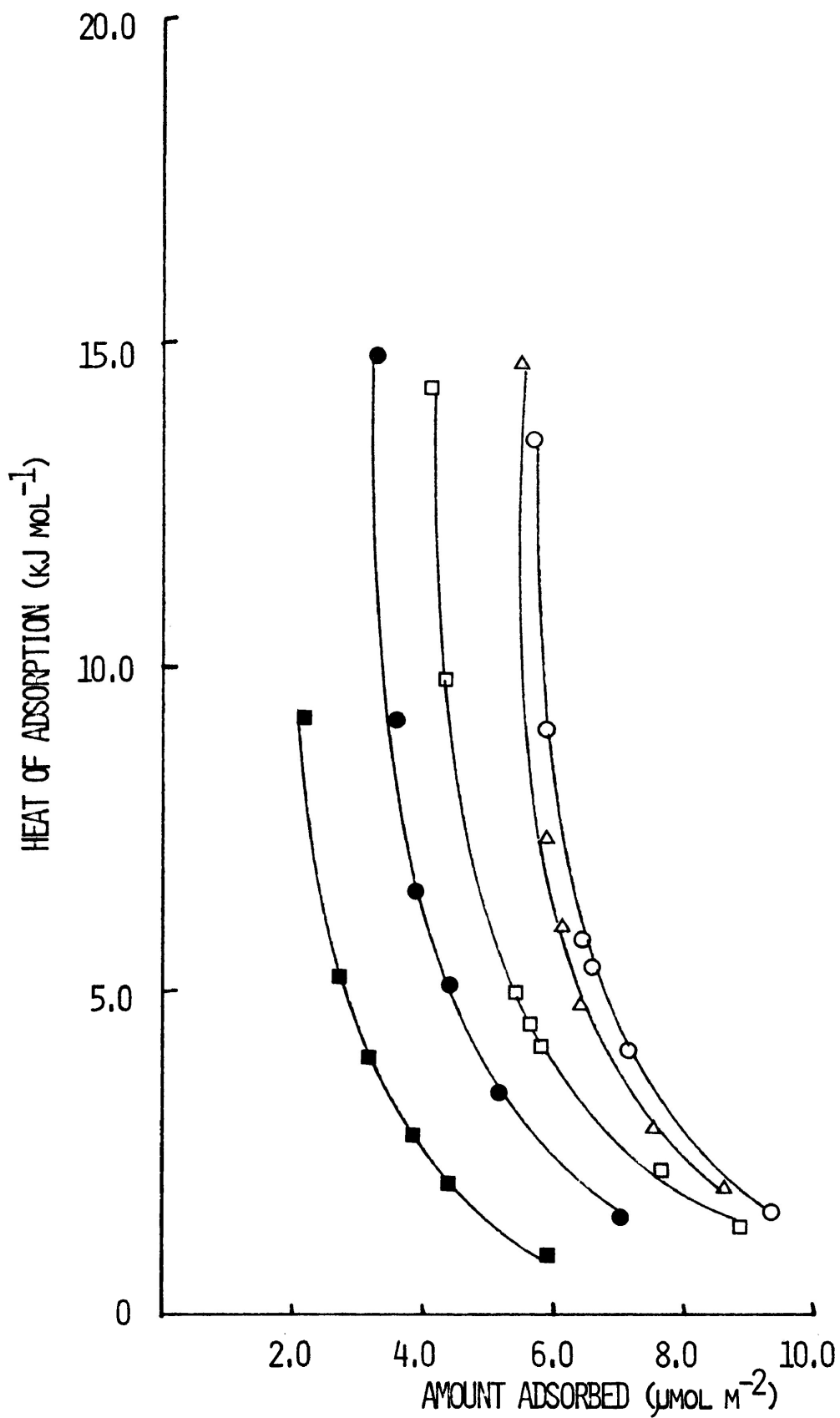


FIGURE 13 VARIATION OF HEAT OF ADSORPTION WITH AMOUNT OF AMMONIA ADSORBED ON CALIFORNIAN CHRYSOTILE HEAT-TREATED AT 500 C. ○, 266; △, 273; □, 288; ●, 298; ■, 308K.

for the experiments performed at 266, 273, 288, 298 and 308 K all tended to a "limiting" value of approximately 1.0 kJ mol^{-1} . It should be stressed again that "limiting" is a term of convenience and is not accurate in the true sense of the word. Actually we look at trends toward a fairly steady value which does not reach infinity.

The placement of the heat curves was directly related to the operating temperature. For example, the curve corresponding to experiments at 266 K indicated that the highest heat value occurred at a surface coverage of $5.7 \mu\text{mol m}^{-2}$; whereas the curve for the 308 K experiments was at its highest recorded point at a coverage of $2.0 \mu\text{mol m}^{-2}$ and reached its "limiting" value at $6.0 \mu\text{mol m}^{-2}$. The remaining three curves occurred, in order, between these two described.

3.3.2 Entropy Calculations

The variation of the experimental differential molar entropy with surface coverage for the adsorption of ammonia at 266, 273, 288, 298 and 308 K on Californian chrysotile heat-treated at 500°C is shown in Figure 14.

An interesting pattern can be noted in the entropy curves. The curve for the experiment at 266 K progressed upward from an initial low value of $120 \text{ J deg}^{-1} \text{ mol}^{-1}$ at $4.9 \mu\text{mol m}^{-2}$ to a "limiting" value corresponding closely to the curve calculated for a fully mobile adsorbed phase. Conversely, the entropy curve for the experiment at 308 K shows

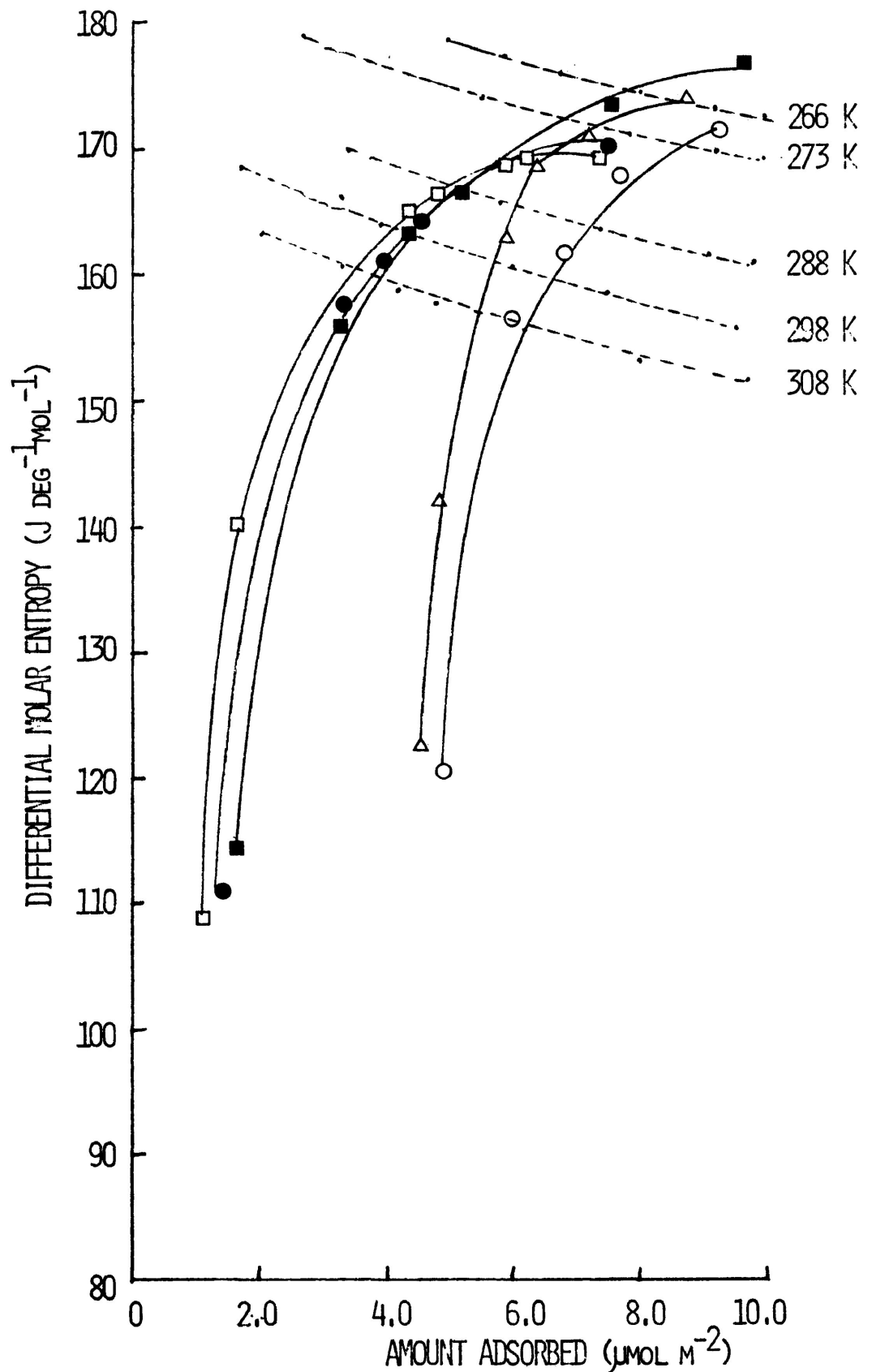


FIGURE 14 EXPERIMENTAL DIFFERENTIAL MOLAR ENTROPIES OF ADSORPTION FOR AMMONIA AT 266 (○), 273 (△), 288 (□), 298 (●), AND 308 (■) K ON CALIFORNIAN CHRYSOTILE HEAT-TREATED AT 500°C. -----"MOBILE" ENTROPY CURVES

an initial value of $108 \text{ J deg}^{-1} \text{ mol}^{-1}$ at $1.10 \mu\text{mol m}^{-2}$ and progresses up to a "limiting" value of $177 \text{ J deg}^{-1} \text{ mol}^{-1}$ at $9.7 \mu\text{mol m}^{-2}$ which is $25 \text{ J deg}^{-1} \text{ mol}^{-1}$ higher than that expected from the mobile adsorption model for 308 K. The other three experiments performed at temperatures between these two extremes gave results falling between the above examples but, in each case, as the operating temperature was increased, the difference between the experimental differential entropy and that for the mobile phase became more pronounced.

3.3.3. Adsorption/Desorption Isotherms

The adsorption/desorption isotherms of ammonia at 266, 273, 288, 298 and 308 K on Californian chrysotile heat-treated at 500°C are shown in Figure 15. In general, the curves showed a slight decrease of amounts adsorbed, with increased operating temperature. The corresponding desorption isotherms again showed incomplete desorption, i. e. a certain amount of irreversible adsorption. The only exception was the isotherm measured at 308 K. In general, the adsorption isotherms for the lower temperature experiments tended to level out at approximately $6.5 \mu\text{mol m}^{-2}$ at an ammonia pressure of 80 kPa but the 308 K isotherm continued to increase from a value of $9.5 \mu\text{mol m}^{-2}$ at the same pressure of ammonia. The 308 K adsorption isotherm showed the expected decrease in adsorption at low pressures of ammonia ($< 17 \text{ kPa}$) after which it showed an unexpected increase in adsorption capacity to the above value.

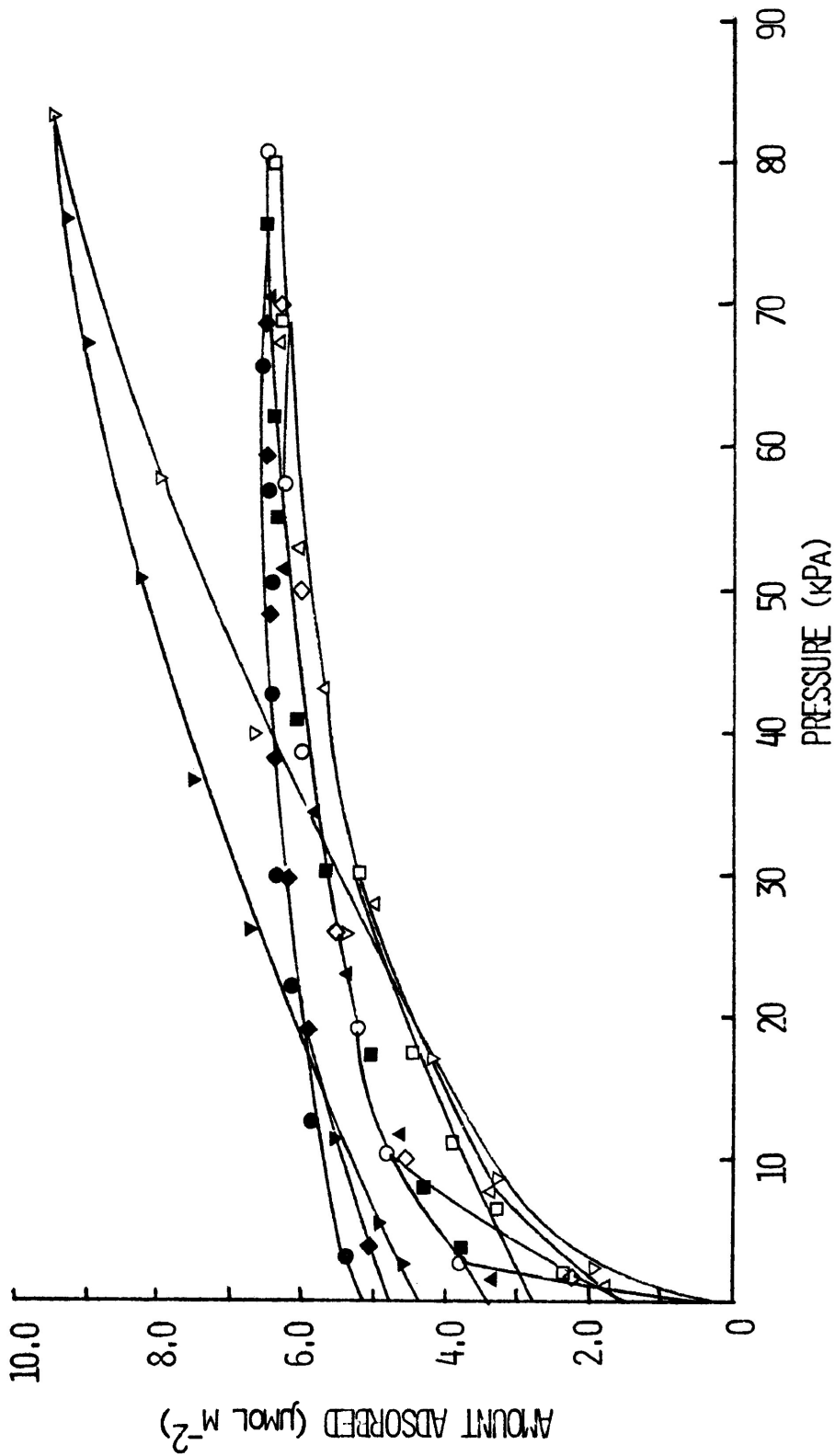


FIGURE 15 ADSORPTION/DESORPTION ISOTHERMS FOR AMMONIA ON CALIFORNIAN CHRYSOTILE HEAT-TREATED AT 500°C. EXPERIMENTAL TEMPERATURES 266 (○), 273 (◇), 288 (△), 298 (◻), AND 308 (▽) K.

Despite this irregularity, the desorption isotherm at 308 K indicated the same degree of irreversible adsorption.

3.4 Adsorption/Desorption of Ammonia on Quebec Chrysotile at 273 and 298 K

3.4.1. Calorimeter Experiments

Heats of adsorption were determined at 273 and 298 K for ammonia on Quebec chrysotile heat-treated at 150, 300, 500 and 700°C, Figures 16 and 17. Heats were obtained over a range of surface coverage from 1.0 to 7.0 $\mu\text{mol m}^{-2}$. At 298 K, monolayer coverage approximated to 11.94 $\mu\text{mol m}^{-2}$.

The heat curves were similar in shape to those for Californian chrysotile, Figures 7 and 8. In general, the "limiting" heats were reached at a slightly lower surface coverage and were approximately 1 kJ mol^{-1} higher than those given by the Californian samples. At 273 K the heat curves showed an orderly progression in their placement from the 150 to the 700°C samples, i. e. the "limiting" heat was attained at the highest surface coverage, 7.0 $\mu\text{mol m}^{-2}$, for the 150°C sample and the lowest, 4.5 $\mu\text{mol m}^{-2}$, for the 700°C sample. The 150 and 300°C samples gave approximately the same "limiting" heat, 3.2 kJ mol^{-1} , while the 500 and 700°C samples reached their limits at a slightly higher value, 3.6 kJ mol^{-1} .

The same progression in the placement of the heat curves was observed for runs at 298 K as in the 273 K experiments but, in general, the "limiting" heats were slightly lower.

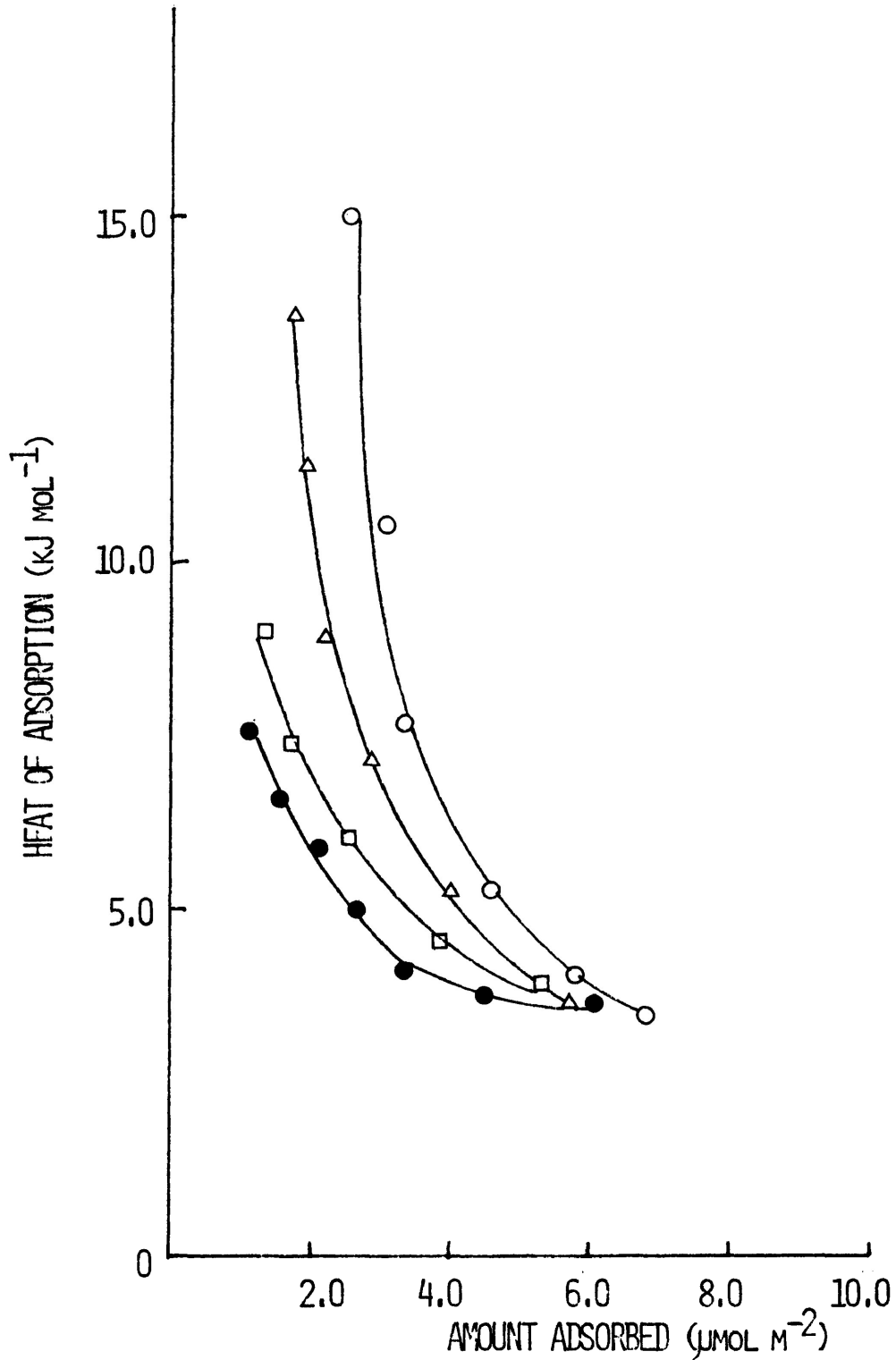


FIGURE 16 VARIATION OF HEAT OF ADSORPTION OF AMMONIA WITH AMOUNT ADSORBED ON HEAT-TREATED QUEBEC CHRYSOTILE. HEAT TREATMENT AT 150 (○), 300 (△), 500 (□), AND 700 (●)°C. EXPERIMENTS AT 273K.

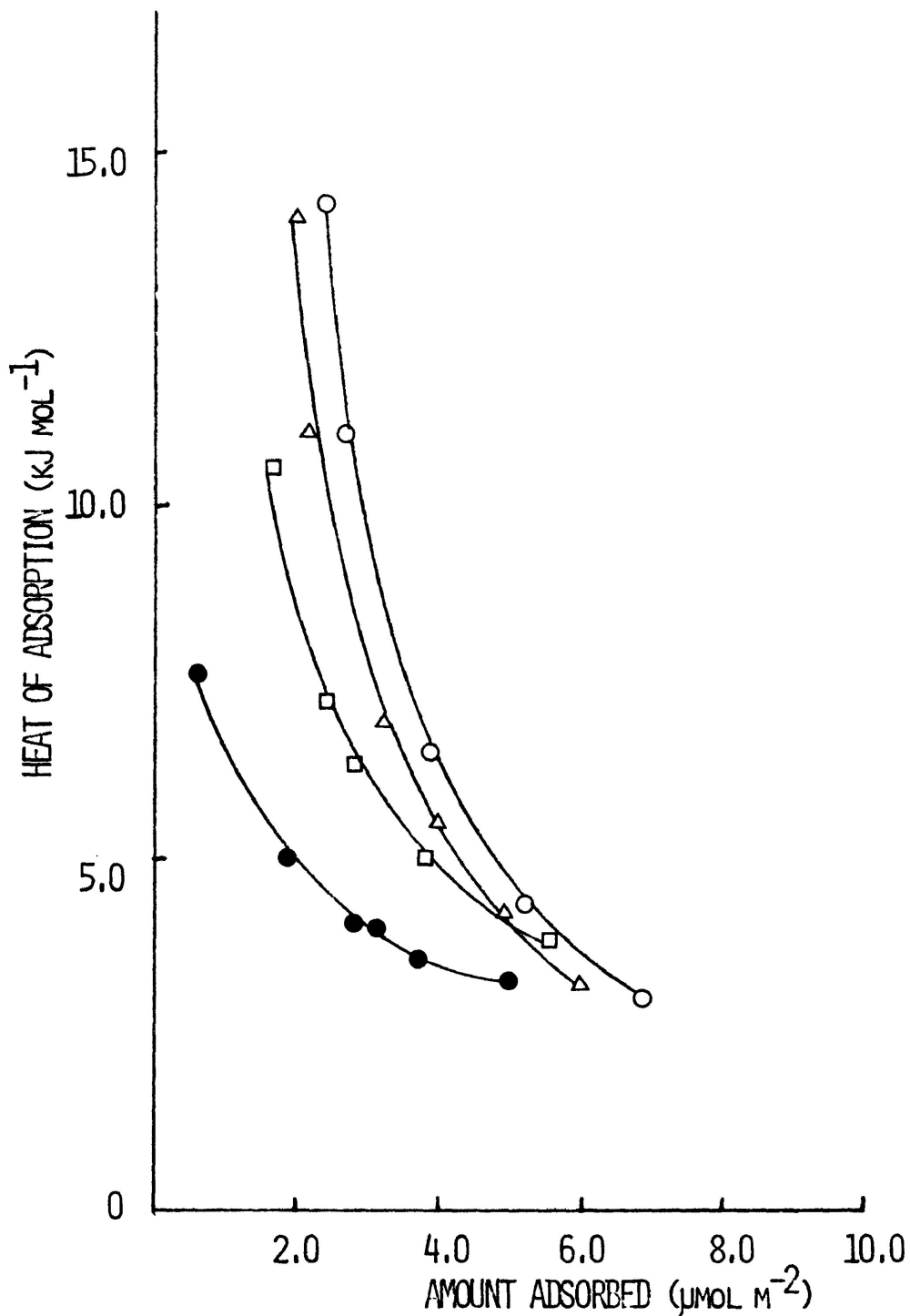


FIGURE 17 VARIATION OF HEAT OF ADSORPTION OF AMMONIA WITH AMOUNT ADSORBED ON HEAT-TREATED QUEBEC CHRYSOTILE. HEAT TREATMENT AT 150 (○), 300 (△), 500 (□), AND 700 (●)°C. EXPERIMENTS AT 298 K.

The 150 and 300°C samples gave "limiting" values of about 2.5 kJ mol⁻¹ while the 500°C sample levelled out at about 3.5 kJ mol⁻¹, only slightly higher than the 700°C sample at 3.2 kJ mol⁻¹.

3.4.2 Entropy Calculations

Figures 18 and 19 show the variation of the experimental differential molar entropy as a function of surface coverage for the adsorption of ammonia at 273 and 298 K on Quebec chrysotile heat-treated at 150, 300, 500 and 700°C.

The sets of entropy curves for the 273 and 298 K experiments had very similar shapes and "limiting" values. The main difference lay in the lateral placement of the curves along the axis of surface coverage. The 298 K curves were placed, in general, at a degree of surface coverage 1 μmol m⁻² lower than their counterparts at 273 K. For both sets of experiments there seemed to be two distinct surfaces, one for the 150 and 300°C samples and the other for the 500 and 700°C samples. In each case the two sets of curves were quite separate from each other. All the entropy curves appeared to "limit" themselves at values of 30 to 40 J deg⁻¹ mol⁻¹ above the curve corresponding to the model for a mobile adsorbed phase. The 150 and 300°C curves appeared to level out about 10 J deg⁻¹ mol⁻¹ lower than those for the 500 and 700°C materials.

3.4.3. Adsorption/Desorption Isotherms

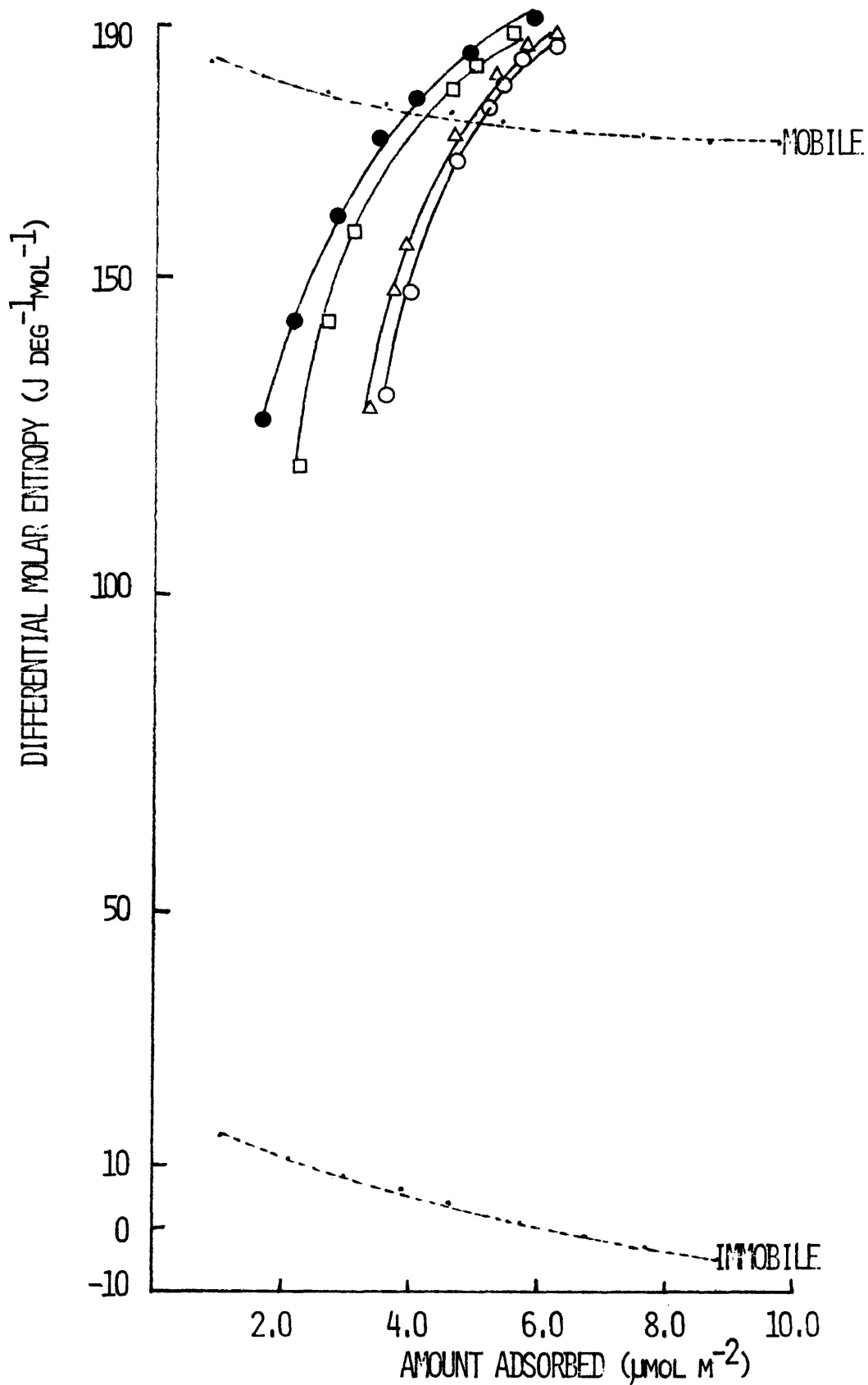


FIGURE 18 EXPERIMENTAL DIFFERENTIAL MOLAR ENTROPIES OF AMMONIA ADSORBED AT 273 K ON QUEBEC CHRYSOTILE HEAT-TREATED AT 150 (○), 300 (△), 500 (□), AND 700 (●)°C.

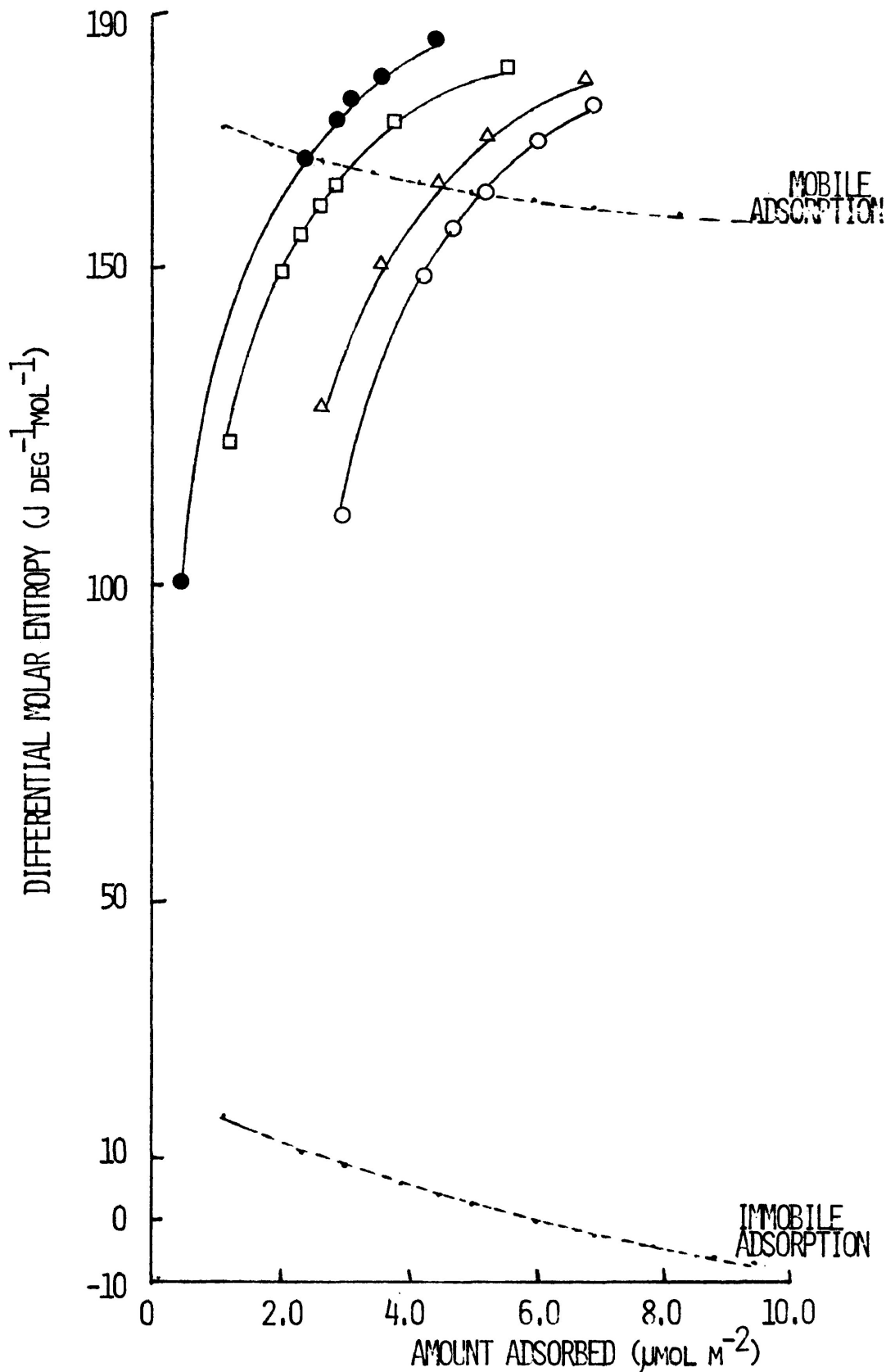


FIGURE 19 EXPERIMENTAL DIFFERENTIAL MOLAR ENTROPIES OF AMMONIA ADSORBED AT 298 K ON QUEBEC CHRYSOTILE HEAT-TREATED AT 150 (○), 300 (△), 500 (□), AND 700 (●)°C.

Adsorption/desorption isotherms for ammonia at 273 and 298 K on the four heat-treated Quebec chrysotiles were determined, Figures 20 and 21. It is evident from the isotherms that the adsorption behaviour of the ammonia on the Quebec samples was affected by the operating temperature. The amount adsorbed at low pressures was generally greater at 273 K but lower as the pressure of ammonia was increased. The isotherms for both operating temperatures seemed to indicate, as with the entropy curves, that there were two distinct types of surface formed with heat-treatment, one at 150 and 300°C and another at 500 and 700°C. At 273 K, the 150 and 300°C samples had very similar adsorption capacities, the only difference being that the adsorption isotherms for both samples were identical at low pressures, < 7.5 kPa, but diverged slightly with the 150°C sample showing a slightly greater adsorption capacity at 80 kPa, $5.2 \mu\text{mol m}^{-2}$, than the 300°C sample, $5.1 \mu\text{mol m}^{-2}$. The 500 and 700°C samples also exhibited similar adsorption patterns at low pressures, < 2.5 kPa, but soon diverged to level out at $3.6 \mu\text{mol m}^{-2}$, 500°C, and $3.0 \mu\text{mol m}^{-2}$, 700°C, at 80 kPa of ammonia pressure.

The 298 K experiments indicated two distinctive surfaces as noted at 273 K. However, in this case the isotherms did not level out in the same manner as those at 273 K. The 150°C sample showed higher adsorption capacity than that of the 300°C material over the entire length of the isotherm. The isotherms determined on 500 and 700°C samples had similar adsorption

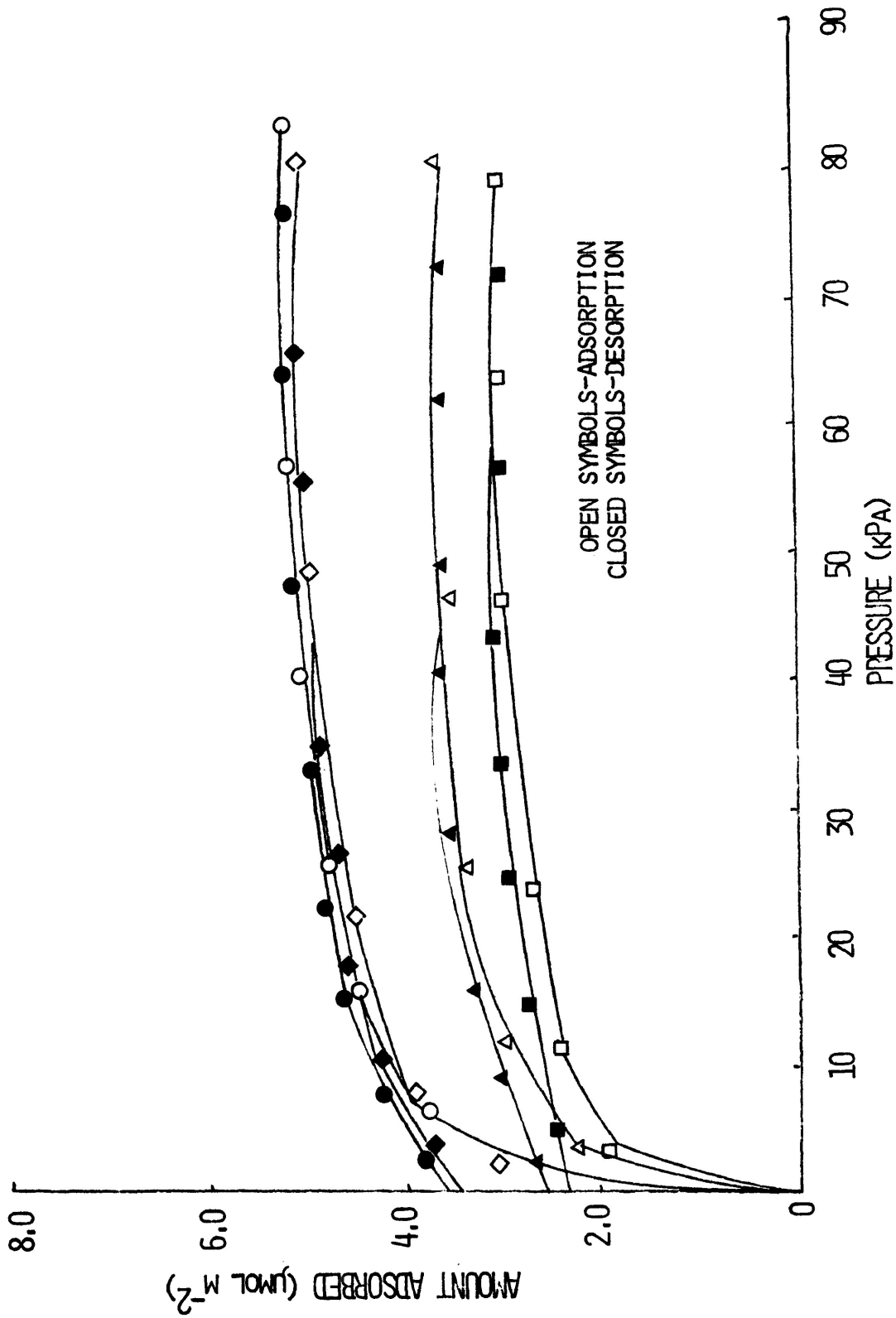


FIGURE 20 ADSORPTION/DESORPTION ISOTHERMS FOR AMMONIA AT 273K ON HEAT-TREATED QUEBEC CHRYSOTILE. HEAT TREATMENT AT 150 (○), 300 (◇), 500 (△), AND 700 (□)°C.

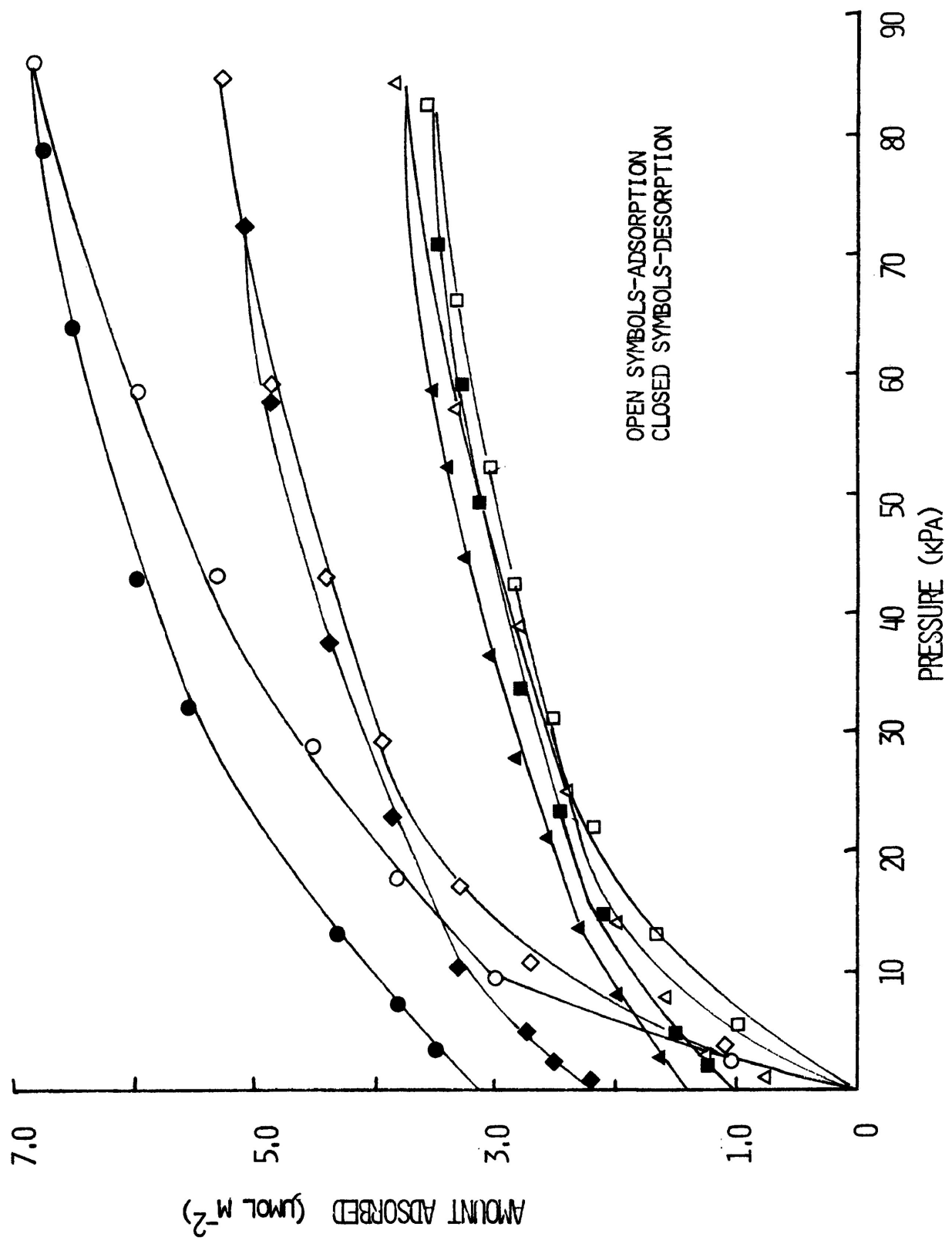


FIGURE 21 ADSORPTION/DESORPTION ISOTHERMS FOR AMMONIA AT 298 K ON HEAT-TREATED QUEBEC CHRYSOTILE, HEAT TREATMENT AT 150 (○), 300 (◇), 500 (△), AND 700 (□)°C.

capacities to that of the 500°C sample, slightly higher over the entire curve.

As with the Californian chrysotile analyzed under similar conditions, all the desorption isotherms indicated some degree of irreversibility.

Table 3.2 summarizes the adsorption characteristics of ammonia adsorbed on each of the heat-treated samples at the two operating temperatures.

3.5 A Comparison of the Sorption Characteristics at 266, 273, 288, 298 and 308 K of Ammonia on Quebec Chrysotile Heat-Treated at 500°C

3.5.1. Calorimeter Experiments

The calorimeter was operated adiabatically to determine the heat of adsorption at 266, 273, 288, 298 and 308 K for ammonia on Quebec chrysotile heat-treated at 500°C, Figure 22.

The shape of the heat curves was similar to that for all previous systems, falling rapidly from a high initial value at low surface coverage to a "limiting" value at higher surface coverage. However, the placement of the curves for the Quebec chrysotile differed from that of the Californian samples. Whereas the curves for the Californian samples all fell to approximately the same "limiting" value at varying surface coverages, those for Quebec samples fell to different "limiting" values at similar degrees of surface coverage. The "limiting" values varied in a systematic manner from the value at 266 K, 5 kJ mol⁻¹ at

Table 3.2
Surface Areas, Adsorption Capacities and "Limiting" Heats and Entropies of
Adsorption of Ammonia on Heat-Treated Quebec Chrysotile

Operating Temperature (K)	Temperature of Heat Treatment (°C)	Surface Area (m ² g ⁻¹)	Adsorption Capacity at 30 kPa (μmol m ⁻²)	"Limiting" Heat of Adsorption (J deg ⁻¹ mol ⁻¹)	"Limiting" Entropy at 7.0 μmol m ⁻² (J deg ⁻¹ mol ⁻¹)
273	150	40	4.9	3.4	186
"	300	40	4.8	3.2	187
"	500	40	3.5	3.9	190
"	700	42	2.9	3.6	192
298	150	40	4.6	2.8	176
"	300	40	4.0	2.6	180
"	500	40	2.6	3.6	182
"	700	42	2.5	3.2	190

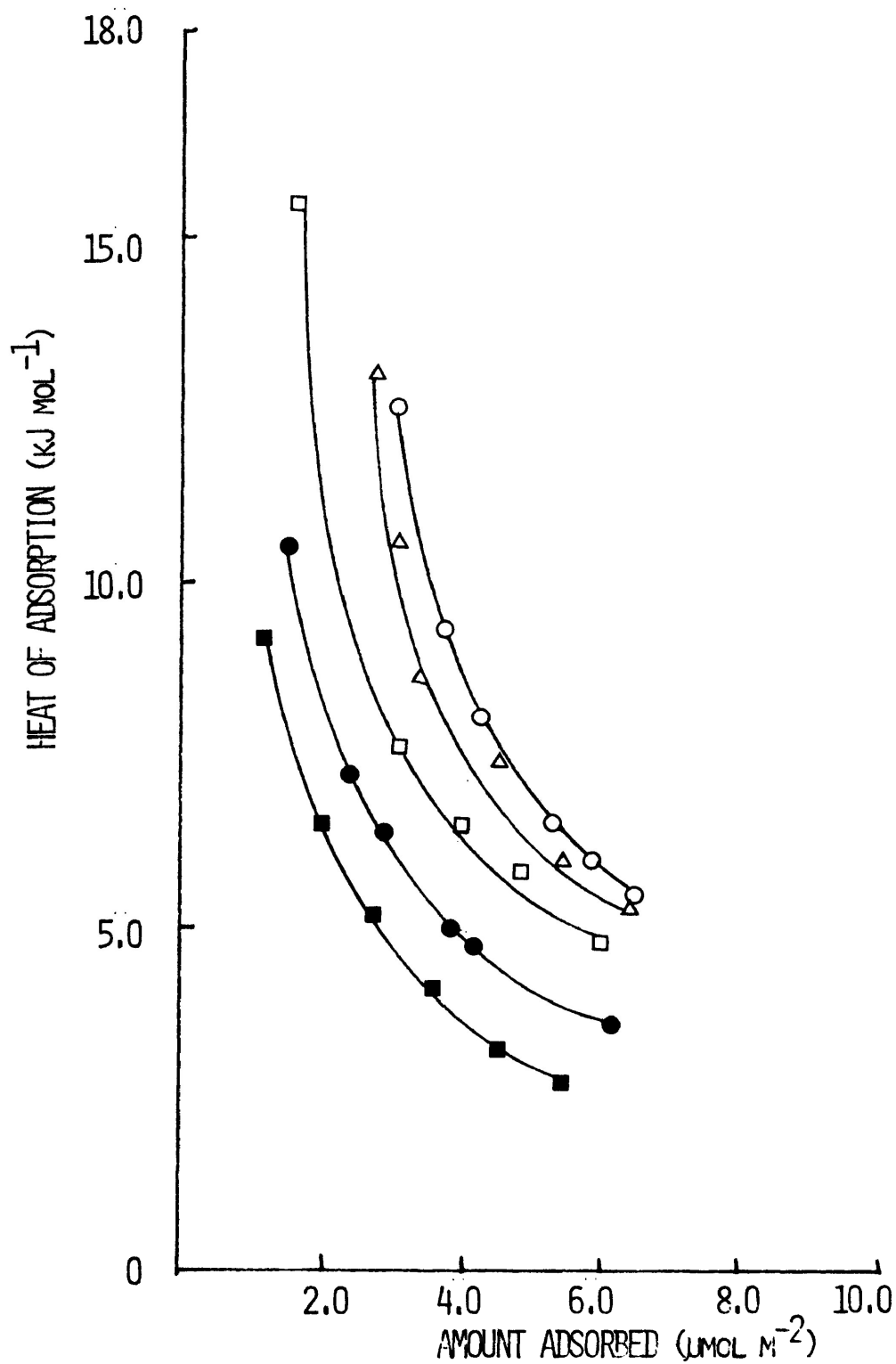


FIGURE 22 VARIATION OF HEAT OF ADSORPTION WITH AMOUNT OF AMMONIA ADSORBED ON QUEBEC CHRYSOTILE HEAT-TREATED AT 500°C, ○, 266; △, 273; □, 288; ●, 298; ■, 308 K.

$7.0 \mu\text{mol m}^{-2}$, to that at 308 K, 2.5 kJ mol^{-1} at $6.0 \mu\text{mol m}^{-2}$.

3.5.2 Entropy Calculations

The variation of the experimental differential molar entropy with surface coverage for the adsorption of ammonia from 266 to 308 K on Quebec chrysotile heat-treated at 500°C is shown in Figure 23. The adsorption patterns were similar to those for Californian samples. Each entropy curve began at a low value and rose rapidly to a "limiting" point. Again, the experimental entropy for the 266 K experiment "limited" itself at a value slightly below the curve calculated for a mobile adsorbed phase. The 273 K curve approached the mobile model very closely but the curves determined at 288, 298 and 308 K were all "limited" at values progressively higher than those for the mobile model for their particular temperature. The 308 K entropy curve was $20 \text{ J deg}^{-1} \text{ mol}^{-1}$ higher than that for the 308 K mobile model.

3.5.3. Adsorption/Desorption Isotherms

The adsorption/desorption isotherms of ammonia at 266, 273, 288, 298 and 308 K on Quebec chrysotile heat-treated at 500°C are shown in Figure 24. As in the case of the Californian samples, the curves generally showed decreased adsorption with increased operating temperature except for the 308 K experiment where the adsorption isotherm exhibited an unexpectedly high adsorption capacity over its entire length. The desorption isotherms for all the experiments indicated some degree of irreversible adsorption.

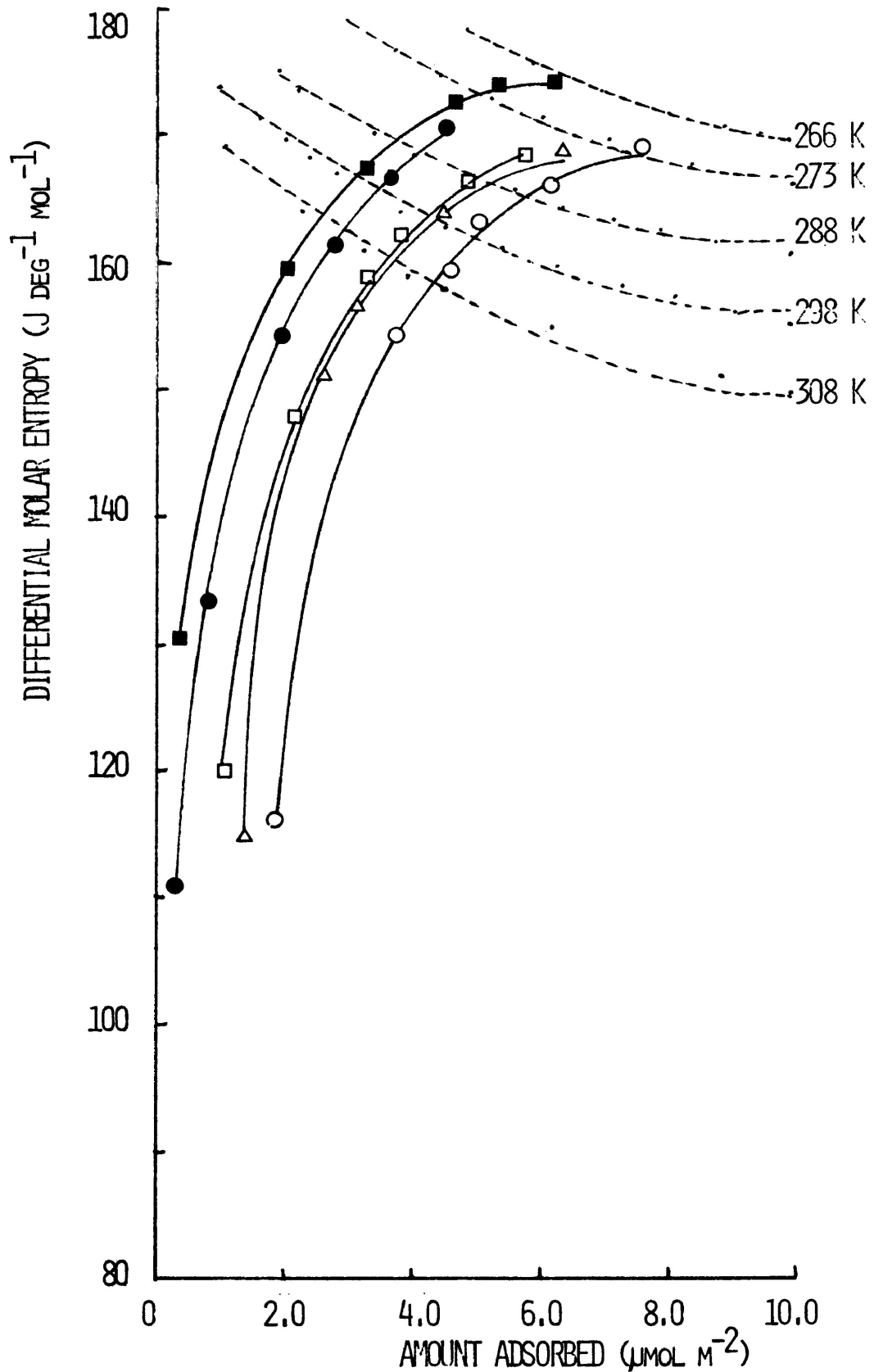


FIGURE 23 EXPERIMENTAL DIFFERENTIAL MOLAR ENTROPIES OF ADSORPTION FOR AMMONIA AT 266 (○), 273 (Δ), 288 (◻), 298 (●), AND 308 (■) K. ON QUEBEC CHRYSOTILE HEAT-TREATED AT 500°C. -----"MOBILE" ENTROPY CURVES

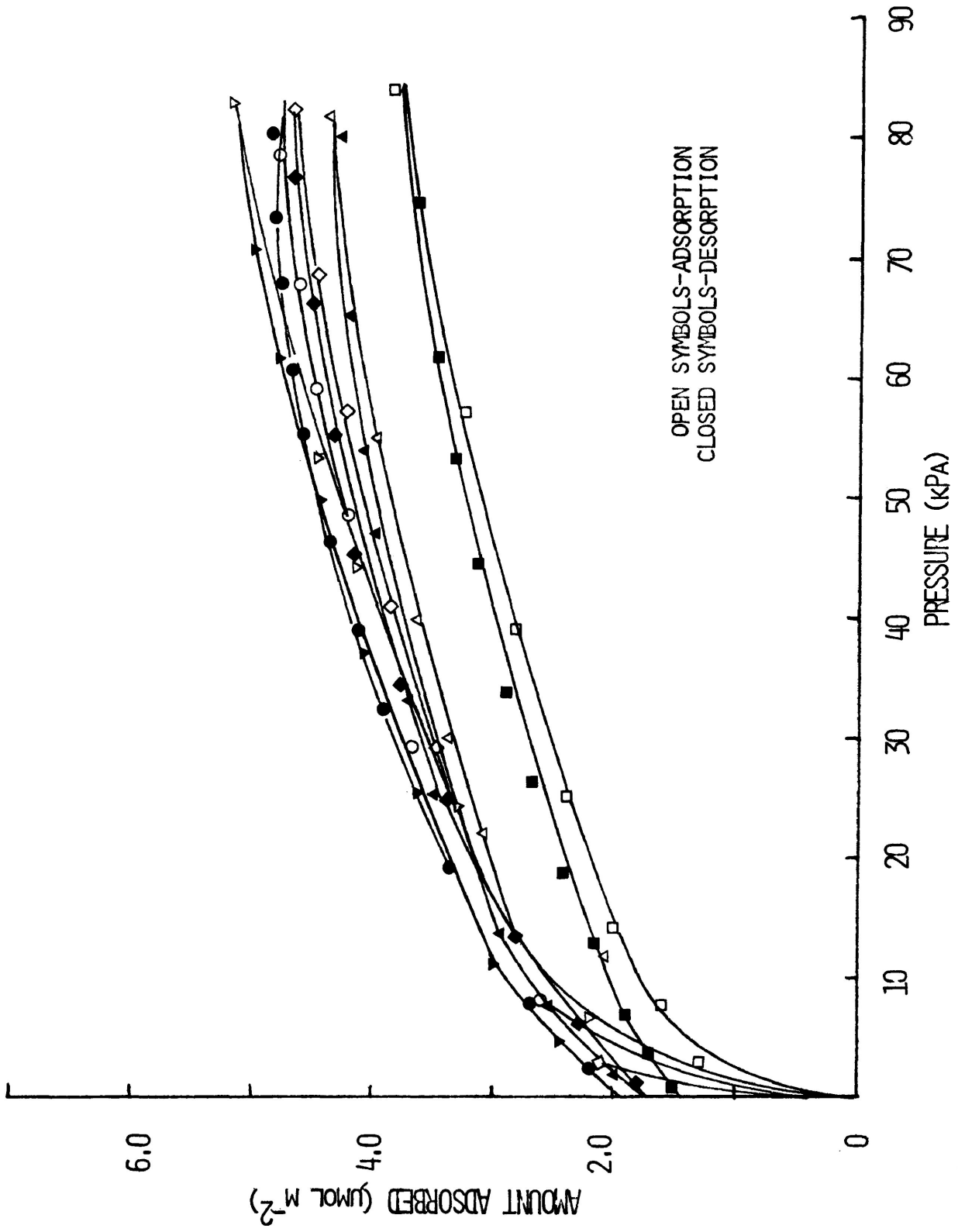


FIGURE 24 ADSORPTION/DESORPTION ISOTHERMS FOR AMMONIA ON QUEBEC CHRYSOTILE HEAT-TREATED AT 500°C, EXPERIMENTAL TEMPERATURES 266 (○), 273 (◇), 288 (△), 298 (□), AND 308 (▽) K.

3.6. Adsorption/Desorption of Ammonia on Californian Chrysotile Pre-treated with Boiling Water

3.6.1. Calorimeter Experiments

The calorimeter was operated adiabatically to determine the heat of adsorption at 298 K for ammonia on Californian chrysotile which had been pre-treated for five hours in boiling water, Figure 25. When this heat curve was compared to that for the untreated (150°C) Californian sample it was noted that for the lower surface coverages, $< 8.0 \mu\text{mol m}^{-2}$, the heats were generally much higher for the water-treated sample. However, the "limiting" heat appeared to be similar for both samples i. e. 6 kJ mol^{-1} for the untreated sample and 8 kJ mol^{-1} for the water-treated sample. The curve for the water-treated sample was "limited" at a higher degree of surface coverage, $10.0 \mu\text{mol m}^{-2}$, than the curve for the untreated sample, $8.0 \mu\text{mol m}^{-2}$.

3.6.2. Entropy Calculations

Figure 26 shows the variation of the experimental entropy with surface coverage for the adsorption of ammonia at 298 K on Californian chrysotile treated with boiling water.

The entropy of the adsorbed ammonia increased from 40.0 to $160.0 \text{ J deg}^{-1} \text{ mol}^{-1}$ between 6.7 and $11.0 \mu\text{mol m}^{-2}$, and above $10.0 \mu\text{mol m}^{-2}$ the curve lay above that for the mobile model of adsorption.

3.6.3. Adsorption/Desorption Isotherms

A complete adsorption/desorption isotherm was measured

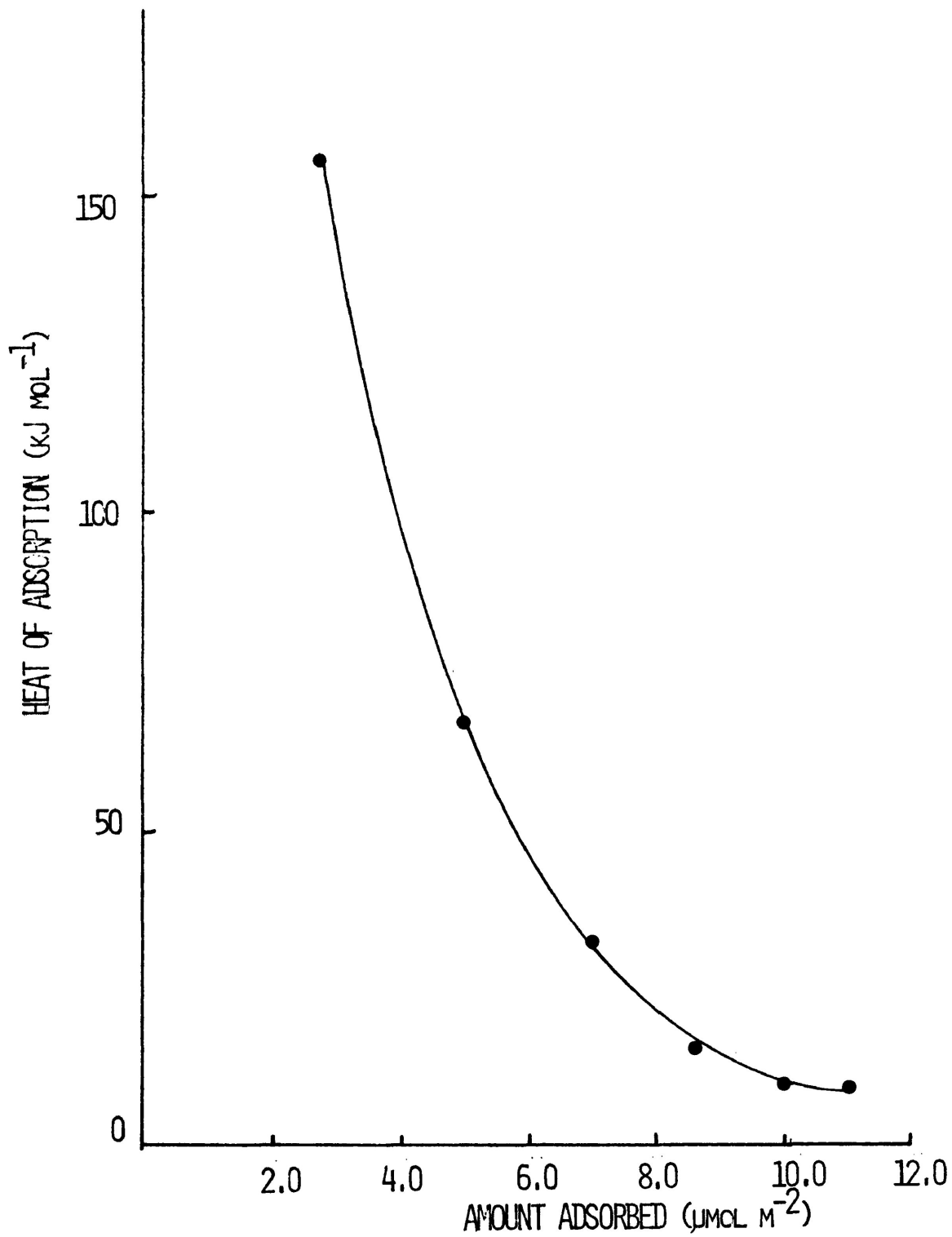


FIGURE 25 HEAT OF ADSORPTION FOR AMMONIA AT 298 K ON CALIFORNIAN CHRYSOTILE TREATED WITH WATER

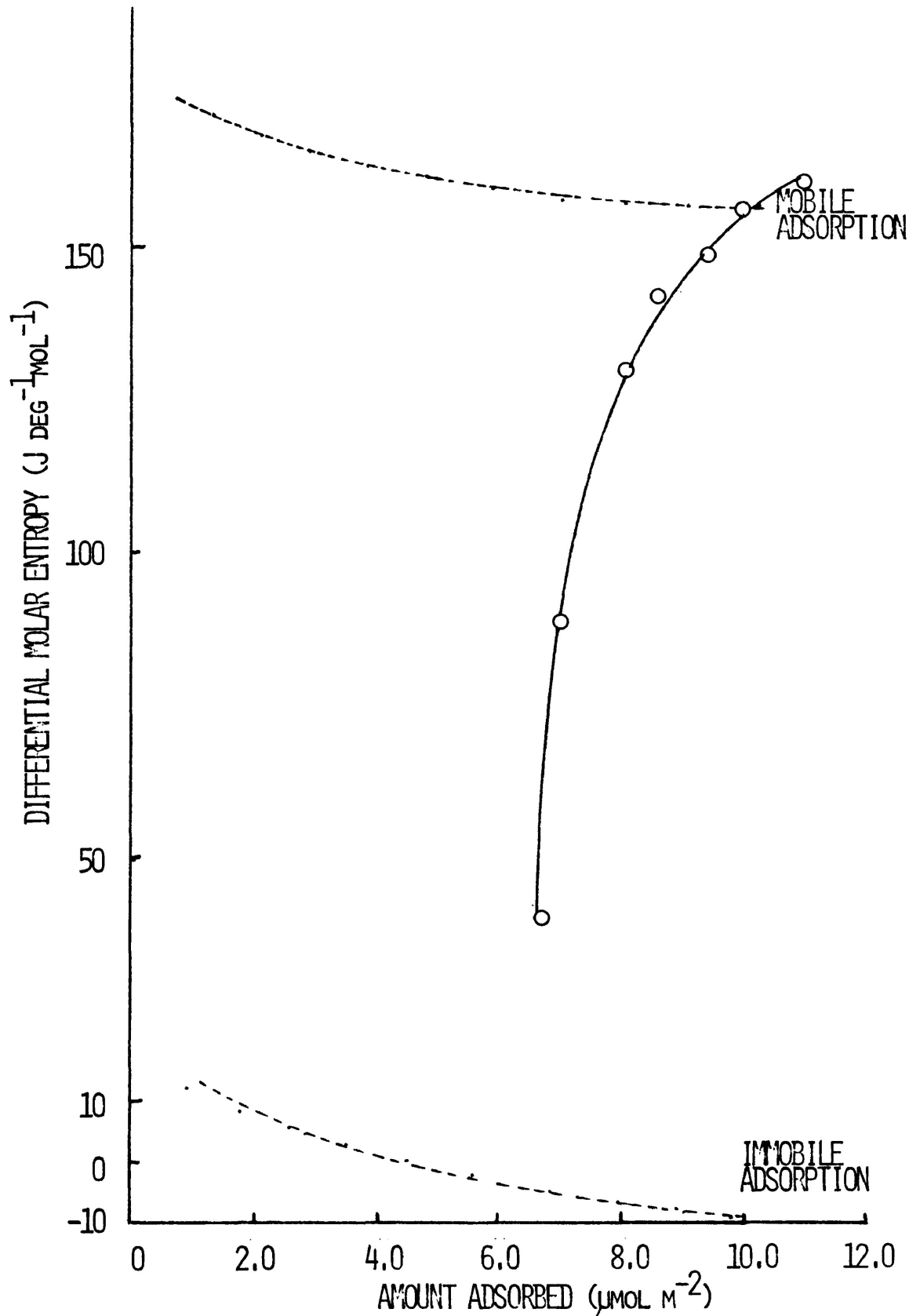


FIGURE 26 EXPERIMENTAL DIFFERENTIAL MOLAR ENTROPY OF AMMONIA ADSORBED AT 298 K ON CALIFORNIAN CHRYSOTILE TREATED WITH WATER.

for ammonia at 298 K on water-treated Californian chrysotile, Figure 27. The adsorbed amount increased to $12.2 \mu\text{mol m}^{-2}$ at 80 kPa. The desorption isotherm followed the adsorption curve from 80.0 kPa to 57.5 kPa where it began to diverge above the adsorption isotherm. Again, some irreversible adsorption was indicated.

3.7 Adsorption/Desorption of Ammonia on Californian Chrysotile Pre-treated with Sodium Nitrate

3.7.1. Calorimeter Experiments

Adiabatic calorimetric heats of adsorption were determined for ammonia at 298 K on Californian chrysotile treated, with stirring, at 100°C , for 5 h. in a 5% sodium nitrate in water solution, Figure 28. The chrysotile was shown by flame photometric analysis, to contain 3.7% sodium. The curve resembled that of the water-treated sample in that the heat at lower surface coverages ($< 8.0 \mu\text{mol m}^{-2}$) was generally much higher than for the untreated sample. The only significant difference between the curves for the water-treated sample and the sodium nitrate-treated sample was that the "limiting" heat for the sample treated with water was slightly lower (8.0 kJ mol^{-1}) and was attained at a higher surface coverage ($10.0 \mu\text{mol m}^{-2}$) than that for the sodium nitrate-treated sample (11.0 kJ mol^{-1} at $9.0 \mu\text{mol m}^{-2}$).

3.7.2. Entropy Calculations

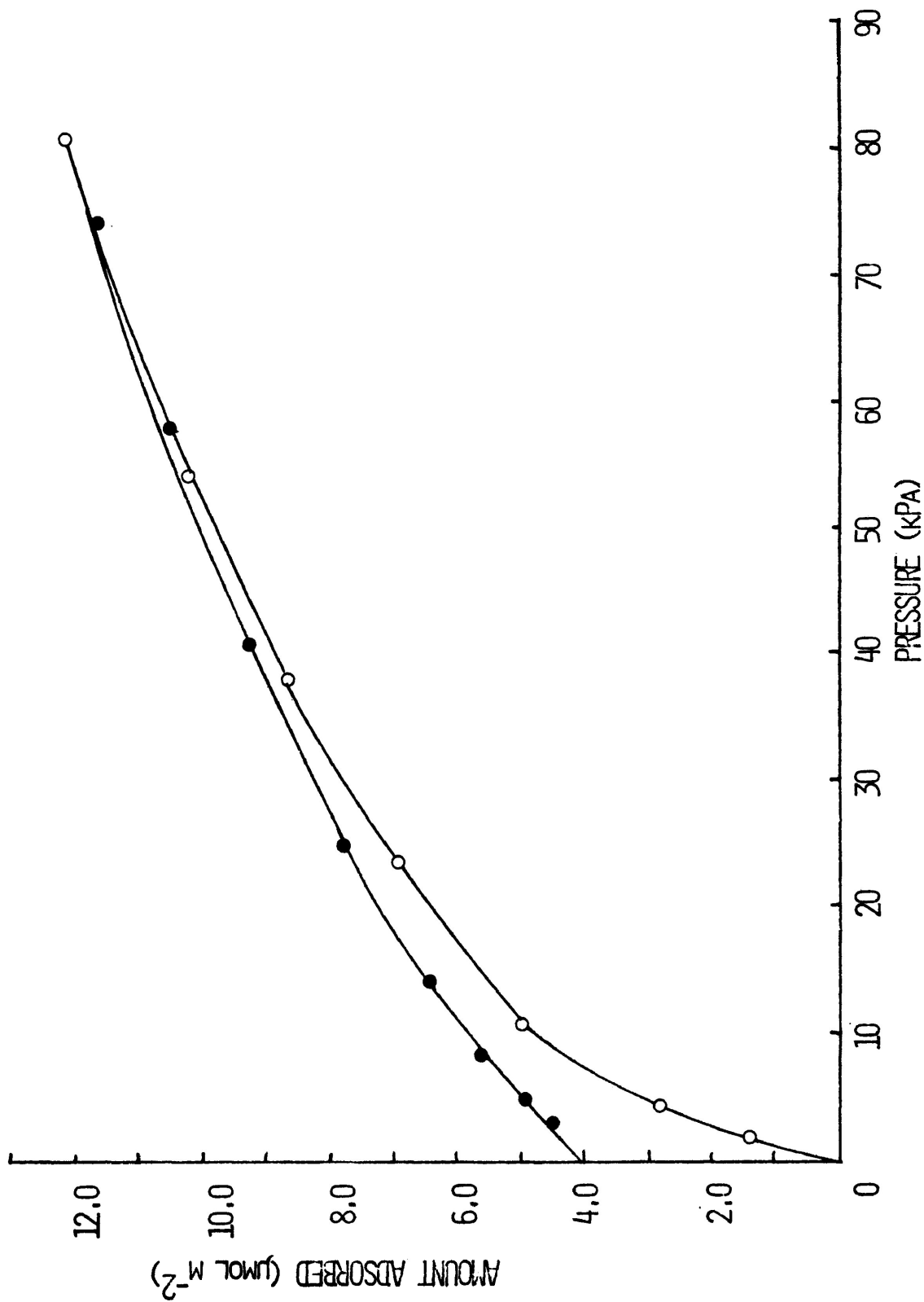


FIGURE 27 ADSORPTION/DESORPTION ISOTHERMS FOR AMMONIA AT 298 K ON CALIFORNIAN CHRYSOTILE TREATED WITH WATER.

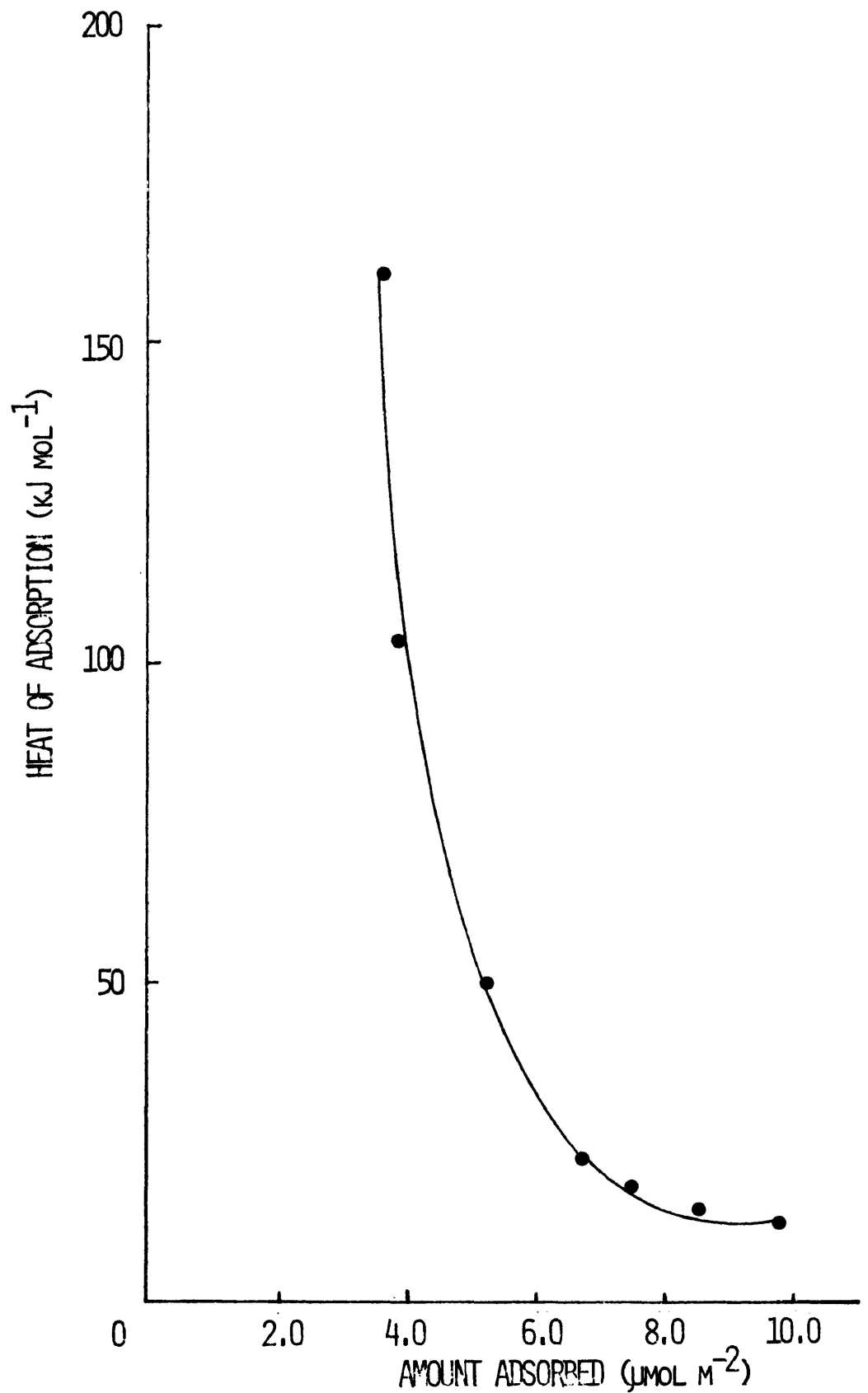


FIGURE 28 HEAT OF ADSORPTION FOR AMMONIA AT 298 K ON CALIFORNIAN CHRYSTILE TREATED WITH SODIUM NITRATE.

Figure 29 shows the variation of the experimental entropy with surface coverage for the adsorption of ammonia at 298 K on Californian chrysotile treated with sodium nitrate.

Whereas the entropy curve for the water-treated sample began to level out at a value slightly greater than that for the mobile model, the curve for the sodium nitrate-treated sample increased rapidly from a value of 30 J deg^{-1} at $4.7 \mu\text{mol m}^{-2}$ to $148 \text{ J deg}^{-1} \text{ mol}^{-1}$ at $9.5 \mu\text{mol m}^{-2}$ which was slightly lower than the curve calculated for the mobile model of entropy.

3.7.3 Adsorption/Desorption Isotherm

A complete adsorption/desorption isotherm for ammonia at 298 K on Californian chrysotile pre-treated with sodium nitrate is shown in Figure 30. This adsorption curve and the one for the water-treated sample followed the same pattern up to 5 kPa of ammonia pressure but at pressures greater than this the adsorption capacity of the sodium nitrate sample was much lower. For example, the adsorption capacity at 80 kPa for the water-treated sample was $12.0 \mu\text{mol m}^{-2}$ while it was only $8.4 \mu\text{mol m}^{-2}$ for the sample impregnated with the sodium salt. In both cases approximately the same degree of irreversible adsorption was evident, approximately 30%.

3.8. Efficiency of Desorption of Ammonia from Heat-Treated Californian and Quebec Chrysotiles

3.8.1. Introduction

It was observed that when a dose of ammonia was admitted

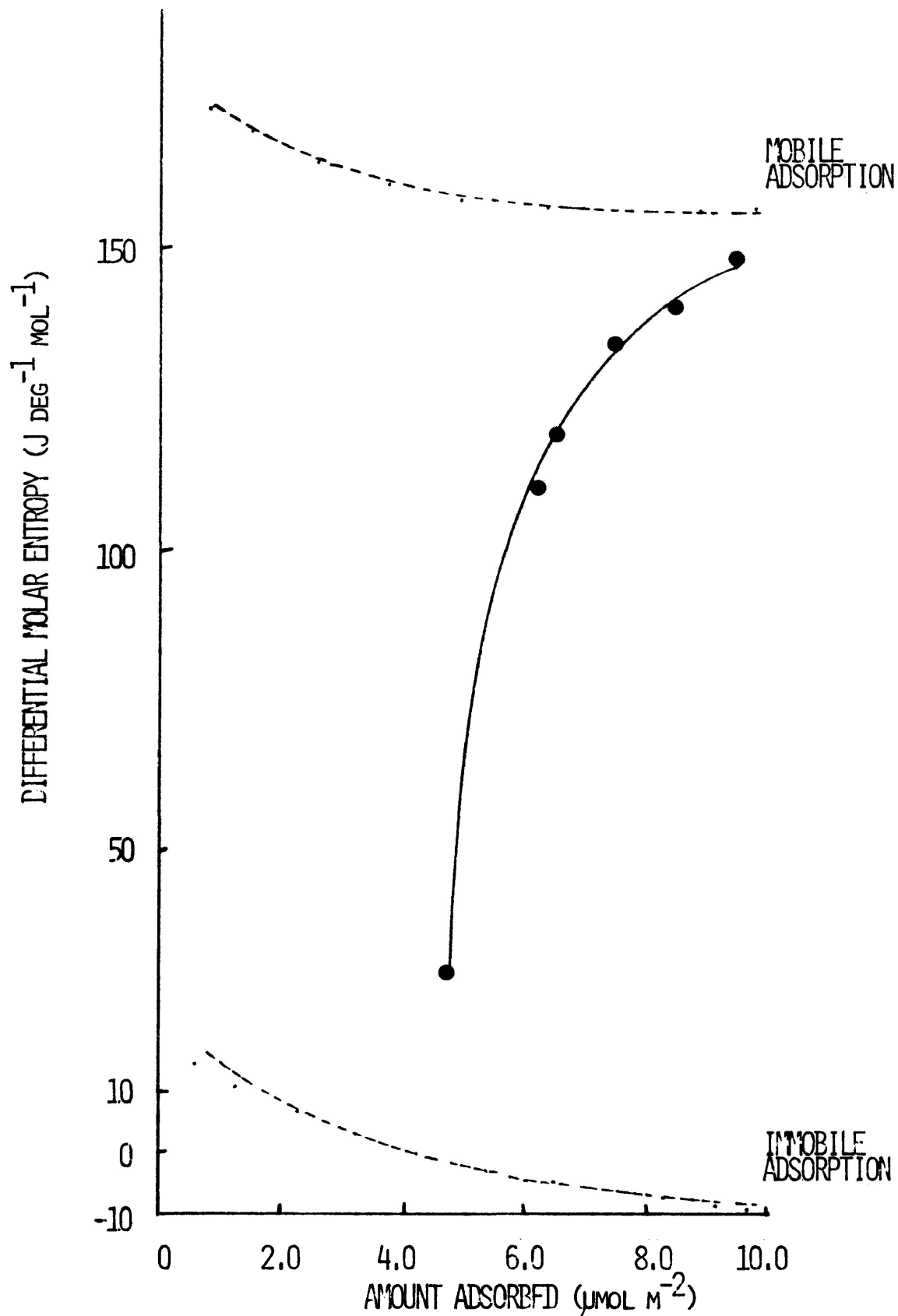


FIGURE 29 EXPERIMENTAL DIFFERENTIAL MOLAR ENTROPY OF AMMONIA ADSORBED AT 298 K ON CALIFORNIAN CHRYSOTILE TREATED WITH SODIUM NITRATE.

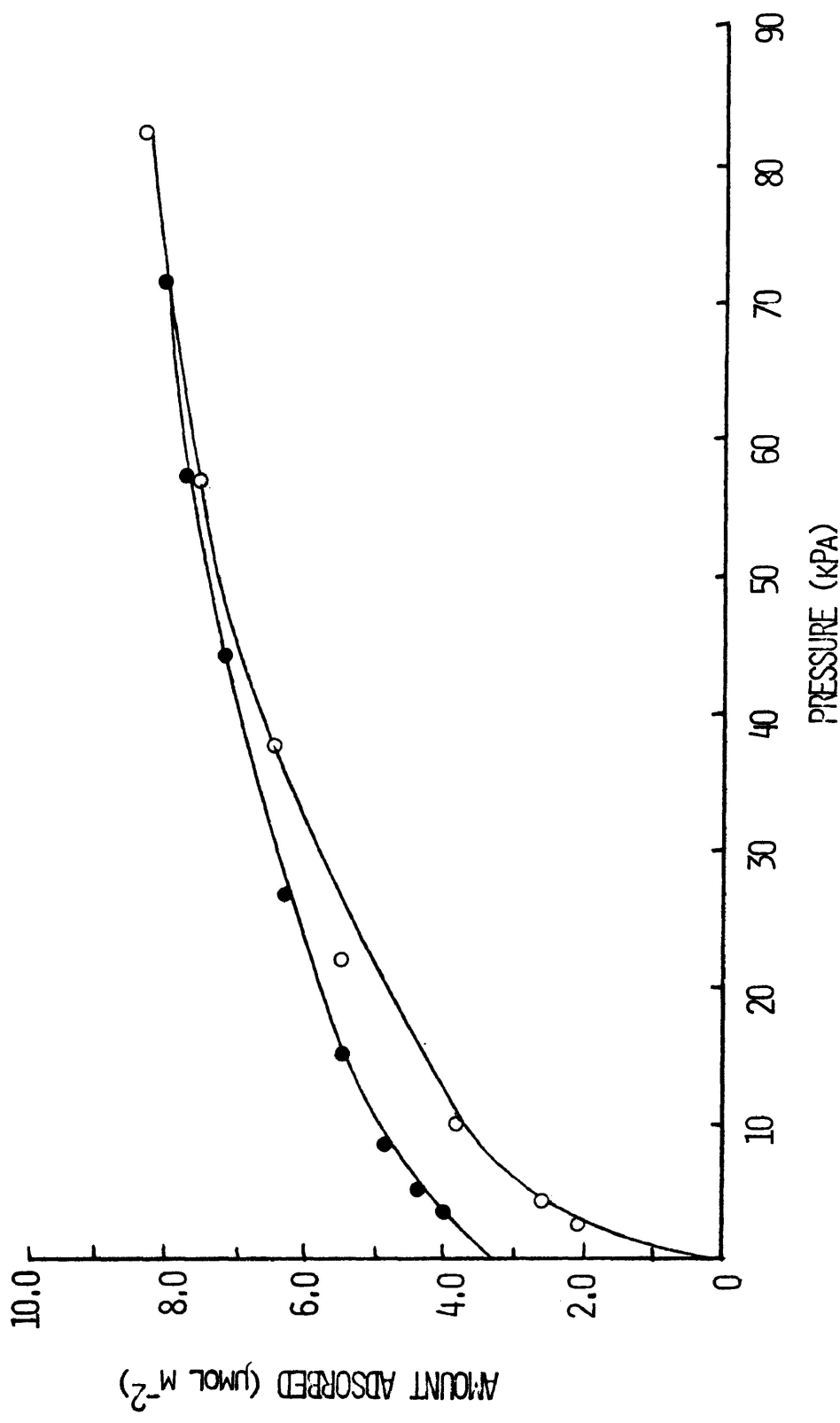


FIGURE 30 ADSORPTION/DESORPTION ISOTHERMS FOR AMMONIA AT 298 K ON CALIFORNIAN CHRYSOTILE TREATED WITH SODIUM NITRATE.

to a chrysotile sample, it could not be desorbed completely. If another dose of adsorbate was then added to the adsorbent only a percentage of that could be removed. Depending on the type of chrysotile and its history of pretreatment, several additions were necessary before an addition of gas could be completely desorbed. A comprehensive series of experiments was performed to determine the number of these gas doses that were needed before complete desorption occurred. The experiments were performed to provide further evidence regarding which samples formed stronger and more numerous "bonds" with the adsorbate.

For each heat-treated sample a dose of gas was allowed to adsorb for 1 h., at which time the tap from the calorimeter was opened and the sample allowed to desorb. The change in the manometer reading was recorded and the precise amount desorbed was calculated. The calorimeter was then closed off and the manometer area evacuated. This desorption procedure was repeated until no further change in the manometer could be detected. The cumulative amount of gas desorbed was calculated and subtracted from the amount adsorbed to determine the amount which remained on the surface. Another dose of ammonia was then admitted to the calorimeter, the amount adsorbed was recorded, and the desorption procedure was repeated for that sample. This experiment was continued until a dose of adsorbed gas was shown to desorb entirely. In all cases the adsorbed gas was left for 1 h. before a reading was taken and all

desorption points were also left 1 h. to ensure complete equilibration. The 1 h. limit on all points was determined by taking successive readings over time to find the point at which the manometer reading ceased to change.

3.8.2. Californian Chrysotile

Table 3.3. summarizes the results obtained in the desorption efficiency experiments on the four heat-treated Californian samples. The results indicate that the strongest adsorption occurred on the 150 and 700°C treated samples while the most readily reversible adsorption occurred with the 300 and 500°C chrysotiles.

3.8.3. Quebec Chrysotile

Table 3.4. shows the results obtained from the desorption efficiency experiments performed on the heat-treated Quebec samples.

The results also showed that the samples from which desorption was least efficient were those heated at 150 and 700°C. However, in contrast to the Californian samples, complete desorption from the Quebec chrysotile was accomplished by the fourth adsorbed dose of gas whereas the Californian sample showed some incomplete desorption up to the fifth dose of ammonia. In this case all samples showed complete desorption by the fourth addition of ammonia.

As in the case of the Californian sample, the 300°C - treated Quebec sample seemed to show the highest degree of

Table 3.3.
Summary of the Desorption Efficiency of Heat-Treated Californian Chrysotile

Temperature of Heat Treatment (°C)	Percentage of Ammonia Remaining on Surface after Desorption				
	1st adsorption	2nd	3rd	4th	5th
150	100%	48%	40%	14%	0
300	72	21	14	0	0
500	66	15	4	0	0
700	100	57	19	17	0

Details of Actual Amounts Adsorbed Described in Appendix C

Table 3.4.

Summary of the Desorption Efficiency of Heat-Treated Quebec Chrysotile

Temperature of Heat Treatment (°C)	Percentage of Ammonia Remaining on Surface after Desorption				
	1st adsorption	2nd	3rd	4th	5th
150	100%	55%	34%	0	0
300	73	0	0	0	0
500	100	64	0	0	0
700	100	55	36	0	0

Details of actual adsorbed/desorbed amounts are given in Appendix C

reversibility of adsorption with the 500°C sample showing the next highest degree of the same.

3.9. Mass Spectrometer Analysis

Over the course of the experimental work, several samples of desorbed gas were collected after ammonia had been adsorbed at a variety of temperatures on both groups of heat-treated chrysotiles. These gas samples were analyzed by a mass spectrometer. In all recorded cases, the only observable desorbed products were ammonia and water.

3.10. Studies of the Physical Structure of the Adsorbents

3.10.1. Introduction

Two independent techniques were used to characterise the surface physical properties of the adsorbent. One involved the determination of low-temperature (77 K) nitrogen adsorption/desorption isotherms. From these, surface area and approximate pore size distributions can be calculated. Such pore size distribution data may be compared with results obtained directly using the electron microscope, which is useful in obtaining information about the topographical features of the adsorbent surface.

3.10.2. Californian Chrysotile

3.10.2.1. Low-Temperature Nitrogen Adsorption

The heat treatment carried out on the chrysotile was the same as that used in the calorimetric experiments. Samples

were outgassed at 100°C for 1 h., after evacuation to 1.33×10^{-4} kPa.

Nitrogen adsorption/desorption isotherms were determined at 77 K on Californian chrysotile heat-treated at 150, 300, 500 and 700°C, Figure 31.

The amount of nitrogen adsorbed at N. T. P. at any given relative pressure value was similar for all the heat-treated samples. The main difference seemed to be in the hysteresis loop obtained for the 700°C sample. While the hysteresis loops for the 150, 300 and 500°C samples were very similar, occurring in the relative pressure range of approximately .25 to .90 p/po, the 700°C loop was located between .30 and .80 p/po and was much narrower than that of the other samples. Equilibration times were relatively long over the range of the isotherms at approximately 45 to 60 minutes.

B. E. T. plots calculated from the adsorption data are shown in Figure 32. The plots were all straight lines from p/po = .025 to .325 and monolayer adsorbed amounts were calculated from the slopes and intercepts of the lines in the usual way. Surface areas were then calculated assuming that the cross-sectional area of the nitrogen molecule was $16.2 \text{ \AA}^2 (.16 \text{ nm}^2)$ at 77 K and these data are presented in Table 3.4.

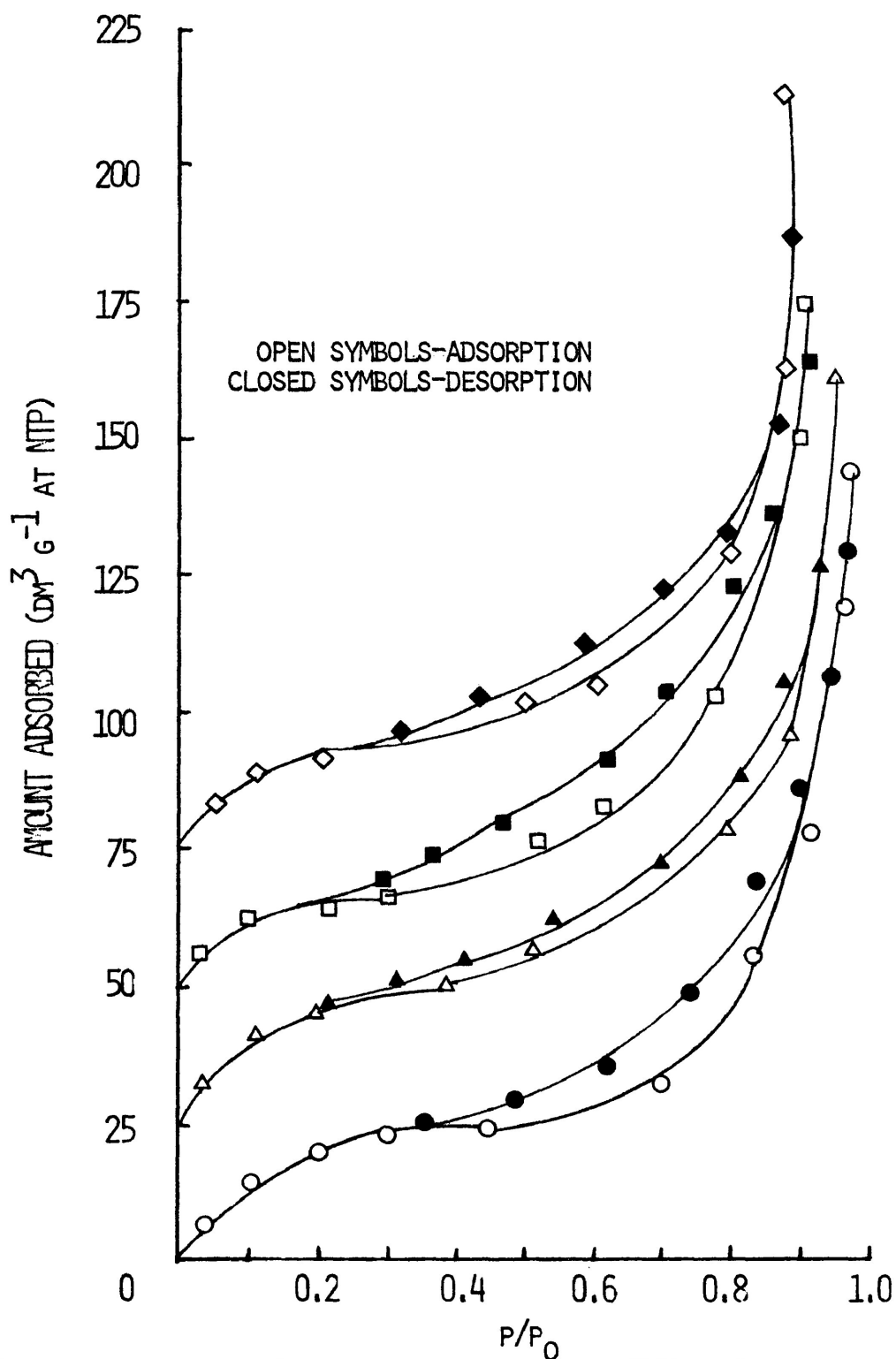


FIGURE 31 NITROGEN ADSORPTION/DESORPTION ISOTHERMS AT 77K ON CALIFORNIAN CHRYSOTILE HEAT-TREATED AT 150°C (○), 300°C (△, ORIGIN DISPLACED TO 25 DM³ G⁻¹), 500°C (□, ORIGIN DISPLACED TO 50 DM³ G⁻¹), AND 700°C (◇, ORIGIN DISPLACED TO 75 DM³ G⁻¹).

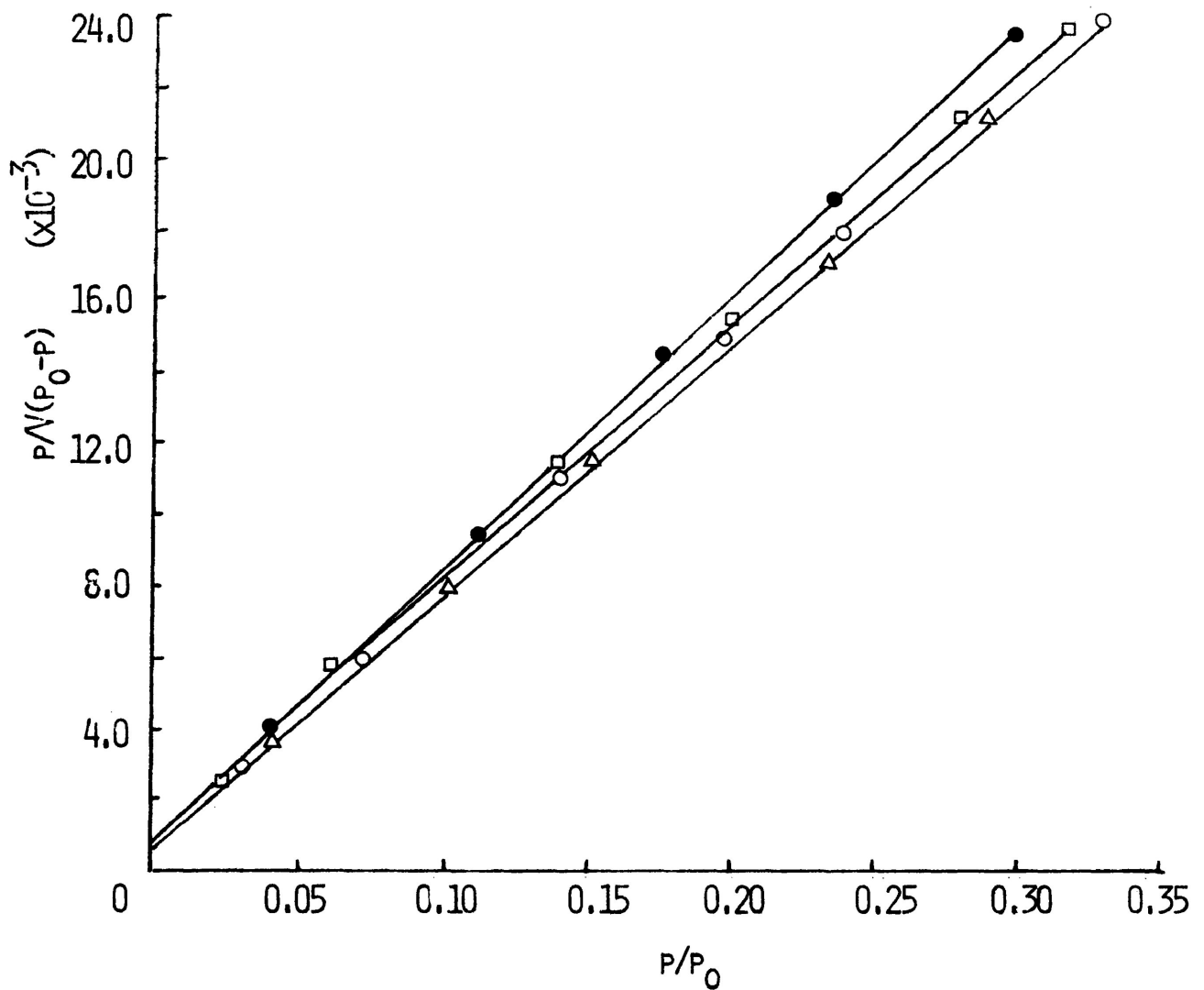


FIGURE 32 B.E.T. PLOTS FOR NITROGEN AT 77K ON HEAT-TREATED CALIFORNIAN CHRYSOTILE. HEAT TREATMENT AT 150 (○), 300 (△), 500 (□), AND 700 (●)°C.

Table 3.4.

Surface Areas for Californian Chrysotile Heat-Treated at 150
300, 500 and 700°C.

	Activation Temperature of Californian Samples (°C)			
	150	300	500	700
Surface Area (m ² g ⁻¹)	61	61	60	62

The method of Cranston and Inkley (49) was used to compute pore size distribution plots on a differential basis from nitrogen desorption data. These showed that the pore diameters ranged from 20 to 200 Å for Californian chrysotile heat-treated at 150, 300, 500 and 700°C, Figure 33. The charts showed that maxima occurred at approximately 35 and 55 Å for all samples.

The method of Dollimore and Heal (50) was also used to calculate pore size distributions from the same data, Figure 34. From these plots it can be noted that heating from 150 to 300°C caused an increase in the percentage of small pores (radius of 20 Å) and a decrease in the number of larger pores at the second maximum (30 Å). Heating to 500°C brought about the collapse of the smallest pores (< 20 Å) and a large increase in the number of larger pores (30 Å). Finally, treatment to 700°C caused the formation of small pores (< 15 Å) and a decrease in the number of larger pores. It may be noted that

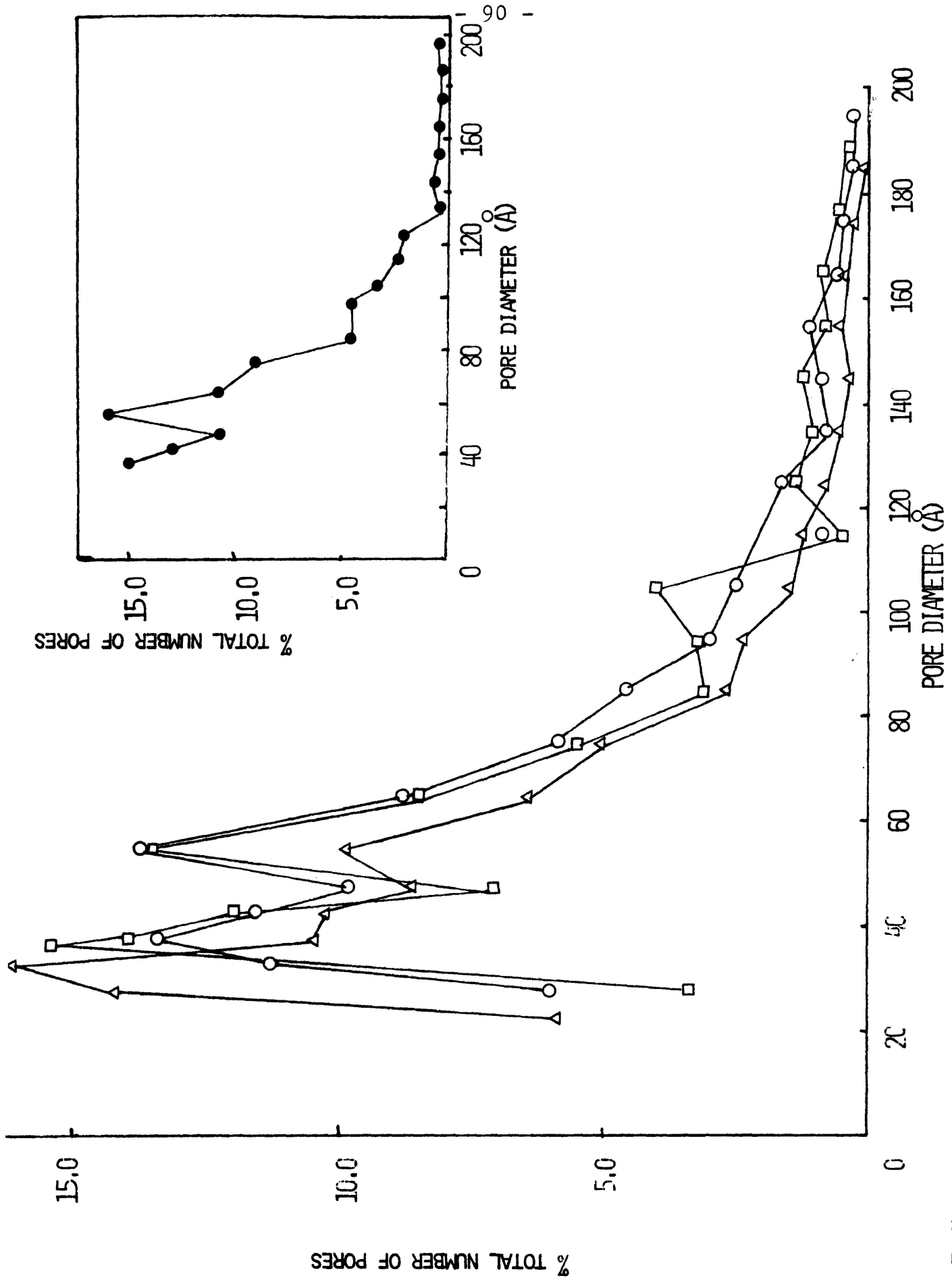


FIGURE 33 PORE SIZE DISTRIBUTION BASED ON NITROGEN DESORPTION AT 77K ON CALIFORNIAN CHRYSOTILE HEAT-TREATED AT 150 (○), 300 (△), 500 (□), AND 700 (●), INSET)°C. BASED ON THE METHOD OF CRANSTON AND INKLEY.

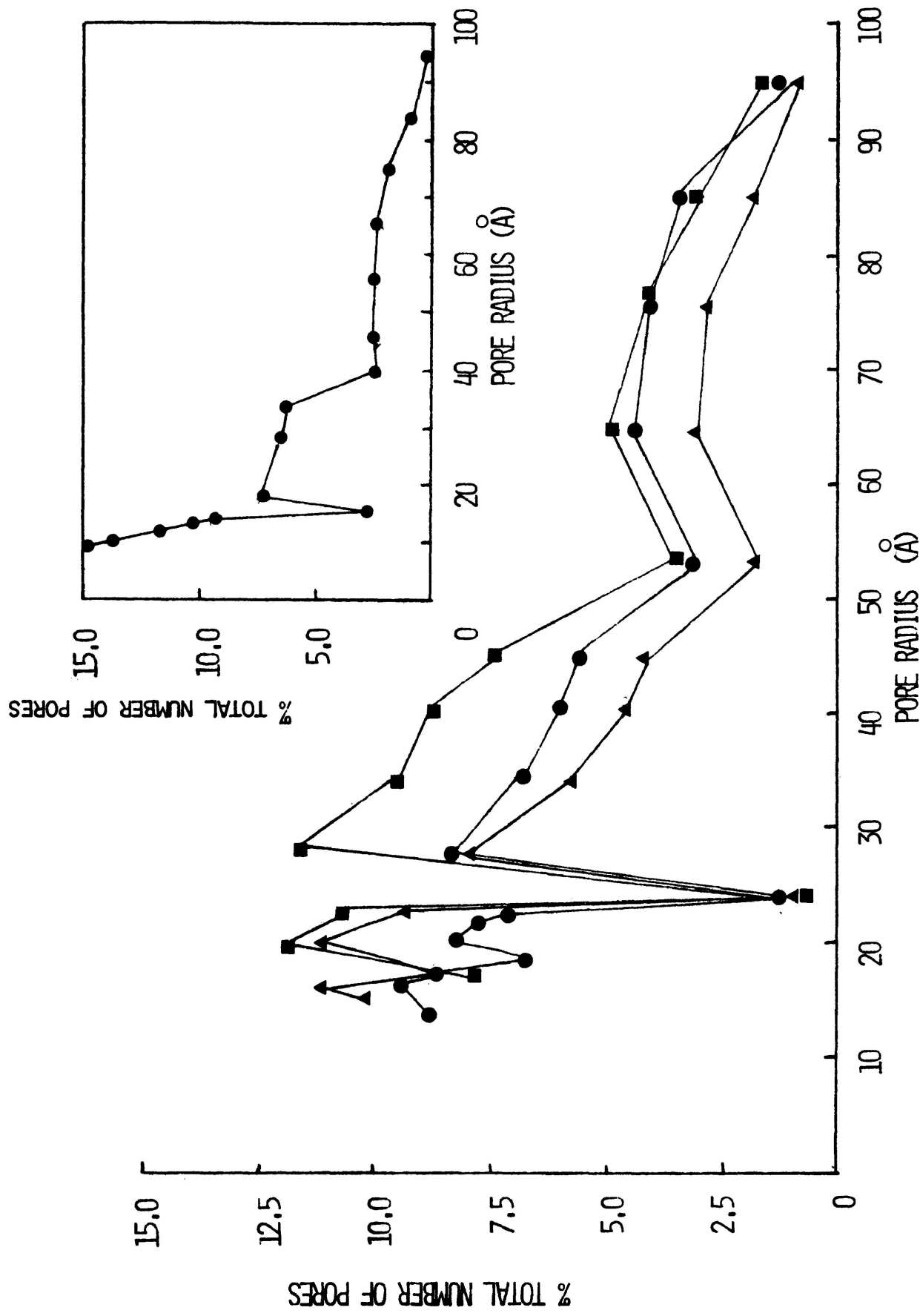


FIGURE 34 PORE SIZE DISTRIBUTION BASED ON NITROGEN DESORPTION AT 77K ON CALIFORNIAN CHRYSOTILE HEAT-TREATED AT 150 (●), 300 (▲), 500 (■), AND 700 (◊)°C. BASED ON THE METHOD OF DOLLIMORE AND HEAL.

the surface area did not change appreciably in any case, particularly in view of the approximate nature of the method of calculation. Although the surface areas were reproducible to within one percent, the "true" surface area may be as much as 10 to 20% higher or lower than that found experimentally using the B. E. T. method (1).

3.10.2.2. Electron Microscopy

Transmission micrographs, Plates 1 (a) - (d), and electron diffraction studies, Plates 2(a) - (d), of Californian samples heat-treated at 150, 300, 500 and 700°C were obtained using the instrument described previously, Section 2.3.4. The only significant difference among the samples was observed with the 700°C material. In all samples, including that from 700°C, the fibrous appearance of the material was retained although structural changes could be observed at the highest treatment temperature. Dehydration caused the fibre to crack and flake but did not reduce it to smaller units. The electron diffraction studies indicated retention of the chrysotile structure through 500°C but the sample became amorphous at 700°C.

3.10.3 Quebec Chrysotile

3.10.3.1. Low-Temperature Nitrogen Adsorption

Heat treatment of Quebec chrysotile was identical to that performed on the samples used in the calorimetric experiments.

Nitrogen adsorption/desorption isotherms were determined

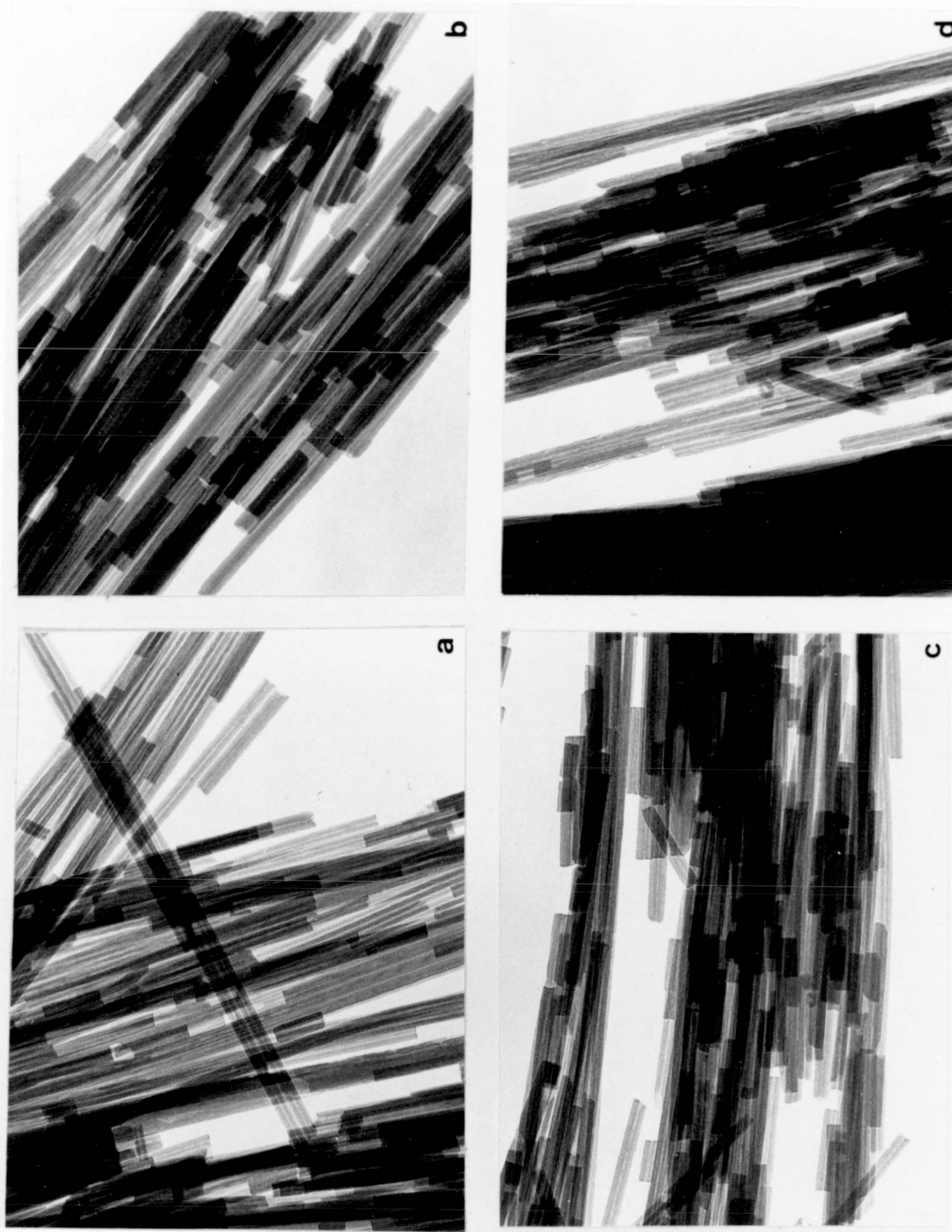


PLATE 1 TRANSMISSION ELECTRON MICROGRAPHS OF CALIFORNIAN CHRYSOTILE HEAT-TREATED AT 150°C (A), 300°C (B), 500°C (C), AND 700°C (D). MAGNIFICATION: 52812X

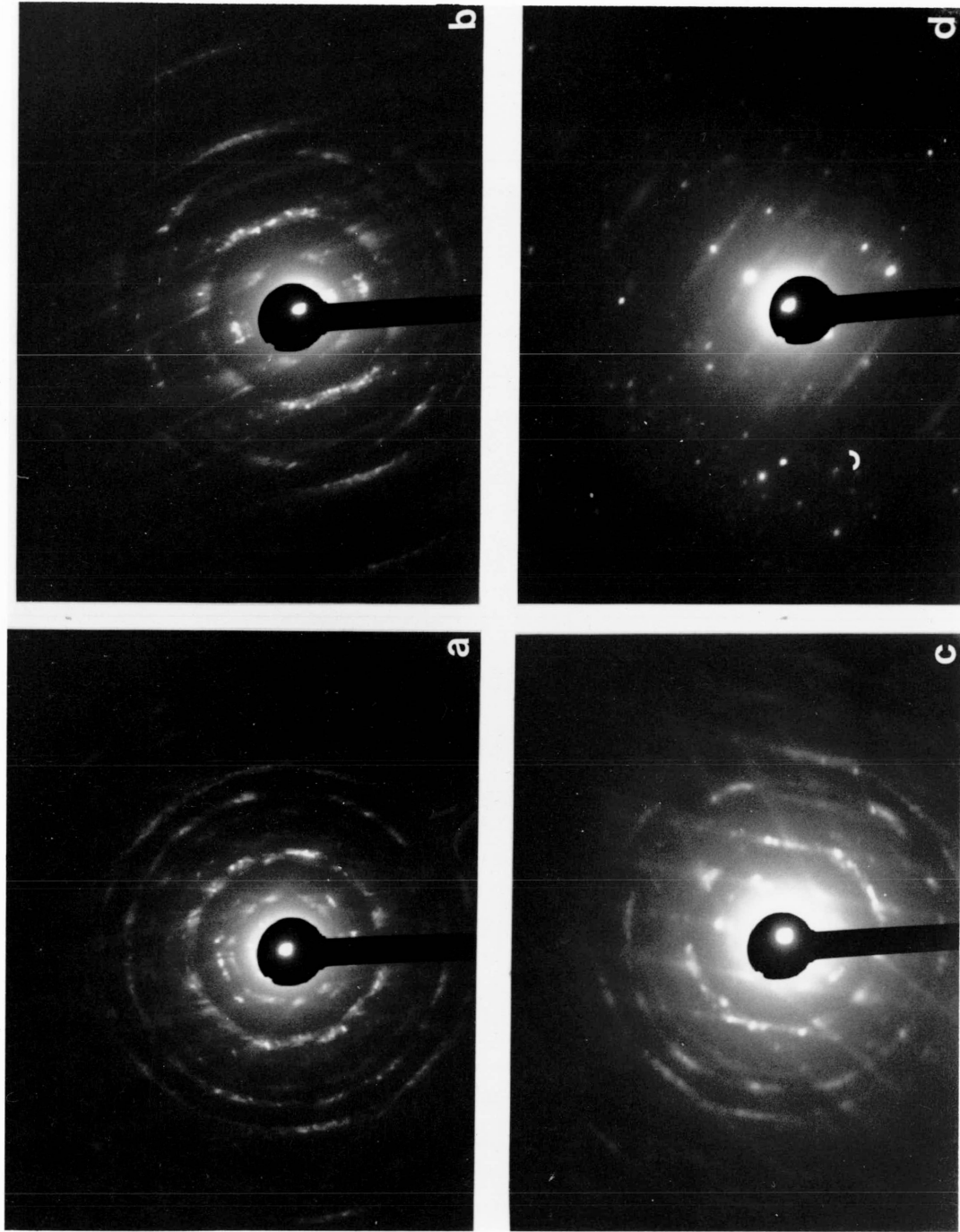


PLATE 2 SELECTED AREA ELECTRON DIFFRACTION STUDIES OF CALIFORNIAN CHRYSOTILE HEAT-TREATED AT 150°C (A), 300°C (B), 500°C (C), 700°C (D).

at 77 K on Quebec chrysotile heat-treated at 150, 300, 500 and 700°C, Figure 35.

As in the case of the Californian samples, the amount of nitrogen adsorbed at N. T. P. at any relative pressure was similar for all the treated Quebec samples. However, unlike the Californian samples, the pattern of hysteresis was somewhat more varied. For example, the height of the hysteresis loop was progressively greater from the 150°C sample to the 700°C sample. Hysteresis began at $p/p_0 = .93$ for all the chrysotiles but the loop closed at 0.10, 0.15, 0.30 and 0.20 for the 150, 300, 500 and 700°C samples respectively. Again equilibration times were long, at approximately 60 minutes for all surfaces.

B. E. T. plots were calculated from the adsorption data, Figure 36. The calculation parameters were identical to those of the Californian chrysotile for the surface area determinations. Surface area results are presented in Table 3.5.

Table 3.5.

Surface Areas for Quebec Chrysotile Heat-Treated at 150, 300 500 and 700°C

	Activation Temperature of Quebec Samples (°C)			
	150	300	500	700
Surface Area ($m^2 g^{-1}$)	37	38	42	42

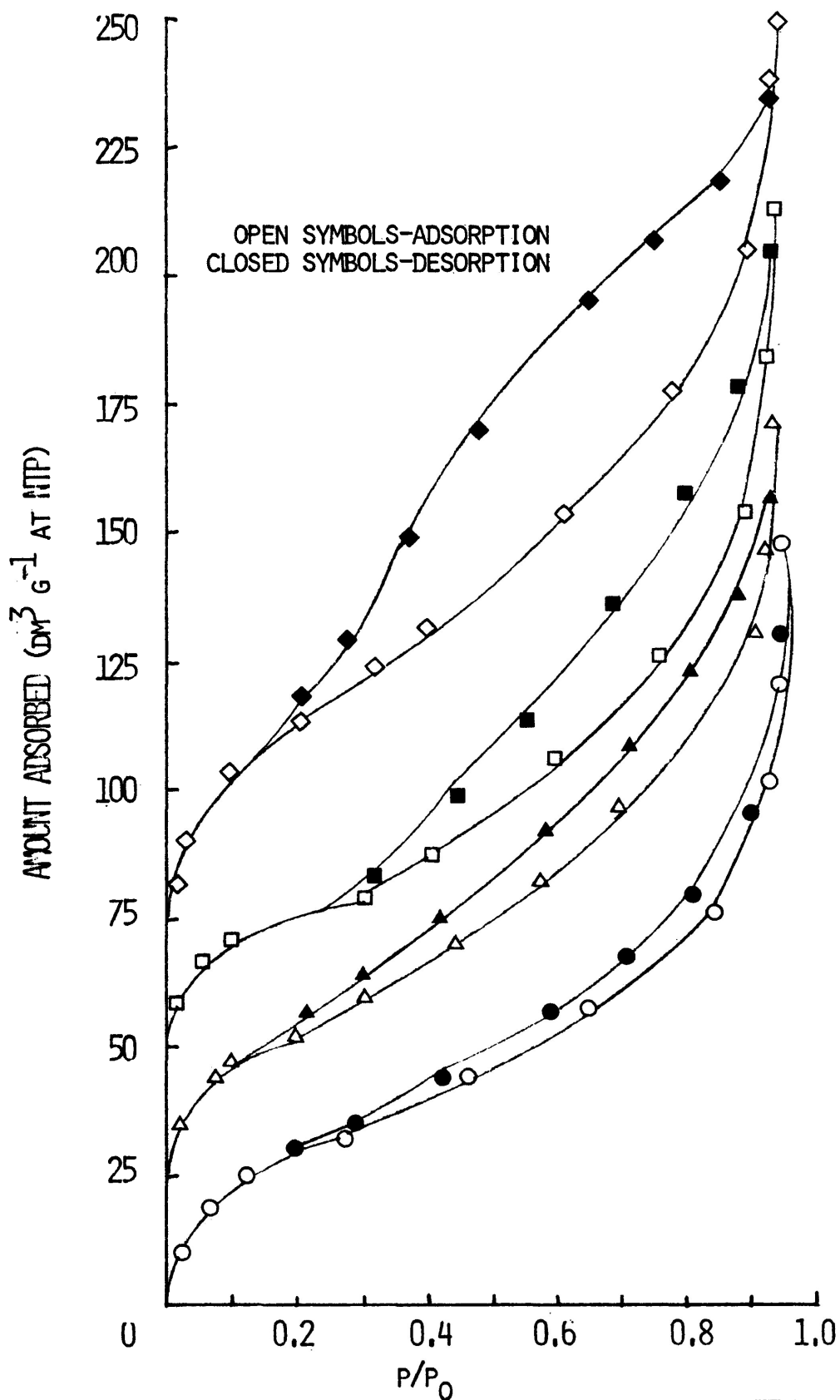


FIGURE 35 NITROGEN ADSORPTION/DESORPTION ISOTHERMS AT 77K ON QUEBEC CHRYSOTILE HEAT-TREATED AT 150 (\circ), 300 (Δ , ORIGIN DISPLACED TO $25 \text{ DM}^3 \text{G}^{-1}$), 500 (\square , ORIGIN DISPLACED TO $50 \text{ DM}^3 \text{G}^{-1}$) AND 700 (\diamond , TO $75 \text{ DM}^3 \text{G}^{-1}$) $^{\circ}\text{C}$

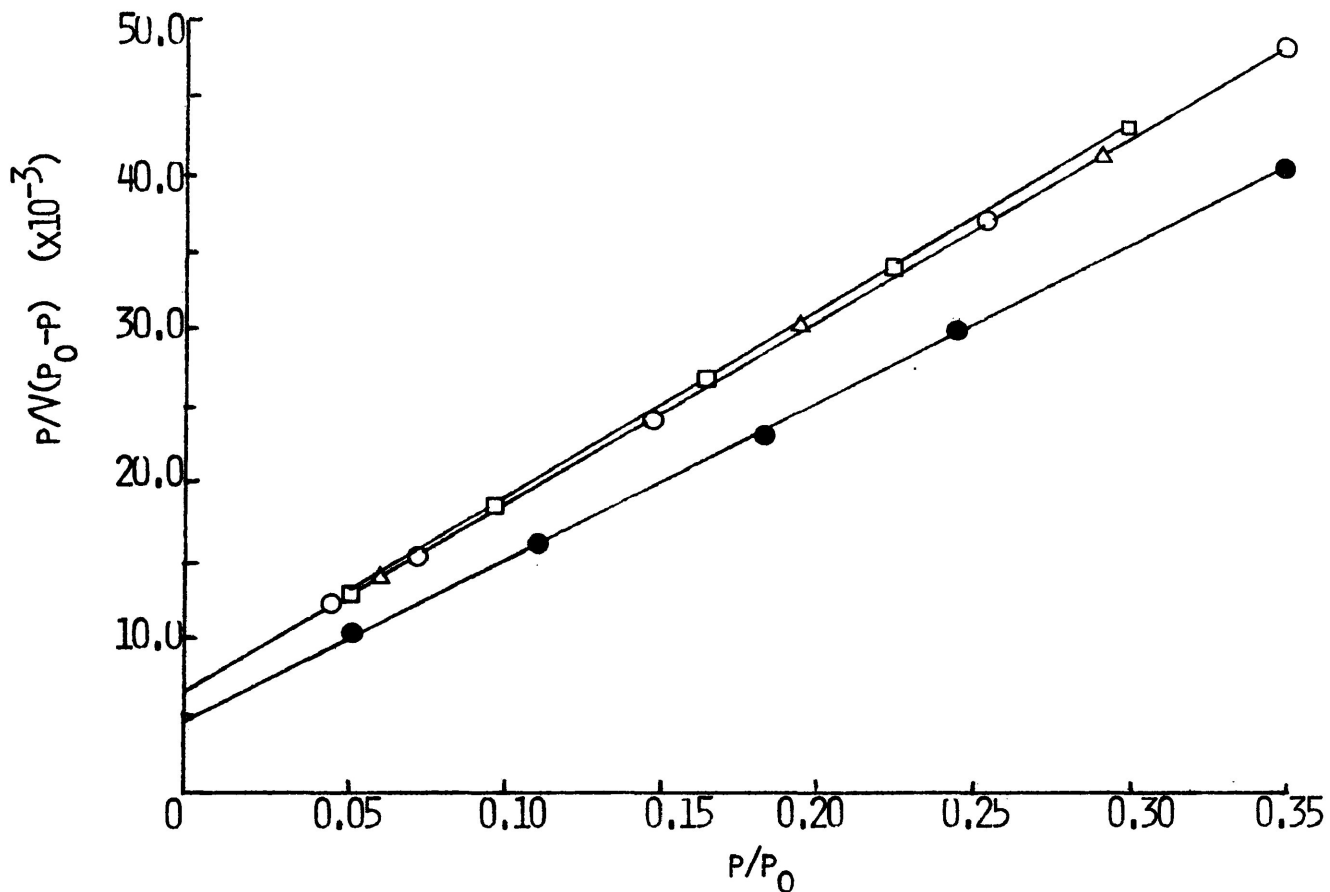


FIGURE 36 B.E.T. PLOTS FOR NITROGEN AT 77K ON HEAT TREATED QUEBEC CHRYSOTILE. HEAT TREATMENT AT 150 (○), 300 (△), 500 (□), AND 700 (●)°C.

The method of Cranston and Inkley (49) was again used to find an approximate pore size distribution plot for each of the heat-treated Quebec chrysotiles, in the same manner that it was used for the Californian material. The pore diameter range for all samples fell between 15 and 200 Å, Figure 37. Maxima for the 150°C sample plot were located at < 20, 30 and 55 Å. The 300°C sample plot indicated that the smallest (< 20 Å) pores collapsed leaving an increased number of 30 and 55 Å pores. The 500°C plot showed a shift of the maximum to the 20 to 25 Å range. This was the sole maximum observed for this activation temperature. A small maximum appeared at 65 Å diameter on the 700°C plot otherwise it was similar to that for the 500°C sample.

As in the case of the Californian samples the Dollimore-Heal method was used to generate pore distribution data, Figure 38. The charts showing the 150, 300 and 500°C samples indicated that the number of small pores (< 20 Å) was decreasing with increasing treatment temperature but there was a fairly constant second maximum for the three samples at a radius of 35 Å. The 700°C sample plot showed a reformation of small pores radius < 20 Å, and a second maximum, as in the other samples, at 35 Å. As might now be expected, the surface changed appreciably for the 700°C sample only.

3.10.3.2. Electron Microscopy

Plates 3(a) - (d) show transmission micrographs and plates 4(a) - (d), electron diffraction studies of Quebec samples heat-treated at 150, 300, 500 and 700°C. Again no significant

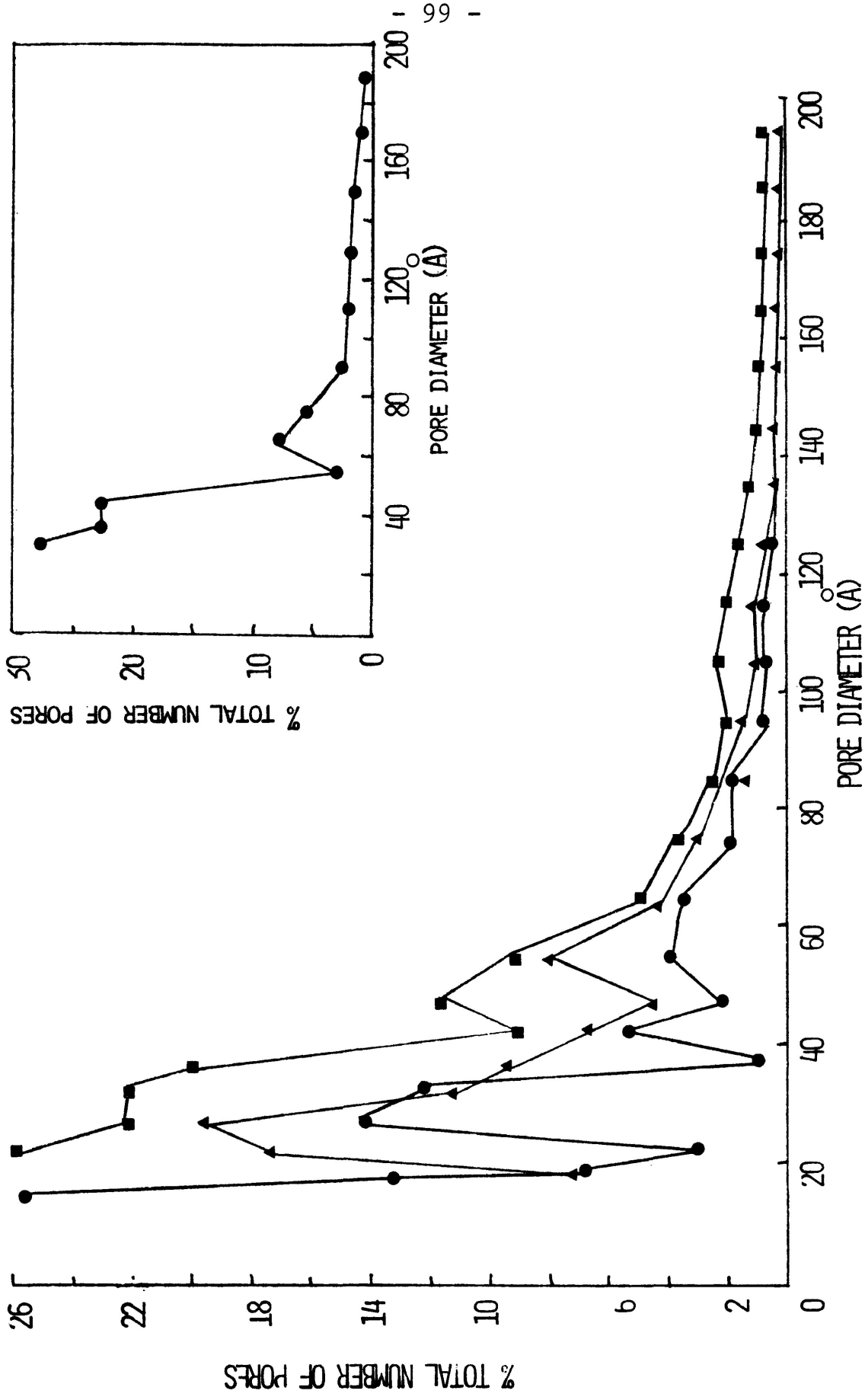


FIGURE 37 PORE SIZE DISTRIBUTION BASED ON NITROGEN DESORPTION AT 77K ON QUEBEC CHRYSOTILE HEAT-TREATED AT 150 (●), 300 (▲), 500 (■), AND 700 (▼) °C. BASED ON THE METHOD OF CRANSTON AND INKLEY.

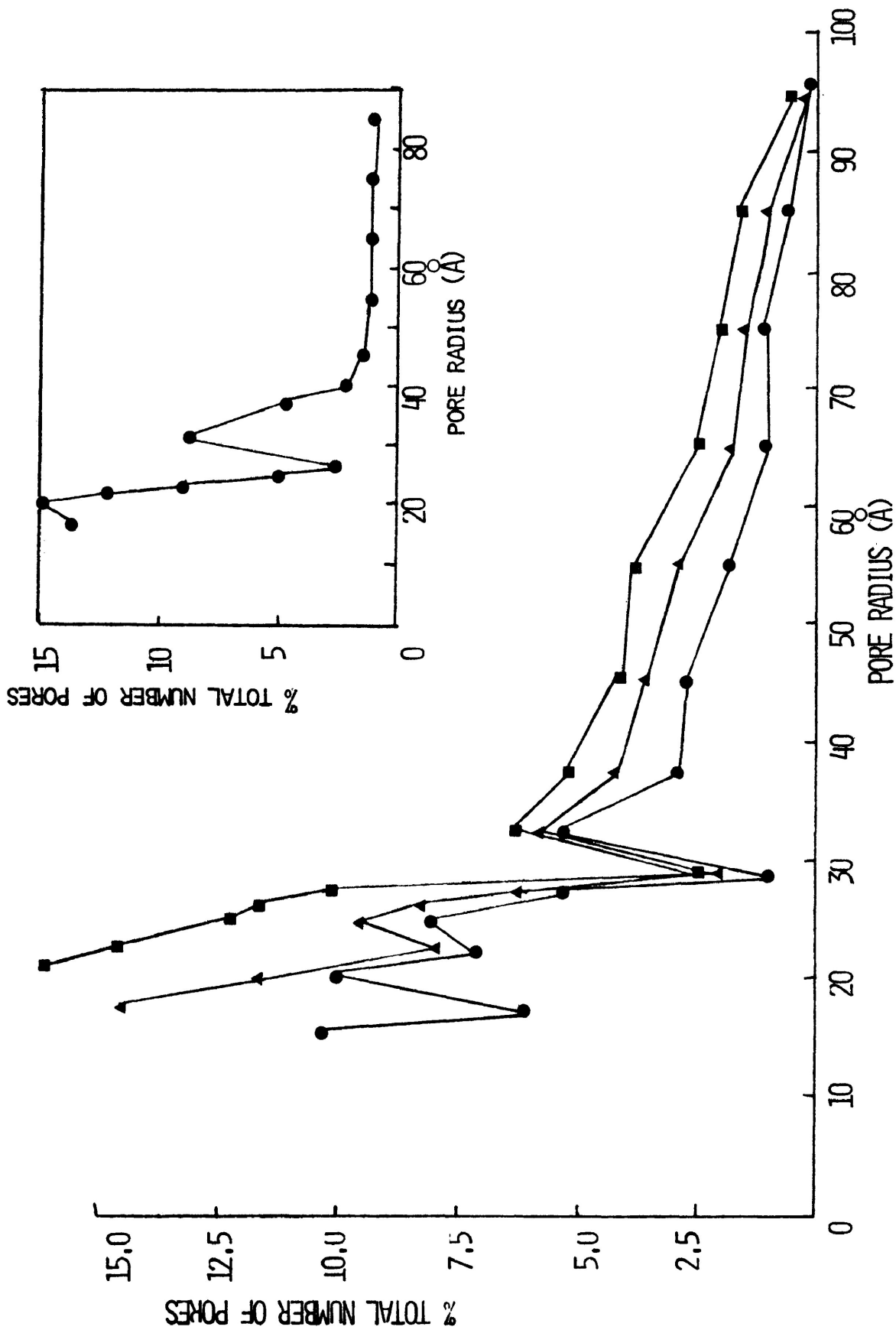


FIGURE 38 PORE SIZE DISTRIBUTION BASED ON NITROGEN DESORPTION AT 77K ON QUEBEC CHRYSOTILE HEAT-TREATED AT 150 (●), 300 (▲), 500 (■), AND 700 (◆), BASED ON THE METHOD OF DOLLIMORE AND HEAL.



PLATE 3 TRANSMISSION ELECTRON MICROGRAPHS OF QUEBEC CHRYSOTILE HEAT-TREATED AT 150°C (A), 300°C (B), 500°C (C), AND 700°C (D). MAGNIFICATION: 52812X

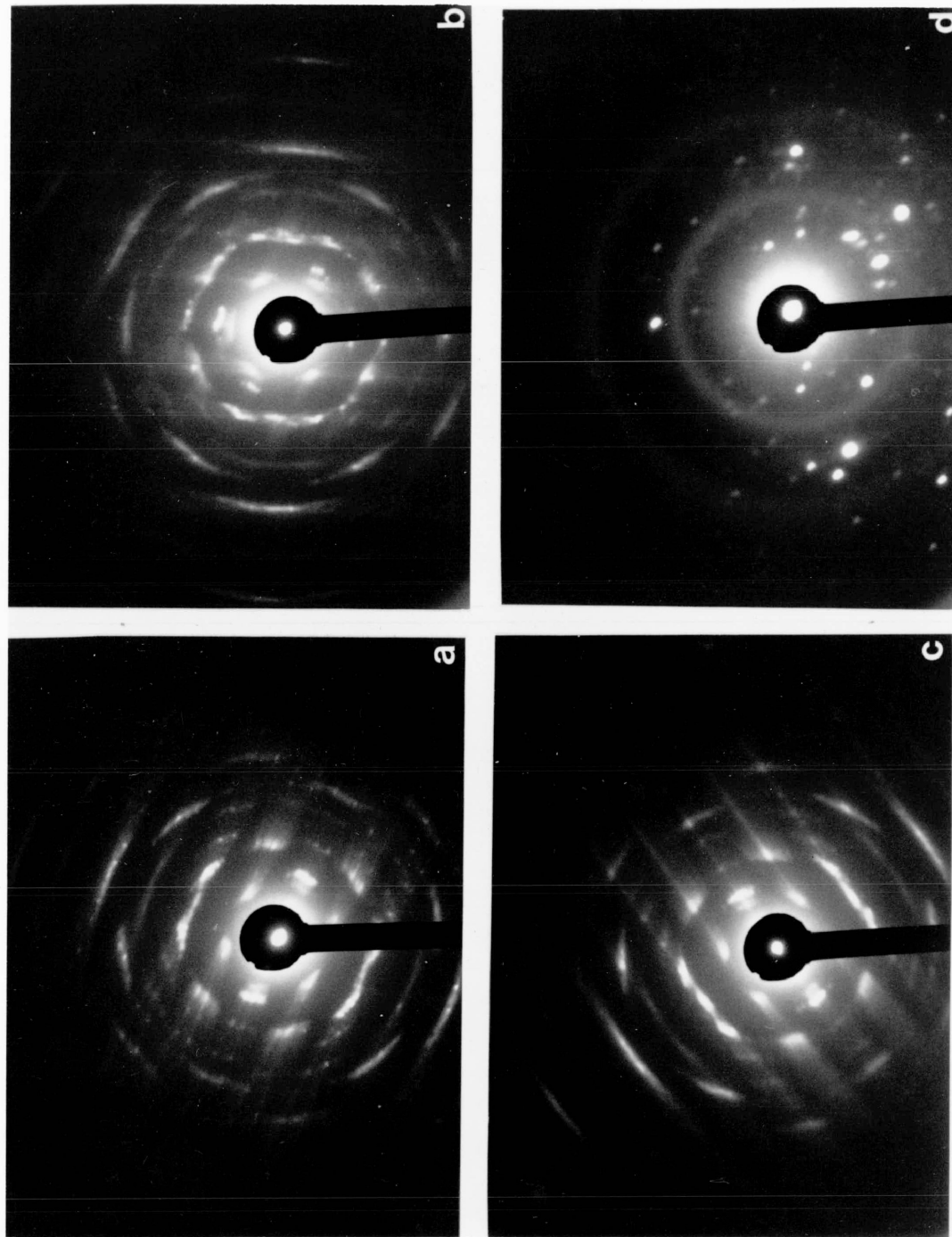


PLATE 4 SELECTED AREA ELECTRON DIFFRACTION STUDIES OF QUEBEC CHRYSOTILE HEAT-TREATED AT 150°C (A), 300°C (B), 500°C (C), AND 700°C (D).

differences in structure were observed until the adsorbent had been heated to 700°C. Whereas the Californian samples were conglomerations of discrete fibres, the Québec material tended to exist as fibre bundles. Some cracking and flaking was observed in the 700°C micrograph, due probably to the dehydration phenomenon. Again, electron diffraction studies showed retention of the chrysotile structure through 500°C but the sample was amorphous at 700°C.

3.10.4. Californian Chrysotile Treated with Water and Sodium Nitrate

3.10.4.1. Low-Temperature Nitrogen Adsorption

Nitrogen adsorption/desorption isotherms were determined at 77 K on Californian chrysotile treated with water and sodium nitrate, Figure 39. The amount of nitrogen adsorbed at any given relative pressure was similar to the heat-treated samples. No apparent difference existed with respect to the hysteresis loops. Equilibration times were also similar to those observed for all of the heat-treated samples.

B. E. T. plots for the two treated samples are shown in Figure 40. Again the plots were good straight lines from which the surface areas were calculated. The B. E. T. surface area for the water-treated sample was $57 \text{ m}^2 \text{ g}^{-1}$. Within the margin of error of the method (1) it may be stated that these values were not significantly different from those of the heat-treated Californian chrysotile (i. e. $60 \text{ m}^2 \text{ g}^{-1}$).

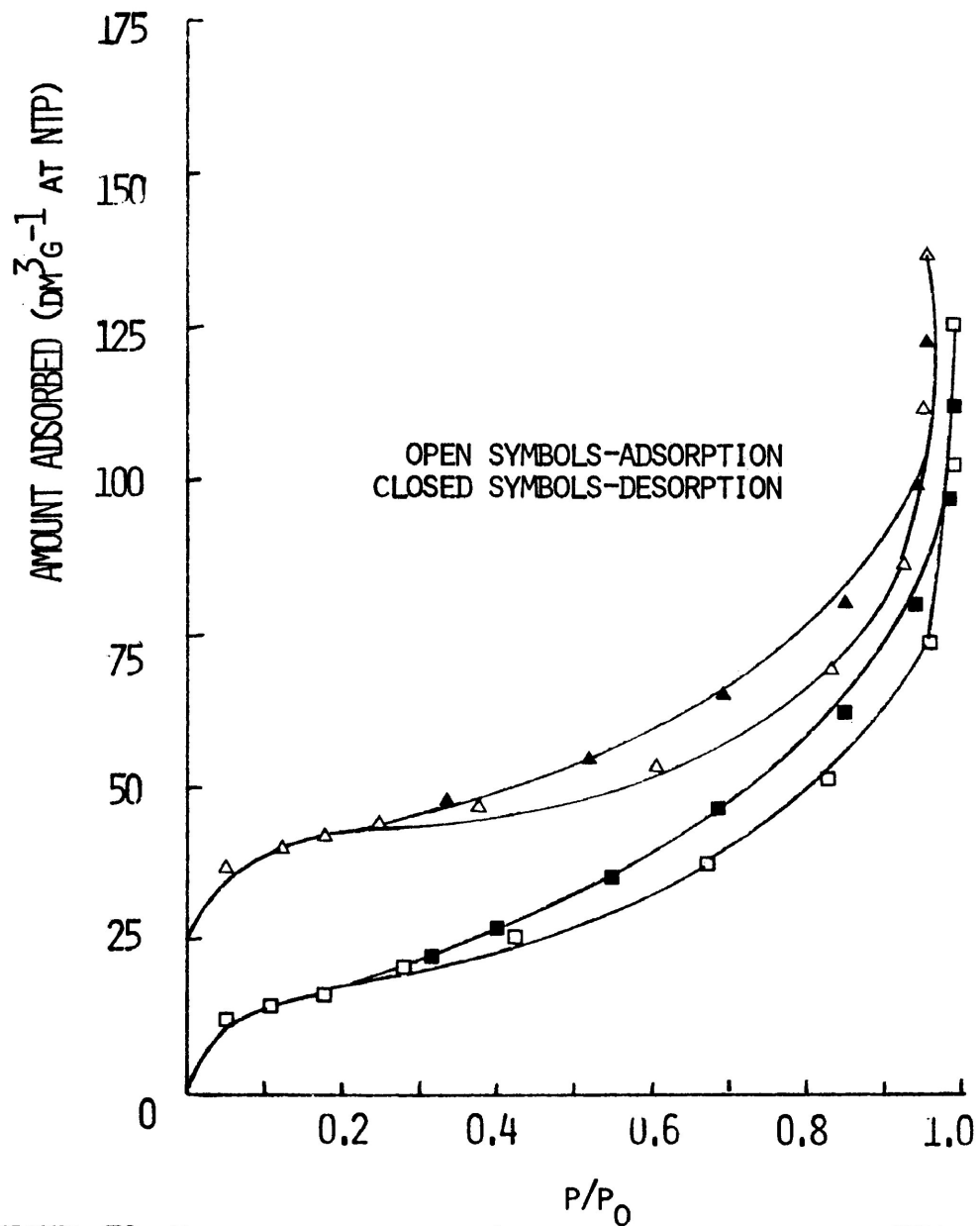


FIGURE 39 NITROGEN ADSORPTION/DESORPTION ISOTHERMS AT 77K ON CALIFORNIAN CHRYSOTILE TREATED WITH WATER (\square) AND SODIUM NITRATE (\triangle , ORIGIN DISPLACED TO $25 \text{ DM}^3\text{G}^{-1}$).

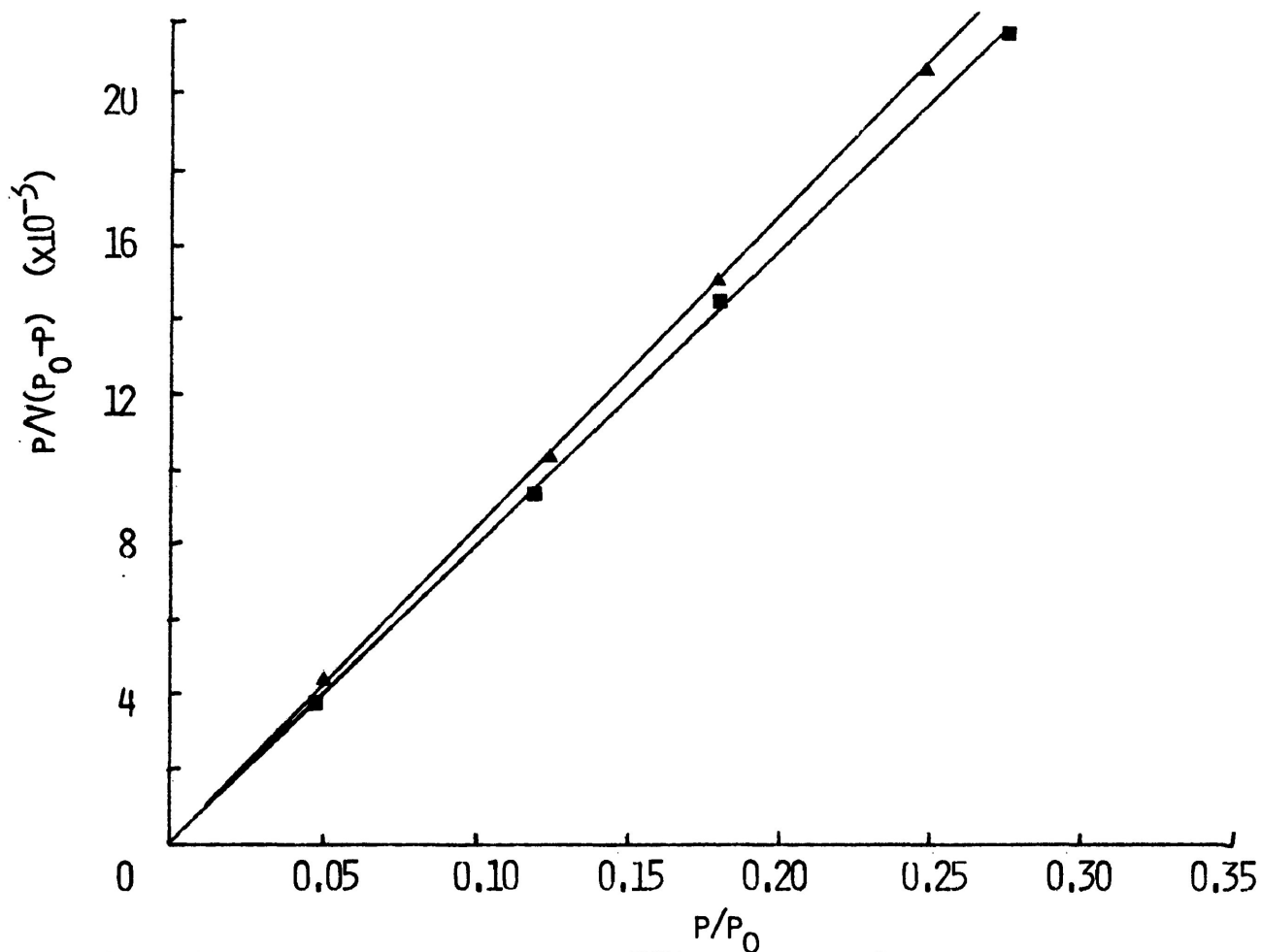


FIGURE 40 B.E.T. PLOTS FOR NITROGEN AT 77K ON TREATED CALIFORNIAN CHRYSOTILE. TREATMENT WITH WATER (\blacksquare), AND SODIUM NITRATE (\blacktriangle).

The Dollimore-Heal method was used to compute approximate pore size distributions for the treated samples, Figure 41. The two charts were virtually identical to each other and were also similar to that for the 150°C sample. The maxima were similar to the latter, the only difference being a decrease in the number of small pores ($< 20 \text{ \AA}$) and a corresponding increase in the second maximum (30 \AA).

3.10.4.2. Electron Microscopy

No electron micrographs or electron diffraction patterns were included for the chemically-treated samples as no differences could be observed between them and those obtained with the 150°C sample. The fibre structure would seem to have remained intact although some chemical changes may have occurred.

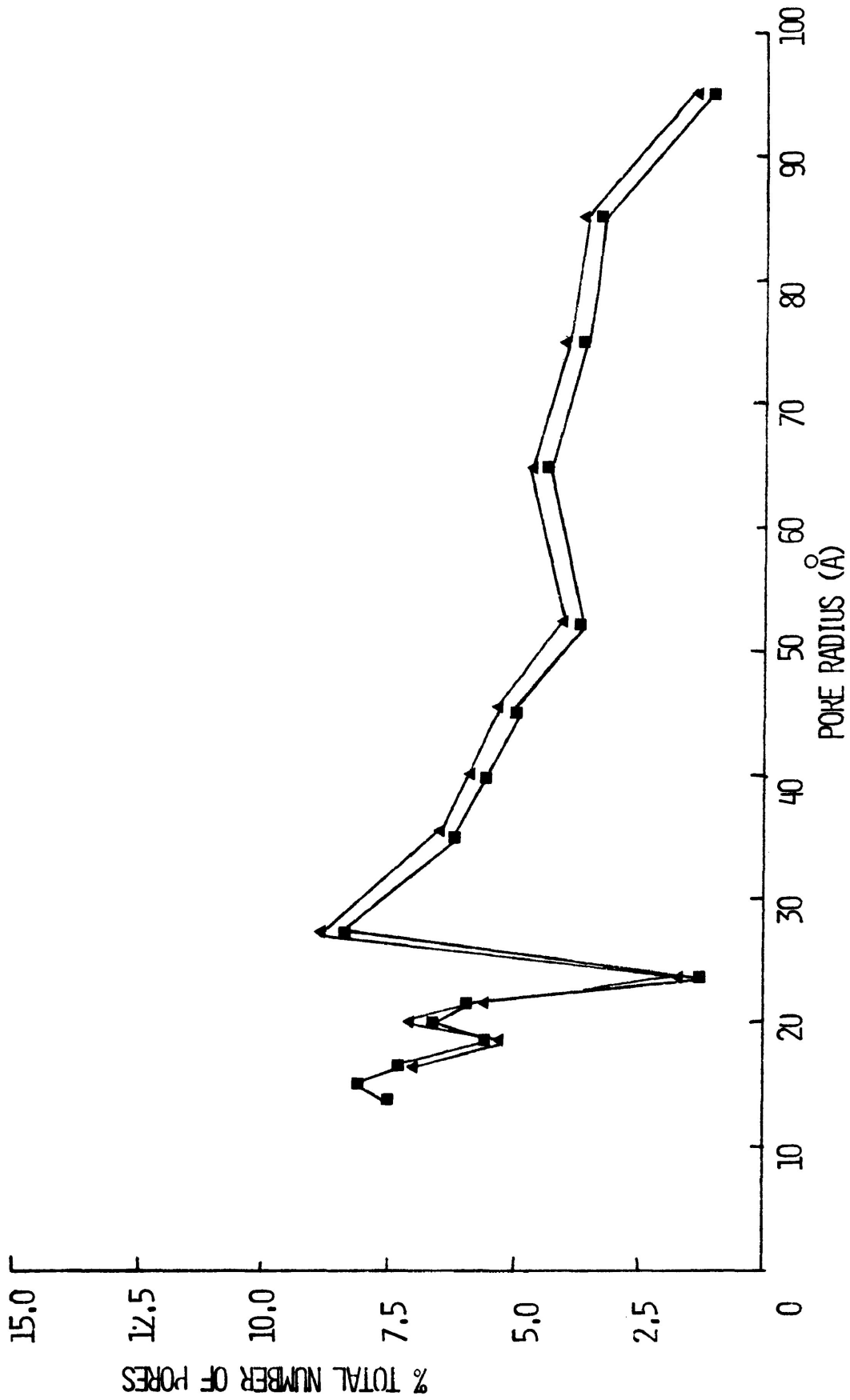


FIGURE 41 PORE SIZE DISTRIBUTION BASED ON NITROGEN DESORPTION AT 77K ON CALIFORNIAN CHRYSOTILE TREATED WITH WATER (■) AND SODIUM NITRATE (▲), BASED ON THE METHOD OF DOLLIMORE AND HEAL.

CHAPTER 1V

4. Discussion

4.1. Introduction

A variety of studies (10-13, 41, 74-79) of ammonia sorption on solid adsorbents have yielded some interesting theories regarding the "binding" of the gas at adsorption sites. A number of the investigations dealt with ammonia adsorbed on silica surfaces (11-13, 74-79) which may have some features in common with ammonia adsorption on chrysotile since it is essentially a porous magnesium silicate. However, comparisons cannot be taken too far because of the small dimensions of the ammonia molecule and the highly porous nature of the chrysotile surface with its fibrous structure and large capillaries which are believed to exercise substantial influence on the results obtained in the present study.

The general conclusion of most authors with respect to the nature of the adsorption of ammonia on silica or silica-like surfaces was that hydrogen-bonding occurred at low surface coverages and that van der Waals forces were responsible for interactions that occurred at higher degrees of coverage. In all of those cases, the heat of adsorption of ammonia exceeded the heat of liquefaction of the gas.

4.2. Adsorptions on Californian Chrysotile

The amount of ammonia adsorbed on Californian chrysotile

decreased with an increase in activation temperature from 150 to 700°C. From 150 to 500°C there was a fairly small decrease in the adsorbed amount while at 700°C there was a significant decrease which may be explained by the observation that on activation to 500°C the Californian sample retained a large degree of chrysotile crystal structure while at approximately 650°C the chrysotile structure disappeared and selected area electron diffraction studies showed that forsterite had formed (27).

In their study of the thermodynamics of ammonia adsorption on silica-alumina surfaces, Clark, Holm and Blackburn (12) observed isotherms somewhat similar to those obtained in this study. The steep initial rise of the isotherm followed by a slower increment possibly indicated that the surface had a variety of sites with adsorption energies from "weak" to "strong" (i. e. the surface was heterogeneous with respect to energy sites). Folman and Yates (41) believed that the decrease in the adsorption gradient was related to differences in the energy of adsorption at various kinds of hydroxyl sites on the surfaces and that as these sites were taken by ammonia molecules, fewer would be adsorbed. Also, desorption may have occurred first from sites of lower adsorption energy and then more slowly from those of higher energy, which perhaps accounted for the large hysteresis effect observed at low pressures.

It is interesting to note that in a study of ammonia adsorption on silica xerogel (13) it was demonstrated that

adsorption was accompanied by a measure of catalytic dehydrogenation. In samples that had been constant in weight, it was shown that additional water was lost on desorption, as confirmed by infrared spectroscopy. It was observed, using mass spectrometry, that in the case of asbestos some of the desorbed material included additional water.

Although thermodynamic studies do not provide enough information to characterise, independently, the types of sites present on the surface, interesting data were obtained and could be related to the nature of bonds formed and the mobility of the adsorbed species.

In all cases the curves of heat of adsorption versus surface coverage for ammonia on heat-treated Californian chrysotile showed an extremely rapid decrease in heat from a high value at low coverage to a low value at high coverage. Other studies of ammonia adsorption on silica surfaces (11-13, 74-79) documented results of the same type. These data would be in agreement with the proposals regarding high and low energy surface sites. Results of this study indicated an increase in the heat of adsorption following the minimum. This phenomenon was also observed by two authors (11, 12) in studies of ammonia sorption on silica. Clark (12) attributed the increase as being due to exothermal interactions between neighbouring ammonia molecules. A corresponding decrease in entropy was also observed in the present results indicating a decrease in the mobility of the adsorbed species possibly

because of these interactions. Hsieh (11) also observed the increase after the minimum but it was very large, approximately 75% of the original height of the curve, followed by a gradual decrease. It could be that in the present work, only the start of the increase was observed since a lower degree of surface coverage was examined. Hsieh (11) reasoned that the initially high heats at low surface coverages were due to a combination of several factors including the possibilities that surface protons combined with ammonia to form adsorbed ammonium ions, that surface hydroxyl groups formed hydrogen bonds with ammonia and that the surface sites acted as Lewis acids and accepted electrons from the lone pair on the nitrogen atom in the ammonia molecule. It was felt that the van der Waals forces and/or induced dipole effect postulated by other authors (12, 80) to account for the unusual increase in heat after the minimum could not account for the large increase observed in this work. The initially high heats were probably due to the neutralization of all types of surface acids forming ammonium ion and highly polarized ammonia molecules. The minimum was reached when all the surface acid had been neutralized at which time "new" ammonia molecules interacted with the ammonium ion and ammonia polarized by coulombic and van der Waals forces associated with the adsorbent surface. The increase in heat was explained by the coulombic interaction and the gradual decrease occurred only when four ammonia molecules were co-ordinated to each ammonium ion, Figure 42.

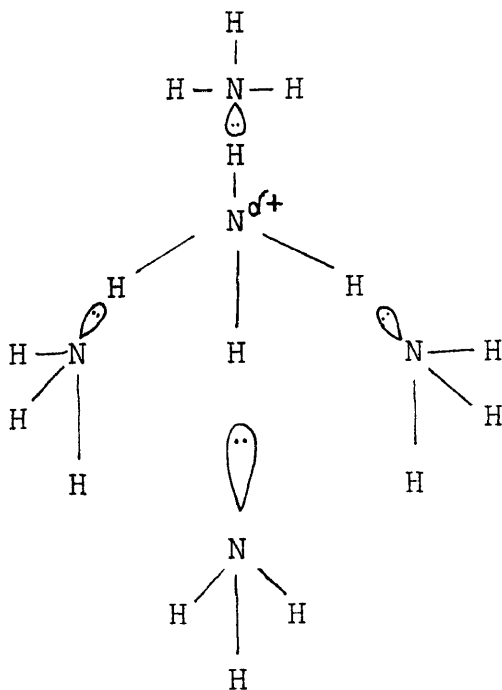


Figure 42. Hsieh's Model of Ammonia Co-ordinated to Ammonium

It was found (11) that high energy sites were deactivated to a large extent on heating, resulting in decreased amounts of gas adsorbed. The slight increase in the heat of adsorption of .2 to .8 kJ observed in the present results was most likely due to a small degree of adsorbate/adsorbate interaction at the surface.

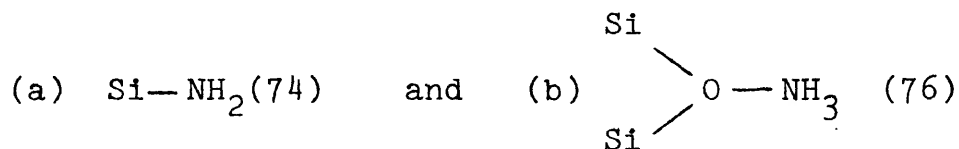
The prevailing concepts regarding the bonding mechanisms associated with ammonia on silica-type surfaces (11-13, 75-79) seemed to involve a combination of hydrogen bonding and van der Waals forces, sometimes in association with more

complex interactions.

The hypothesis of a weak chemisorption at low surface coverages, some degree of hydrogen bonding, followed by an interaction involving weak van der Waals forces at high coverages seemed reasonable also to explain the adsorption of ammonia on chrysotile. Also, an argument will be developed later involving the possibility of molecular diffusion into the capillaries of the asbestos fibre which results in the formation of a highly mobile adsorbed species.

The pattern of the heat of adsorption curves supported the above models as did the entropy curves which showed an increase from a low entropy at low coverages to a high value at high surface coverages. The low initial entropy perhaps indicated that adsorbate molecules were most tightly bound (i. e. chemisorbed) at low coverages while the high values corresponding to the theoretical curves for mobile entropy and, indeed, approaching Kemball's (67) "supermobile" state may have shown that those molecules were physically adsorbed or have diffused into the large capillaries of the fibre.

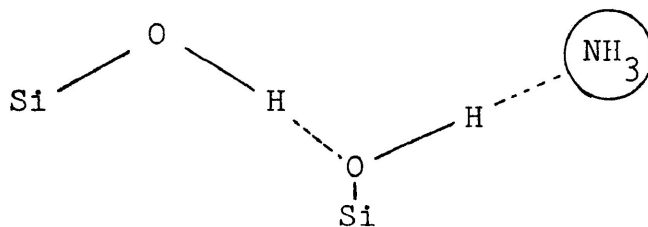
At least two authors (74, 76) felt there was some evidence for the formation of groups of the following nature:



Blomfield and Little (74) found that dehydroxylated silicas contained sites which dissociated ammonia to form species (a)

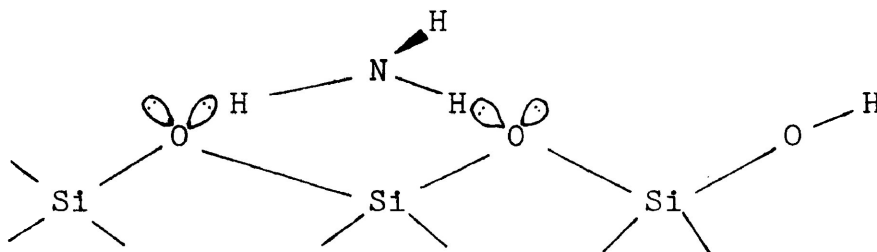
and also claimed infrared evidence to prove its existence. Griffiths et al (76) suggested species (b) but did not evacuate the ammonia from the samples to verify if the gas was indeed bound chemically to the adsorbent. In the present experiments, several trials were performed where the samples holding adsorbed ammonia were evacuated overnight at 1.33×10^{-4} kPa. The following day, fresh ammonia was introduced onto the sample resulting in the same initially high heats as would be expected of a sample not previously exposed to the gas. It was assumed therefore, that the high energy adsorption sites had been cleared and therefore any chemisorption which had occurred must have been reversible and probably weak.

Another interesting theory (74) which might apply to the nature of ammonia adsorption on chrysotile involved the observation that the gas was adsorbed on "free" hydroxyl groups on the silica surface in preference to hydroxyl groups that were hydrogen-bonded to each other. It was also found, as with the present samples, that physical adsorption sites decreased in number as heat-treatment temperatures were increased and also that at low pre-treatment temperatures the bands, on the infrared spectrum, for OH...NH₃ interactions were intense. A corresponding decrease in the band intensity for isolated OH groups was also observed. This would mean that preferred physisorption of ammonia might occur:



Cant and Little (75) indicated that chemisorption of ammonia on porous silica glass was only enhanced when trace oxides were present on the surface. This would suggest that the trace oxides rather than the surface hydroxyl groups were responsible for strong chemisorption phenomena.

In addition to their ammonia/siloxane model Griffiths et al (76) also felt there was sufficient ir evidence to show ammonia hydrogen-bonded to oxygen lone pairs on silicon-oxygen bridges. Their model, below, indicated that a double (and possibly treble) oxygen site was possible.

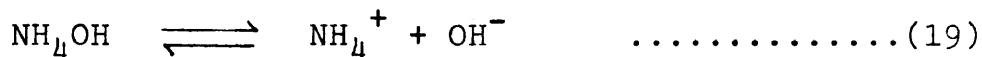
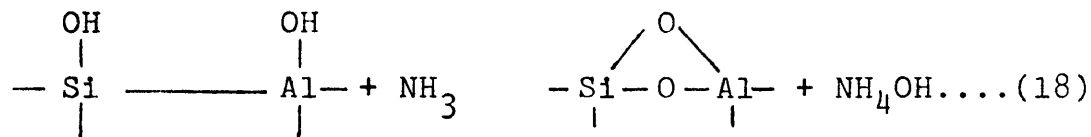


There was good agreement among several authors (77, 78, 81, 82) that hydrogen bonding was the main form of attraction of the adsorbate to the adsorbent in the case of ammonia on silica gel. In addition, Basila and Kantner (77) supported the argument that the silica surface acted as an assembly of Lewis acid sites. In fact, the amount of ammonia adsorbed at a given temperature was used (77) as a measure of the number

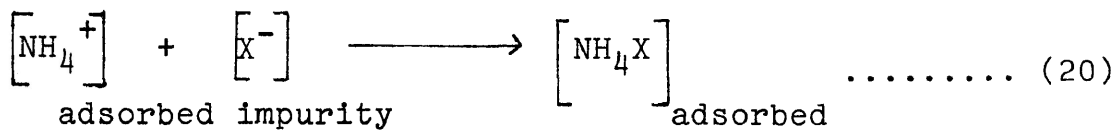
of acid sites of a given strength (defined arbitrarily by temperature) on a catalytic surface. Kvlividge (78) explained the high initial heat of adsorption values by suggesting a donor-acceptor bond between the nitrogen of ammonia and the free 'd' orbitals of the silicon atom aided by a free electron pair. This author also showed that acid-washed silica gel with a surface area of $370 \text{ m}^2 \text{ g}^{-1}$ adsorbed total amounts of ammonia in the order of 6 to $10 \text{ } \mu\text{mol m}^{-2}$. This observation was interesting with respect to the present study where it has been shown that the amount of ammonia adsorbed was of the same order but the surface area of the chrysotile was only 40 to $60 \text{ m}^2 \text{ g}^{-1}$. These features perhaps lend some credence to the concept that there may be diffusion into cylinders not suitable for nitrogen adsorption and therefore all adsorption did not occur at the outer surface. The comparative sizes of the molecules are - nitrogen, $16.2 \text{ } \text{Å}^2$ and ammonia $13.96 \text{ } \text{Å}^2$. It has been found (18) that the apparent surface area for ammonia adsorption was greater than that for nitrogen at normal temperatures with respect to untreated chrysotile. However, as heat-treatment temperatures were increased the surface area determined by either ammonia or nitrogen became similar.

The observations that dehydration occurred with heat-treatment and the amount adsorbed decreased with increased temperature of heat treatment can be related and it may be postulated that the form of attachment of ammonia to the

chrysotile was by hydrogen bonds to the surface hydroxyl groups. It has been determined (81) that the heat of formation of one hydrogen bond can vary from 12 to 25 kJ mol⁻¹ and hence some hydrogen bond formation might be expected particularly between the first dose of ammonia and the solid surface. The heat evolved by the adsorption of the first dose was invariably too great to be measured by the present system but it may be assumed that it was at least 100 kJ mol⁻¹ in magnitude. It must not be inferred, however, that the high heats of the first dose of gas are due to classical hydrogen bonding as the heat would be too high to account for that possibility. Instead we may consider that the high initial heat could be due to ammonia adsorption on an impurity in the chrysotile. The surface was not prepared or cleaned in order to avoid the presence of low concentration levels of heterogeneous materials. There could be anions or cations capable of reaction with the ammonia in the presence of hydroxyl groups (present through dehydration) to yield salts of ammonium or ammonium complexes. For example, ammonium ion could be formed thus:



The ion might then react with an impurity (X) in the following manner to yield an adsorbed complex:



The hydroxide from ammonium hydroxide itself, though not an impurity could be (X) in equation (20). Therefore, the most labile hydroxyl groups, when placed in juxtaposition, could react to give ammonium hydroxide. The heat of formation for the hydroxide is $-366.5 \text{ kJ mol}^{-1}$ which is very high but it could be that only a few molecules of ammonia react in this way, even within the first dose, and therefore a heat of adsorption of approximately 100 kJ mol^{-1} could include ammonium hydroxide formation "diluted" with less powerful forces of adsorbate/adsorbent interactions. It is possible that this reaction and others involving trace impurities (possibly transition metals) could occur giving very small amounts of salts and/or complexes as reaction products.

The first point recorded on each of the heat of adsorption versus surface coverage plots was actually the heat from the second dose of adsorbate admitted to the calorimeter vessel and it was generally between 15 and 20 kJ mol^{-1} , sufficiently high to be associated with hydrogen bond formation. The decrease in the limiting heat of adsorption with increase in activation temperature observed for the Californian chrysotile was consistent with the theory of a reduction in the number of surface hydroxyl sites with heat treatment.

One of the most difficult observations to explain was

that the "limiting" heat in all cases of ammonia adsorption on chrysotile was 15 to 20 kJ lower than the heat of liquefaction of ammonia, $21.55 \text{ kJ mol}^{-1}$ at 273 K. De Boer (8) cited an example of water adsorption on charcoal where the same phenomenon occurred and similar explanations may apply to ammonia on chrysotile. The van der Waals forces associated with a molecule of a volatile substance on the surface of a solid will generally be greater than the van der Waals forces which contribute to the binding of the molecule in its own liquid. Therefore, in most cases, the heat of adsorption is greater than the heat of liquefaction (3, 4). There are exceptions to this rule including the aforementioned water on charcoal example where water molecules were weakly bound and the polar character of the species did not aid in the process. In this case the heat of adsorption was less than the heat of liquefaction. Adsorption, however, did occur because the influence of entropy dominated. Thus the entropy of the adsorbed state was higher than in the solid or liquid state and therefore the adsorbed molecules had a greater degree of freedom than molecules in the liquid or solid state. This might apply to ammonia adsorption on chrysotile where the entropy of the adsorbed state at 298 K was approximately $170 \text{ J deg}^{-1} \text{ mol}^{-1}$ and the entropy of liquid ammonia at that temperature is $108.91 \text{ J deg}^{-1} \text{ mol}^{-1}$. For chrysotile, ammonia adsorption approached the "supermobile" model for entropy (67) where the value was close to that expected of a three-dimensional

gas. In other words, the degree of translational freedom perpendicular to the surface that was lost to the adsorbate on adsorption became a vibration of low frequency in that direction (8). The entropy value of the mobile film increased to an extent which depended on the frequency of that particular vibration but, as can be noted from the plots of the entropy of ammonia adsorbed at various temperatures on 500°C chrysotile, when temperature was decreased, the frequency of the vibration decreased and the "limiting" entropy value approached that of a mobile film. In the case of these unusual adsorption processes the entropy was indeed high enough for adsorption to occur but the transfer of an adsorbate molecule from the liquid state to the surface of the adsorbent was endothermic rather than exothermic resulting in unexpectedly low "limiting" heats.

Another possible explanation for the low "limiting" heats could involve capillary adsorption (8). Molecules of the adsorbate could penetrate into the capillaries of the chrysotile fibre and this might be treated as a diffusion process. Both the lengthy equilibration time and the irreversible adsorption might indicate that a process such as this was occurring. The mechanism of diffusion could be one of a number of possibilities (8). It could be that the adsorbent molecules collided with the capillary wall, evaporated immediately, collided again etc. resulting in no energy of activation or they could have collided with the capillary wall, rested

for a time, re-evaporated, collided again, rested, etc., thus the energy of activation would equal the heat of adsorption. Thirdly, the molecules might migrate along the capillary wall, over a time in a "hopping" motion causing shorter rest times and an energy of activation less than the heat of adsorption. The diffusion process was endothermic and would therefore result in a heat of adsorption lower than expected (8).

In summary, ammonia adsorption on Californian chrysotile seemed to involve a mixture of a weak chemisorption, perhaps related to the Lewis acid sites on the surface (11) or to the presence of an impurity, and an attraction which is mostly "physical" in nature and which might be explained by some hydrogen bonding of ammonia to the surface hydroxyl groups with a contribution from weaker van der Waals forces. The irreversibility of adsorption evident from all the isotherms suggested some stronger attraction but overnight evacuation of the sample resulted in an ammonia-free surface which supported the concept of a slow return to reversibility through the mechanisms outlined which involved somewhat weaker forces than those normally expected in a strong chemisorption process.

Only ammonia and water were detected in the desorbed gas by mass spectrometry which indicated that any other species formed only played an intermediate role on the surface. The inordinately low heats of adsorption in relation to the heat of liquefaction could be related to De Boer's (8) theories regarding the importance of entropy in adsorption phenomena

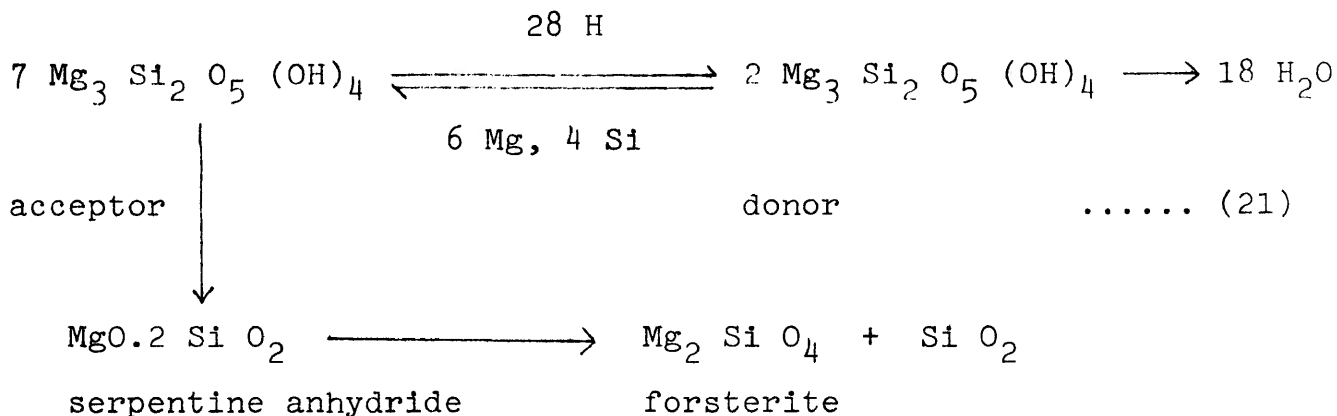
or by a balancing contribution from an endothermic process such as diffusion into the large capillaries of the fibre surface.

4.3. Adsorption on Quebec Chrysotile

With respect to the adsorption of ammonia, Quebec chrysotile appeared to possess two distinct surfaces as a result of heat treatment. One was associated with samples treated up to 300°C and another with samples treated at 500 and 700°C. This was not in agreement with results collected in an earlier study of the sorption of sulfur dioxide on heat-treated chrysotile (14) which suggested that a large degree of the chrysotile structure was retained on activation to 500°C and therefore there was little change in the amount adsorbed. The structural information may be applicable but perhaps the ammonia molecule with its differing size and chemistry reacted in a different manner at the surface than the sulfur dioxide.

Generally the mechanisms of attachment of the ammonia to the surface were probably similar to that suggested for the Californian sample, the major difference being the presence of the brucite (magnesium hydroxide) impurity. It has been shown (39) that the brucite impurity stabilized the chrysotile with respect to thermal degradation but the brucite itself was destabilized, forming magnesium oxide. As outlined in the literature (14), the magnesium oxide may perturb the donor-acceptor region equilibrium in the Taylor-Ball or Brindley-Hayami mechanisms (33-35) for chrysotile dehydration

by acting as a sink for migratory protons and upsetting the balance of cation migration between the donor and acceptor regions as in equation (21).



Both the donor and the acceptor regions are necessary for dehydration.

A steady decrease in the heat of adsorption at low surface coverage for ammonia on Quebec chrysotile could have been due to a decrease in the number of labile hydroxyl groups associated with brucite. The heat curves for the 150/300°C and the 500/700°C samples tended to merge together at higher surface coverage perhaps implying that the same sites are responsible for adsorption at higher coverage on the related surfaces. It may also be noted that the 500 and 700°C samples tended to level out, with respect to heat of adsorption, at a value higher than that for the 150 and 300°C samples. This effect was consistent with the observation that there was a decrease in the stabilizing effect of the magnesium oxide on the surface hydroxyl groups. Whether or not it was significant, it has been shown (29) that heat treatment after 600°C of

chrysotile containing magnetite (magnetic iron oxide - Fe_3O_4) impurity, such as the Quebec sample, caused the Fe_3O_4 to partially convert to Fe_2O_3 which is non-magnetic.

It is evident from the entropy versus surface coverage curves for the Quebec chrysotile that it behaved in a similar manner to the Californian material with respect to mobility. Again the mobility of the adsorbed species was much higher than the entropy of liquid ammonia possibly indicating a mildly endothermic contribution to the adsorption process. Such a process might again explain the extremely low heats of adsorption found for Quebec chrysotile (8).

All entropy curves approximated the mobile or "supermobile" model for entropy (67). The higher the isotherm temperature, the more mobile the adsorbed species became but as the temperature was lowered the experimental differential molar entropy curve approximated or fell slightly below the mobile model for entropy. It may be that the vibration perpendicular to the surface decreased along with a drop in temperature and the nature of the adsorbed gas was more closely related to that indicated by the two-dimensional model (8).

It may also be noted that the amount of gas adsorbed on the Quebec and Californian chrysotiles was in approximately the same proportion as the surface areas of the two adsorbents, i. e. a 2:3 ratio (39).

It is also possible that there was some adsorption of ammonia

onto surface impurities in this chrysotile as well as in the Californian material. With respect to the magnetite and brucite impurities, especially, there could have been some formation of salts and complexes thus helping to account for the very high initial heats of adsorption.

4.4. Desorption Efficiency of Californian Chrysotile

It appeared that the least efficient desorption occurred with the samples heat-treated at 150 and 700°C. For both samples the first dose adsorbed did not desorb at all and the second dose was only 50% desorbed. At least some of the gas remained on the surface up to the fifth addition at which time all the adsorbed gas was desorbed. The gas on the 300 and 500°C samples was more rapidly desorbed with approximately 30% of the first addition being desorbed and greater amounts for the second and third aliquots. By the fourth gas addition, all the ammonia was desorbed.

These results may perhaps be interpreted using the pore size distributions obtained for the various treated samples. The maxima of the 300 and 500°C sample pore distributions occurred at sizes less than 40 Å while both the 150 and 700°C samples tended to have slightly larger pores. It may be that ammonia molecules adsorbed on the 300 and 500°C surfaces did not penetrate into the small pores as readily as the larger pores of the 150 and 700°C samples. It could also be that the 150°C sample had more available sites suitable for hydrogen bonding (i. e. hydroxyl groups) which held the adsorbate to

the surface. When these sites were depleted the regular weak, reversible forces such as van der Waals attractions took over and adsorption became reversible. It may only be speculated as to why the 700°C surface retained the adsorbate so efficiently. Perhaps some weak chemisorption occurred involving the nitrogen lone pair of the ammonia and the empty 'd' orbitals of the silicon atoms on the dehydroxylated surface. The results indicated that the most efficient desorption occurred with the 300 and 500°C samples suggesting that the forces were weak, perhaps hydrogen bonds to the hydroxyl groups which remained on the surface. Van der Waals forces probably played some role in the adsorption also.

4.5. Desorption Efficiency of Quebec Chrysotile

These results showed that overall the desorption efficiency of Quebec chrysotile was better than that of the Californian samples. Invariably desorption was complete by the fourth dose of adsorbate. Again the adsorbate was most persistently held on the surface of the 150 and 700°C samples. The 300 and 500°C surfaces allowed desorption to occur after the least number of adsorbate doses i. e. one for the 300°C and two for the 500°C surface. These results were difficult to interpret but again it may be speculated that weak chemisorption occurred for the first three additions of gas to the 150 and 700°C surfaces and only for the first one and two aliquots on the 300 and 500°C surfaces, respectively. Overall, chemisorption must have occurred at fewer sites on Quebec than Californian surfaces as complete desorption was possible after fewer additions of

adsorbate. This was perhaps due to the stabilizing influence of the brucite layer in the Quebec samples.

4.6. Adsorption of Ammonia on Californian Chrysotile Treated With Water and Sodium Nitrate

With respect to heats of adsorption the samples treated with water and sodium nitrate were identical, beginning with extremely high heats which could not be recorded with the present system and descending to just above 150 kJ mol^{-1} for the second adsorbate addition. After that point the descent was steep to a "limiting" value of 10 kJ mol^{-1} . Overall the values both at low surface coverages and at the "limiting" heats were greater by about three times than the heats recorded for the heat-treated materials. According to the literature (22) when chrysotile was extracted in water by Soxhlet extraction, it was shown that the chrysotile decomposed by dissolution of magnesium leaving a residue of colloidal silica that hydrolyzed to orthosilicic acid. Since the amount of ammonia adsorbed on the water and sodium-nitrate treated material was greater by 20 to 40% than that on the heat-treated sample at 150°C , it might indicate that the methodology used in these experiments brought the chrysotile to the colloidal silica phase onto which ammonia would be readily adsorbed at the hydroxyl sites. The removal of the magnesium possibly cleared a number of new sites for ammonia adsorption. This adsorption at the hydroxyl sites might also have promoted the kind of salt formation of ammonium hydroxide outlined in Section 4.2.

The main differences between the water and sodium nitrate-treated samples was in the amount adsorbed and in the position of the entropy curve with respect to the mobile model.

The amount of ammonia adsorbed on the sodium nitrate-treated samples was only about 70% of the amount desorbed on the water-treated sample at ammonia pressures greater than 15 kPa. This might be explained if the ammonia molecules from the first doses were attracted to the available hydroxyl sites but when these were occupied it was found that sodium atoms were blocking some sites on the sodium nitrate-treated surface. Therefore there would be less adsorption on that surface than on the water-treated surface where more sites remained free. Whether true ion exchange took place with respect to sodium atoms or if they were only distributed on the silica surface is not known as the 3.7% sodium determination was established by a differential method. Further experimentation in this area would be necessary because two experiments were not regarded as sufficient to form any firm conclusions.

The experimental differential molar entropy of the two chemically-treated samples were similar with some difference emerging in that the species adsorbed on the water-treated sample was more mobile than that on the sodium nitrate-treated material. A possible reason for this could be that more ammonia was able to penetrate the capillaries (8) in the surface of the

water-treated chrysotile than the other sample where sodium may have made some pores inaccessible. The highly mobile species in the capillaries of the water-treated samples might have made a significant contribution to the total entropy making it slightly (6 to $10 \text{ J deg}^{-1} \text{ mol}^{-1}$) higher than that for the sodium nitrate-treated material.

4.7. The Physical Structure of the Adsorbents

4.7.1. Californian Chrysotile

Many studies have been conducted which dealt with the surface structure of alumino-silicates (84), chrysotile (16, 37, 85-89) and heat-treated chrysotile (30-36, 39). The nitrogen adsorption/desorption isotherms, surface areas and pore size distribution results for Californian chrysotile heat-treated at 150, 300, 500 and 700°C were in general agreement with those obtained earlier (39). The major difference in results obtained between the Cranston and Inkley (49) and Dollimore and Heal (50) applications lay in the increase in the number of points in the crucial small pore ($< 40 \text{ \AA}$ radius) region of the plot of Dollimore and Heal (50). From 150 to 300°C the percentage of "small" to "large" pores increased possibly due to water plug removal (39, 85, 86). Heat treatment at 500°C was perhaps coincident with the first part of the main dehydration step of chrysotile (30-35), in other words a partially disordered serpentine anhydride was formed. Neither electron microscopy nor selected area electron diffraction techniques confirmed this however, so structural differences must have

been minimal and confined to a short-range effect. Heating to 700°C caused the Californian chrysotile to dehydrate and form forsterite (90). Selected area electron diffraction (Plate 2(d)) showed that the material formed had little ordered arrangement since no clear electron diffraction pattern was observed. A surface area decrease such as that described by Murphy and Ross (39) was not observed, in fact it remained virtually the same through 150 to 700°C treatment. This is not in agreement either with Girgis (91) where it was observed that a collapse of the structure occurred reducing the surface area. It is possible that since less disorder was observable with the present 500°C sample, the 700°C sample would also not have reached the extent of disorder reported in the literature (39, 91). Transmission electron micrographs (Plate 1(d)) also showed very little flaking and cracking which corroborated that result.

4.7.2. Quebec Chrysotile

These results also were basically in agreement with those observed previously (39). Heating from 150 to 300°C resulted in some dehydration of brucite to magnesium oxide. No increase in surface area was observed over this temperature range so little dissociation of the fibre bundles could have occurred; indeed it had not occurred up to 500°C. An increase in temperature from 500 to 700°C resulted in a surface area increase of $2 \text{ m}^2 \text{ g}^{-1}$ unlike the increase of $15 \text{ m}^2 \text{ g}^{-1}$ observed

by Murphy and Ross (39). Although some cracking and flaking was observed in the transmission electron micrograph (Plate 3(d)) no fibre dissociation seemed evident. Selected area electron diffraction studies, however, showed no structural organization at 700°C (Plate 4(d)). The forsterite formed at that temperature was thus shown to be disordered in structure.

4.7.3. Water and Sodium Nitrate-Treated Californian Chrysotile

Similar nitrogen adsorption/desorption isotherms, surface areas and pore size distributions were observed for the chemically-treated samples. These data compared closely with those observed for the 150°C Californian chrysotile. Transmission electron micrographs and selected area electron diffraction studies showed no difference in appearance or diffraction pattern from the 150°C samples. Although ammonia adsorption results showed considerable differences from the 150°C samples nitrogen adsorption data and electron microscopy did not. As stated previously this could be due in part to the relative sizes of the ammonia and nitrogen molecules. Chemical changes in the chemically-treated samples seemed to be present but the physical structure remained essentially the same throughout the treatment.

4.8. Conclusion

It is considered that this work has provided novel and important quantitative data on the nature of the interactions at various temperatures from 266 to 308 K between ammonia and two natural and modified chrysotiles.

The calorimetric determination of the heat of adsorption and subsequent calculation of the entropy of adsorption have helped to clarify the nature of the gas-solid interactions involved. Electron microscopy as well as nitrogen adsorption/desorption data, surface area measurements and pore size distribution data have helped to characterize the adsorbents.

Further work should be undertaken to elucidate certain features of the adsorbate/adsorbent system. The use of in-line infrared spectroscopy or mass spectrometry in particular, would provide direct evidence as to the type of adsorbed complex. Also, in the present work, the distribution of the sodium ions on the chemically-treated chrysotile surface was not known adequately. Further studies are therefore necessary with respect to the chemically-treated chrysotile.

REFERENCES

1. Gregg, S. J., and Sing, K. S. W., "Adsorption, Surface Area and Porosity," New York: Academic Press, (1967).
2. Clark, A., "The Theory of Adsorption and Catalysis", ed. Loebel, E. M., London: Academic Press, 3 (1970).
3. Ross, S., and Oliver, J. P., "On Physical Adsorption," New York: John Wiley and Sons, Inc., (1964).
4. Young, D. M., and Crowell, A. D., "Physical Adsorption of Gases," London: Butterworths, (1962).
5. Steele, W. A., "The Solid - Gas Interface," ed. Flood, E. A., New York: Marcel Dekker, Vol. 1, 307 (1966).
6. Glass, R. W., Thesis, The Queen's University of Belfast, Northern Ireland (1972).
7. Scholten, J. J. F., and Kruyer, S., "Physical and Chemical Aspects of Adsorbents and Catalysts," ed. Linsen, B. G., London: Academic Press, (1970).
8. de Boer, J. H., "The Dynamical Character of Adsorption," Oxford: Clarendon Press, (1968).
9. Thomas, J. M., and Thomas, W. J., "Introduction to the Principles of Heterogeneous Catalysis," London: Academic Press, (1967).
10. Bomchil, G. et al, J. Chem. Soc. Faraday Trans. 1, 75 (7), 1535 (1979).
11. Hsieh, P. Y., J. Catalysis, 2, 211 (1963).
12. Clark, A., J. Catalysis, 1, 244 (1962).
13. Boyle, T. W., Gaw, W. J., and Ross, R. A., J. Chem. Soc., 37, 240 (1965).
14. Murphy, W. J., and Ross, R. A., J. Phys. Chem., 81, 1078 (1977).
15. Murphy, W. J., and Ross, R. A., Can. J. Chem., 56, 1847 (1978).
16. Fripiat, J. J., and della Faille, M., Clays and Clay Minerals Proc. 15th Conf., New York: Pergamon Press, 305 (1964).

17. Gorski, C. H., and Stettler, L. E., American Industrial Hygiene Association Journal, 36 (4), 292 (1975).
18. Hodgson, A. A., "Asbestos Vol. 1 Properties, Applications and Hazards," ed. Michaels, L. and Chissick, S. S., Toronto: John Wiley and Sons, (1979).
19. Myers, J. L., Soc. Plast. Eng; Tech. Pap., 20, 207 (1974).
20. Papirer, E., Clays and Clay Min., 29 (1), 69 (1981).
21. Gibson, J. C., Composites, 3 (2), 57 (1972).
22. Kramer, J. R., Murdoch, O., and Tihor, S., "Asbestos in the Environment," Report to Environment Canada, May, 1974.
23. Report to the Advisory Committee on Asbestos Cancers, Br. J. Ind. Med., 30, 180 (1973).
24. Shugar, S., "Effects of Asbestos in the Canadian Environment," Report to NSERC, (1979).
25. Wright, G. W., "Statement Before the U. S. Department of Labour, Occupational Health and Safety Hearing on Proposed Occupational Asbestos Standards," March 6, 1972.
26. Selikoff, I. J., Hammond, E. C., and Cheng, J., J. Am. Med. Assoc., 204 (2), 104 (1968).
27. de Sousa Santos, H., Clays and Clay Min., 27 (3), 161 (1979).
28. Martinez, E., Can. Min. Metall. Bull., 69, 1305 (1966).
29. Badollet, M. S., and Streib, W. C., Can. Min. Metall. Bull., 63, 65 (1955).
30. Brindley, G. W., and Zussman, J., Am. Miner. 42, 461 (1957).
31. Brindley, G. W., and Hayami, R., Clays and Clay Minerals, Proc. 12th Conf., New York: Pergamon Press, 35 (1964).
32. Brindley, G. W., and Hayami, R., Clays and Clay Minerals, Proc. 12th Conf., New York: Pergamon Press, 49 (1964).
33. Brindley, G. W., and Hayami, R., Miner. Mag. 35, 189 (1965).
34. Ball, M. C., and Taylor, H. F. W., Miner. Mag. 32, 754 (1961).
35. Ball, M. C., and Taylor, H. F. W., Miner. Mag. 33, 467 (1963)

36. Woodrooffe, H. M., Can. Min. Metall. Bull., 59, 363 (1956).
37. Naumann, A. W., and Drescher, W. H., Am. Miner., 51, 1200 (1966).
38. Nagy, B., and Bates, T. F., Am. Miner., 37, 1055 (1952).
39. Murphy, W. J., and Ross, R. A., Clays and Clay Min., 25, 78 (1977).
40. Mapes, J. E., and Eischens, R. P., J. Phys. Chem., 58, 1059 (1954).
41. Folman, M., and Yates, D. J. C., J. Phys. Chem., 63, 183 (1953).
42. Beebe, R. A., and Young, D. M., J. Phys. Chem., 58, 93 (1954).
43. Kemball, C., and Rideal, E. K., Proc. Roy. Soc. (A), 187, 53 (1946).
44. Everett, D. H., Trans. Faraday Soc., 46, 453, 942, 957 (1950).
45. Lippens, B. C., Linsen, B. G., and de Boer, J. H., J. Catal., 3, 32 (1964).
46. Taylor, A. H., and Ross, R. A., J. Chem. Eng. Data, 14 (31), 347 (1969).
47. van Nordstrand, R. A., Kreger, W. E., and Ries, H. E., J. Phys. and Colloid Chem., 55, 621 (1951).
48. Brunauer, S., Emmett, P. H., and Teller, E., J. Am. Chem. Soc., 60, 309 (1938).
49. Cranston, R. W., and Inkley, F. A., Adv. Catalysis, 9, 143 (1957).
50. Dollimore, D., and Heal, G. R., J. Appl. Chem., 14, 109 (1964).
51. Smith, P. A. S., "The Chemistry of Open-Chain Organic Nitrogen Compounds. Volume 1," New York: W. A. Benjamin, (1965).
52. "International Critical Tables", ed. Washburn, E. W., New York: McGraw-Hill Book Co., (1926).
53. "The Encyclopedia of Chemistry," ed. Hampel, C. A. and G. G. Hawley, Toronto, Van Nostrand Reinhold Co., (1973).

54. Pace, E. L., "The Solid - Gas Interface," ed. Flood, E. A., New York: Marcel Dekker, (1967).
55. Pace, E. L., Heric, E. L., and Dennis, K. S., J. Chem. Phys., 21, 1215 (1953).
56. Bobka, R. J., Dininny, R. E., Siebert, A. R., and Pace, E. L., J. Phys. Chem., 61, 1646 (1957).
57. Holmes, J. M., "The Solid - Gas Interface," ed. Flood, E. A., New York: Marcel Dekker, Vol. 1, (1966).
58. Garner, W. E., and Veal, F. J., J. Chem. Soc., 1436 (1935).
59. Beeck, O., Adv. Catalysis, 2, 151 (1950).
60. Murphy, W. J., Ross, R. A., and Glass, R. W., Ind. Eng. Chem. Prod. Res. Dev., 16, 69 (1977).
61. Smith, W. R., and Ford, D. G., J. Phys. Chem. 69 (10), 3587 (1965).
62. Everett, D. H., Proc. Chem. Soc., 28, 246 (1957).
63. Thomas, J. M., J. Chem. Educ., 38, 138 (1961).
64. "Handbook of Chemistry and Physics," West Palm Beach, Fla.: Chemical Rubber Co. Press, (1978).
65. Haar, L., and Gallagher, J. S., J. Phys. Chem. Ref. Data, 7 (3), 635 (1978).
66. Karapet'yants, M. Kh., and Karapet'yants, M. L., "Thermodynamic Constants of Inorganic and Organic Compounds," Ann Arbor: Humphrey Science Publishers, (1970).
67. Kemball, C., Adv. Catalysis, 2, 237 (1950).
68. Emmett, P. H., and Brunauer, S., J. Am. Chem. Soc., 59, 1553 (1937).
69. Pope, M. I., Educ. Chem. 2 (5), 246 (1965).
70. Parkash, S., Chemtech, 10 (9), 572 (1980).
71. Livingstone, H. K., J. Colloid Sci., 4, 450 (1949).
72. Barrett, E. P., Joyner, L. G., and Halenda, P. H., J. Am. Chem. Soc., 73, 373 (1951).

73. Joyner, L. G., "Scientific and Industrial Glassblowing and Laboratory Techniques," ed. Barr, W. E., and Arhorn, W. J., Pittsburg: Instruments Publishing Company, (1949).
74. Blomfield, G. A., and Little, L. H., Can. J. Chem., 51, 1771 (1973).
75. Cant, N. W., and Little, L. H., Can. J. Chem., 46, 1373 (1968).
76. Griffiths, D. W. L., Hallam, H. E., and Thomas, W. J., Trans. Faraday Soc., 64, 3361 (1968).
77. Basila, M. R., and Kantner, T. R., J. Phys. Chem., 71, 467 (1967).
78. Kvlividge, V. I., Brants, R. A., Kisselev, V. F., and Bliznakov, A. M., J. Catalysis, 13, 255 (1969).
79. Stone, F. S., and Whalley, L., J. Catalysis, 8, 173 (1967).
80. Titoff, A. Z., Physik Chem. 74, 641 (1910).
81. Kiselev, A. V., Lygin, V. I., and Titova, T. I., Zh. Fiz. Khim., 38, 2730 (1964).
82. Bliznakov, E., Markov, I., and Bakardjnew, I., Commun. Dept. Chem. Bulgarian Acad. Sci., 1, 211 (1968).
83. Kumli, K. F., "Introductory Chemistry," Englewood Cliffs, New Jersey: Prentice - Hall, Inc., (1974).
84. Fripiat, J. J., Clays and Clay Minerals. Proc. 12th Conf., New York: Pergamon Press, 327 (1964).
85. Young, G. J., and Healey, F. H., J. Phys. Chem., 58, 881 (1954).
86. Healey, F. H., and Young, G. J., J. Phys. Chem., 58, 885 (1954).
87. Pundsack, F. L., J. Phys. Chem., 59, 802 (1955).
88. Pundsack, F. L., J. Phys. Chem., 65, 30 (1961).
89. Carton, B., and Kauffer, E., Atmospheric Environment, 14, 1181 (1980).
90. Brindley, G. W. and Zussman, J., Miner. Mag., 32, 107 (1956).
91. Girgis, B. S., Trans. J. Br. Ceram. Soc., 74 (4), 135 (1975).

APPENDIX A

A.1. Calculations

A.1.1. Calorimetric Heats of Adsorption

Adiabatic calorimetric heats of adsorption were determined using the technique described earlier. Full details of the method of calculation of the results are given in Table 2.1. and part of a typical calculation is shown below:

sample		Quebec chrysotile 7T-5 (150°C)
weight	(g)	0.71349
surface area	(m ² g ⁻¹)	40
experimental temperature	(K)	273
room temperature	(K)	298
burette "dead space" volume	(dm ³)	17.22
calorimeter "dead space" at 273 K	(dm ³)	48.56
calorimeter "dead space" at 298 K	(dm ³)	46.80
conversion factor from cm. to dm ³		1.75
0.0 value on the manometer	(cm)	50.833

Ammonia adsorption on 7T-5 (150°C)

Mercury Levels in the Manometer (cm)

<u>Before NH₃</u>		<u>After NH₃</u>	
<u>h₁</u>	<u>h₂</u>	<u>h₃</u>	<u>h₄</u>
26.420	30.920	27.735	28.754
25.273	32.837	26.492	30.743

1st point

initial volume NH₃ at S.T.P. = (4.5)(59.94)(.0123) = 3.32 dm³

equilibrium volume NH₃ at S.T.P. = (1.02)(57.64)(.0123) = .72 dm³

calorimeter d.s. volume at S.T.P. = $\frac{1.02 \times 48.56}{273} \times \frac{273}{76} = .652 \text{ dm}^3$

amount NH₃ adsorbed at equilibrium is:

$$3.32 - (.72 + .652) = 1.95 \text{ dm}^3$$

or $\frac{1.95 \times 44.615}{.71349 \times 40} = 3.05 \text{ } \mu\text{mol m}^{-2}$

As outlined in the text the recorder reading for this value was off scale so no heat was calculated.

2nd point

initial V_{S.T.P.} = (7.56)(61.95)(.0123) = 5.76 + .652 = 6.41 dm³

equil. V_{S.T.P.} = (3.98)(59.82)(.0123) = 2.93 dm³

cal d.s. V_{S.T.P.} = 2.54 dm³

amount NH₃ adsorbed at equilibrium is

$$6.41 - (2.93 + 2.54) = .94 \text{ dm}^3 \text{ or } 1.47 \text{ } \mu\text{mol m}^{-2}$$

Cumulative amount adsorbed = 4.52 $\mu\text{mol m}^{-2}$

Joules produced = 1.54

Heat of adsorption = $\frac{1.54 \times 22414}{4.52} = 7637 \text{ J or } 7.64 \text{ kJ}$

C.2 Low-Temperature Nitrogen Adsorption

Nitrogen adsorption/desorption isotherms were determined at 77 K using the technique described earlier. Full details of the method of calculation of the results are given in Table 2.2. and part of a typical calculation is shown below:

Heights of mercury in the manometer (cm)

<u>Before N₂</u>		<u>After N₂</u>	
<u>h₁</u>	<u>h₂</u>	<u>h₃</u>	<u>h₄</u>
60.873	66.058	61.588	65.255
58.621	68.496	58.913	68.187
sample size		.06445 g	
barometric pressure		743.1 Torr (99.64 kPa)	
0.0 value on manometer		93.984 cm.	

1st Point

- (1) volume of gas in burette at S. T. P. before admission to sample tube:

$$51.81 \times .0123 \times 5.19 = 3.30 \text{ dm}_3$$

- (2) vol. gas in burette after admission to s. t. but above liquid N₂:

$$52.90 \times .0123 \times 3.67 = 2.39 \text{ dm}_3$$

- (3) vol. gas below liquid N₂ and above sample=

$$\begin{aligned} & 23.9 \times .004605 \times .81 \times .9356 \times (23.9 \times 6.6 \times 10^{-5} + 1) \\ & = .0834 \times 1.0016 \\ & = .0835 \text{ dm}^3 \end{aligned}$$

(4) vol. gas in s.t. above and below liquid N₂ =

$$.0024 \times 3.67 = .009 \text{ dm}^3$$

(5) amt adsorbed = 3.30 - (2.39 + .0835)

$$= .83 \text{ dm}^3 \text{ or } \frac{.83}{.06445} = 12.88 \text{ dm}^3 \text{ g}^{-1}$$

2nd point

(1) vol. gas before admission to S. T. =

$$53.63 \times .0123 \times 9.875 = 6.514 \text{ dm}^3$$

(2) vol. gas in s. t. above and below liquid N₂ =

$$.0024 \times 9.274 = .0223 \text{ dm}^3$$

(3) vol. gas in burette after admission to S. T. but

below liquid N₂ =

$$55.20 \times .0123 \times 9.274 = 6.297 \text{ dm}^3$$

(4) vol. gas below liquid N₂ and above sample =

$$9.274 \times .004605 \times .81 \times .9356 \times (9.274 \times 6.6 \times 10^{-5} + 1)$$

$$= .0324 \times 1.001$$

$$= .0324 \text{ dm}^3$$

(5) amt adsorbed = (6.514 + .009 + .0835) - (6.297 + .0324)

$$= 6.607 - 6.3294$$

$$= 0.278 \text{ dm}^3 \text{ or } \frac{0.278}{.06445} = 4.307 \text{ dm}^3 \text{ g}^{-1}$$

(6) Cumulative amount adsorbed = 17.19 dm³ g⁻¹

APPENDIX B

Copies of APL programmes for the DEC2020 computer used
in this study follow:

```

VADDERMICALMETLDDIV
ABSORBCALCULET1;H1;H2;H3;H4;H5;H6;N1;N2;N3;N4;N5;N6;S1;S2;S3;S4;S5;S6
ENTER ALL H VALUES IN GMS
ENTER YOUR VALUES FOR H1
H1;(H1+0)
(ENTER ) ;(TFH1);* VALUES FOR H2
H2+0
(ENTER ) ;(TFH1);* VALUES FOR H3
H3+0
(ENTER ) ;(TFH1);* VALUES FOR H4
H4+0
(ENTER ) ;(TFH1);* VALUES FOR H5
H5+0
(ENTER ) ;(TFH1);* VALUES FOR H6
H6+0
ENTER CALORIMETER DEAD SPACE
N+0
ENTER WEIGHT OF SAMPLE
W+0
ENTER SURFACE AREA OF SAMPLE
S+0
M+(10*H)F0
M1;]+(((69.717-H1)*X1.75)+17.22)*0.0123XF1+H2-H1
M2;]+(((69.717-H3)*X1.75)+17.22)*0.0123XF2+H4-H3
M3;]+(((69.717-H5)*X1.75)+17.22)*0.0123XF3+H6-H5
M4;]+NXP2
M5;]+NXP3
M6;]+M1;]+M2;]+M3;]+M4;]+M5;]+M6;]+
M7;]+M1;]+M2;]+M3;]+M4;]+M5;]+M6;]+
X+*+2
C1;M[6;]+M[1;]+M[5;]+(X-1)]-(M[4;]+X]+M[2;]+X])
M[7;]+M[1;]+M[5;]+(X-1)]-(M[5;]+X]+M[3;]+X])
+(((X+2+Z+1)*(M)AZIH)/CI
P1
PRESSURES AT PEAK MAXIMUM
P2
EQUILIBRIUM PRESSURE
P3
VOLUME OF GAS ABSORBED / DOSE (IN CC) AT PEAK MAXIMUM
M[6;]
VOLUME OF GAS ABSORBED / DOSE (IN CC) AT EQUILIBRIUM
M[7;]
M[7;]+M[7;]*A4.615+WXS
VOLUME OF GAS ABSORBED / DOSE (M,MM\METER SB) AT EQUILIBRIUM
M[7;]
M[8;]+M[7;]
0+2
C2;M[8;]+M[7;]+(0)]+M[8;]+(0-1)]
+((0+0+1)*(H)/02
P2+M[8;]
TOTAL VOLUME ABSORBED (AFTER LEAK DOSE) IN MICROGRAMS/KETT
BRUM
M[8;]
TOTAL VOLUME ABSORBED (AFTER EACH DOSE) IN CC/GRAM AT EQUILIBRIUM
D1+M[7;]+M[8;]*S+44.515
M[7;]
/OUTPUT

```

9 [1] VADDERMICALMETLDDIV
 [2] ABSORBCALCULET1;H1;H2;H3;H4;H5;H6;N1;N2;N3;N4;N5;N6;S1;S2;S3;S4;S5;S6
 [3] ENTER ALL H VALUES IN GMS
 [4] ENTER YOUR VALUES FOR H1
 [5] H1;(H1+0)
 [6] (ENTER) ;(TFH1);* VALUES FOR H2
 [7] H2+0
 [8] (ENTER) ;(TFH1);* VALUES FOR H3
 [9] H3+0
 [10] (ENTER) ;(TFH1);* VALUES FOR H4
 [11] H4+0
 [12] (ENTER) ;(TFH1);* VALUES FOR H5
 [13] H5+0
 [14] (ENTER) ;(TFH1);* VALUES FOR H6
 [15] H6+0
 [16] ENTER CALORIMETER DEAD SPACE
 [17] N+0
 [18] ENTER WEIGHT OF SAMPLE
 [19] W+0
 [20] ENTER SURFACE AREA OF SAMPLE
 [21] S+0
 [22] M+(10*H)F0
 [23] M1;]+(((69.717-H1)*X1.75)+17.22)*0.0123XF1+H2-H1
 [24] M2;]+(((69.717-H3)*X1.75)+17.22)*0.0123XF2+H4-H3
 [25] M3;]+(((69.717-H5)*X1.75)+17.22)*0.0123XF3+H6-H5
 [26] M4;]+NXP2
 [27] M5;]+NXP3
 [28] M6;]+M1;]+M2;]+M3;]+M4;]+M5;]+M6;]+
 [29] M7;]+M1;]+M2;]+M3;]+M4;]+M5;]+M6;]+
 [30] X+*+2
 [31] C1;M[6;]+M[1;]+M[5;]+(X-1)]-(M[4;]+X]+M[2;]+X])
 [32] M[7;]+M[1;]+M[5;]+(X-1)]-(M[5;]+X]+M[3;]+X])
 [33] +(((X+2+Z+1)*(M)AZIH)/CI
 [34] P1
 [35] PRESSURES AT PEAK MAXIMUM
 [36] P2
 [37] EQUILIBRIUM PRESSURE
 [38] P3
 [39] VOLUME OF GAS ABSORBED / DOSE (IN CC) AT PEAK MAXIMUM
 [40] M[6;]
 [41] VOLUME OF GAS ABSORBED / DOSE (IN CC) AT EQUILIBRIUM
 [42] M[7;]
 [43] M[7;]+M[7;]*A4.615+WXS
 [44] VOLUME OF GAS ABSORBED / DOSE (M,MM\METER SB) AT EQUILIBRIUM
 [45] M[7;]
 [46] M[8;]+M[7;]
 [47] 0+2
 [48] C2;M[8;]+M[7;]+(0)]+M[8;]+(0-1)]
 [49] +((0+0+1)*(H)/02
 [50] P2+M[8;]
 [51] TOTAL VOLUME ABSORBED (AFTER LEAK DOSE) IN MICROGRAMS/KETT
 [52] BRUM
 [53] M[8;]
 [54] TOTAL VOLUME ABSORBED (AFTER EACH DOSE) IN CC/GRAM AT EQUILIBRIUM
 [55] D1+M[7;]+M[8;]*S+44.515
 [56] M[7;]
 [57] /OUTPUT

```

V DESORPTION WORK [U]
V DESORPTION WORK [H1]
V ENTER ALL K VALUES IN GMS.
V ENTER YOUR VALUES FOR H1
H1=(M1E)
V ENTER 1) (YFH1) 2) VALUES FOR H2
M2E
V ENTER 1) (YFH1) 2) VALUES FOR H3
M3E
V ENTER 1) (YFH1) 2) VALUES FOR H4
M4E
V ENTER CALORIMETER DEAD SPACE FACTOR
MDE
V ENTER FINAL P2 VALUE FROM ADSORPTION
V3=MXPF+
V ENTER WEIGHT OF SAMPLE
WE
V ENTER SURFACE AREA OF SAMPLE
SA
V ENTER TOTAL VOLUME ADSORBED IN MICRO MOLES/METER SQ
V FROM CORRESPONDING ADSORPTION XROTHERM
AD40
M+(/,H)F0
M11]J+(((69.717-H1)X1.75)+17.22)X0.0123XP1+H2-H1
M21]J+(((69.717-H3)X1.75)+17.22)X0.0123XP2+H4-H3
M31]J+NXPF2
M41]J+(M21]J+M31]J)-(M11]J+V3)
X+Z+2
C1:M[4]2]J+M[2]X]J+M[3]X]J-M[3]X(X-1)]+M[1]X]
+((X+Z+2+1)H)AZ(H)/C1
V INITIAL PRESSURE
P1
V EQUILIBRIUM PRESSURE
P2
V VOLUME DESORBED / DOSE (CC)
M[4]
M[4]J+M[4]JX44.615+WX5
V VOLUME DESORBED / DOSE [MICROMOLES/METER SQ]
M[4]J
M[5]J1]J+M[4]J1]
G+2
C2:M[5]G]J+M[4]G]J+M[5]G(X-1)]
+((G+R+1)H)/C2
E1+M[5]J
V TOTAL VOLUME DESORBED / DOSE [MICROMOLES/METER SQ]
M[5]J
V VOLUME REMAINING [MICRO MOLES/METER SQ]
V AFTER DESORPTION AT EACH EQUILIBRIUM PRESSURE
C3:VK+M[6]J+AD-M[5]J
VM
V VOLUME REMAINING [IN CC/GRAM]
VC+M[6]JX8-44.615
VC
) OUTPUT

```

```
▽ ADSORBED VOLUME]
  ADSORBED WEIGHT] H1; H2; H3; H4; A1; A2; P0; W; F1; P2; X; S; I] V
  ENTER YOUR VALUES FOR H1'
H+(H1+U)
  ENTER ' '); (YH1)Y' VALUES FOR H2'
H2+U
  ENTER ' '); (YH1)Y' VALUES FOR H3'
H3+U
  ENTER ' '); (YH1)Y' VALUES FOR H4'
H4+U
  ENTER THE 0.0 VALUE FOR THE MANOMETER'
A+U
  ENTER PO IN TORR'
P0+U
  ENTER SAMPLE WEIGHT'
W+U
  SAMPLE DENSITY'
D+U
  F+(10,H)F0
  FL1;] +((A1+A-H1)X0.86)+23.22)X0.00123XP1+(H2-H1)X10
  FL2;] +((A2+A-H3)X0.86)+23.04)X0.00123XP2+(H4-H3)X10
  FL4;] +P2X0.004605X0.81X(1-W+D)X(1+6.60000000E-5 XP2)
  FL5;] +0.0024XP2
  FL6;] +FL1;] - (FL2;] +FL4;] +1]
  X+Z+2]
  C1;] +FL6;] +FL1;] +FL5;] (X-1) +FL4;] (X-1) - (FL2;] X) +FL4;] (X)
  +((X+Z+2+1)(M)AZ(M)/C1
  FL6;] +FL6;] +W
  FL7;] +FL6;] +1]
  L+2]
  C2;] +FL7;] +FL7;] (L-1) +FL6;] L]
  +((L+L+1)(M)/C2
  FL8;] +P2+P0
  FL9;] + (P0-P2)X(P1+FL7;] )
  FL10;] +P2+FL9;]
  VOLUME ADSORBED[CC/GRM]
  FL7;]
  P2+FL8;]
  REDUCED PRESSURE
  FL8;]
  P2/V(P0-P2)
  FL10;]
) OUTPUT
▽
```

```

VOLUME[1] = WADJ*VADJ
RESORBED[1] = WADJ*VADJ
CENTER[1] = WADJ*VADJ
M1 = (YCENTER[1]) / (YFN1)
M2 = (YCENTER[2]) / (YFN2)
M3 = (YCENTER[3]) / (YFN3)
M4 = (YCENTER[4]) / (YFN4)
A = 0.0
W = 0.0
P = 0.0
PO = 0.0
V1 = (X0 + 0.04605 * X) * (1 + W) * X
G1 = (1 + A) * P
G2 = (1 + A) * P
G3 = (1 + A) * P
G4 = (1 + A) * P
G5 = (1 + A) * P
G6 = (1 + A) * P
G7 = (1 + A) * P
G8 = (1 + A) * P
G9 = (1 + A) * P
G10 = (1 + A) * P
G11 = (1 + A) * P
G12 = (1 + A) * P
G13 = (1 + A) * P
G14 = (1 + A) * P
G15 = (1 + A) * P
G16 = (1 + A) * P
G17 = (1 + A) * P
G18 = (1 + A) * P
G19 = (1 + A) * P
G20 = (1 + A) * P
G21 = (1 + A) * P
G22 = (1 + A) * P
G23 = (1 + A) * P
G24 = (1 + A) * P
G25 = (1 + A) * P
G26 = (1 + A) * P
G27 = (1 + A) * P
G28 = (1 + A) * P
G29 = (1 + A) * P
G30 = (1 + A) * P
G31 = (1 + A) * P
G32 = (1 + A) * P
G33 = (1 + A) * P
G34 = (1 + A) * P
G35 = (1 + A) * P
G36 = (1 + A) * P
G37 = (1 + A) * P
G38 = (1 + A) * P
G39 = (1 + A) * P
G40 = (1 + A) * P
G41 = (1 + A) * P
G42 = (1 + A) * P
G43 = (1 + A) * P
G44 = (1 + A) * P
G45 = (1 + A) * P
G46 = (1 + A) * P
G47 = (1 + A) * P
G48 = (1 + A) * P
G49 = (1 + A) * P
G50 = (1 + A) * P
G51 = (1 + A) * P
G52 = (1 + A) * P
G53 = (1 + A) * P
G54 = (1 + A) * P
G55 = (1 + A) * P
G56 = (1 + A) * P
G57 = (1 + A) * P
G58 = (1 + A) * P
G59 = (1 + A) * P
G60 = (1 + A) * P
G61 = (1 + A) * P
G62 = (1 + A) * P
G63 = (1 + A) * P
G64 = (1 + A) * P
G65 = (1 + A) * P
G66 = (1 + A) * P
G67 = (1 + A) * P
G68 = (1 + A) * P
G69 = (1 + A) * P
G70 = (1 + A) * P
G71 = (1 + A) * P
G72 = (1 + A) * P
G73 = (1 + A) * P
G74 = (1 + A) * P
G75 = (1 + A) * P
G76 = (1 + A) * P
G77 = (1 + A) * P
G78 = (1 + A) * P
G79 = (1 + A) * P
G80 = (1 + A) * P
G81 = (1 + A) * P
G82 = (1 + A) * P
G83 = (1 + A) * P
G84 = (1 + A) * P
G85 = (1 + A) * P
G86 = (1 + A) * P
G87 = (1 + A) * P
G88 = (1 + A) * P
G89 = (1 + A) * P
G90 = (1 + A) * P
G91 = (1 + A) * P
G92 = (1 + A) * P
G93 = (1 + A) * P
G94 = (1 + A) * P
G95 = (1 + A) * P
G96 = (1 + A) * P
G97 = (1 + A) * P
G98 = (1 + A) * P
G99 = (1 + A) * P
G100 = (1 + A) * P

```

```

4  CONCENT 11.94
5  CENTER VOLUME ABSORBED (MICRO MOLIES/METER SQ )
6  S+(FV+U )/FO
7  X+1
8  S[X]+78.314*(#(A+1)-A+VIX)+11.94))
9  +((X+X+1)/(FV)/Zi+1)*S
10 DIFFERENTIAL COMPUTATIONAL ENTROPY ZS+
11 S
12 )OUTPUT
13
14 ]

```



```

V
[1]
[2]
[3]
[4]
[5]
[6]
[7]
[8]
[9]
VOLUME FLOW
MOLE FLOW
CENTER VOLUME ABSORBER (MICRO MOLES/METER SQ)
SS4(PV+1) *FC
CENTER MUL SUBSTRATE TEMPERATURE (DEGREES C)
P2273+1+0
K41
POLYMER 1.4+83281+5.3144X10(1721X10000-(V1A3X1000000000000E23 ))+53.8
7((XPA+1)17V77-1+I26
TEMPERATURE OF A 2D MOBILE FILM IS:-1
53
)
) OUTPUT
V

```


APPENDIX C

Table C. 1. shows actual amounts ($\mu\text{mol m}^{-2}$) of ammonia adsorbed and desorbed in the desorption efficiency experiments.

TABLE C. 1.

Desorption Efficiency of Heat-Treated Californian and Quebec Chrysothiles

	Californian				Quebec			
	150°C	300°C	500°C	700°C	150°C	300°C	500°C	700°C
1st amount adsorbed ($\mu\text{mol m}^{-2}$)	1.04	2.74	2.69	2.00	1.07	2.49	0.96	1.85
1st desorption	0	0.42	0.26	0	0	0.14	0	0
2nd	0	0.12	0.33	0	0	0.21	0	0
3rd	0	0.10	0.13	0	0	0.15	0	0
4th	0	0.12	0.13	0	0	0.053	0	0
5th	0	0	0.03	0	0	0.13	0	0
% remaining	100%	72%	66%	100%	100%	73%	100%	100%
2nd amount adsorbed	2.17	1.51	1.20	2.51	1.87	1.15	0.86	1.08
1st desorption	0.30	0.45	0.30	0.34	0.27	0.39	0.14	0.23
2nd	0.30	0.22	0.26	0.21	0.20	0.30	0.015	0.12
3rd	0.23	0.24	0.16	0.28	0.18	0.29	0.087	0.02
4th	0.15	0.19	0.13	0.20	0.14	0.17	0.073	0.12
5th	0.14	0.045	0.06	0.053	0.06	0	0	0
% remaining	48%	14%	15%	57%	55%	0	64%	55%

Table (continued)

	Californian				Quebec			
	150°C	300°C	500°C	700°C	150°C	300°C	500°C	700°C
3rd amount adsorbed	2.40	1.69	1.15	1.19	1.12	0.42	0.56	
1st desorption	0.41	0.33	0.32	0.33	0.33	0.17	0.21	
2nd	0.18	0.42	0.27	0.23	0.21	0.22	0.15	
3rd	0.19	0.26	0.30	0.20	0.17	0.11	0	
4th	0.16	0.21	0.16	0.16	0.034	0	0	
5th	0.21	0.12	0.05	0.07	0	0	0	
% remaining	52%	21%	4%	17%	34%	0	36%	
4th amount adsorbed	1.22	1.07	1.06	1.49	1.06	0.58	0.16	
1st desorption	0.32	0.39	0.32	0.42	0.35	0.16	0.18	
2nd	0.32	0.37	0.26	0.31	0.31	0.094	0.13	
3rd	0.25	0.25	0.24	0.13	0.21	0	0	
4th	0.16	0.15	0.16	0.23	0.20	0	0	
5th	0	0	0.10	0.11	0	0	0	
% remaining	14%	0	0	19%	0	0	0	

Table (continued)

	Californian				Quebec			
	150°C	300°C	500°C	700°C	150°C	300°C	500°C	700°C
5th adsorption	1.43			1.49				
1st desorption	0.53			0.47				
2nd	0.36			0.37				
3rd	0.26			0.17				
4th	0.31			0.17				
5th	0			0.27				
% remaining	0			0				